

Biochemie

**MORPHOLOGICAL AND FUNCTIONAL CHARACTERISATION OF A
NEW MURINE SERUM-FREE *IN VITRO* MODEL OF THE
BLOOD-BRAIN BARRIER**

Inaugural-Dissertation
zur Erlangung des Doktorgrades
der Naturwissenschaften im Fachbereich Chemie und Pharmazie
der Mathematisch-Naturwissenschaftlichen Fakultät
der Westfälischen Wilhelms-Universität Münster

vorgelegt von
CHRISTIAN WEIDENFELLER
aus Oberhausen

-2003-

Dekan: Prof. Dr. J. Leker
Erster Gutachter: Prof. Dr. H.-J. Galla
Zweiter Gutachter: Prof. Dr. K.-H. Klempnauer

Tag der mündlichen Prüfung: 18.11.2003
Tag der Promotion: 18.11.2003

Meinen Eltern

Vielen Dank!

Bedanken möchte ich mich:

bei Prof. Dr. H.-J. Galla für die interessante Themenstellung, die freundliche Unterstützung und die stetige Diskussionsbereitschaft,

bei Priv. Doz. Dr. Thomas Rauen für die Unterstützung bei der Mauskultur und die Anregungen für die molekularbiologischen Arbeiten,

bei Dr. Joachim Wegener für die unglaubliche Hilfsbereitschaft in allen Lebenslagen (ob physikalisch oder nicht...),

bei Markus für die tolle Zusammenarbeit und den Beitrag im Rahmen seiner Diplomarbeit,

bei Alla, Bernd, Joe, Susanne, Tina und Thomas für das Durchsehen des Manuskripts,

für die Unterstützung bei den Messungen: Sabine (Zellkultur & Permeabilitäten), Sebastian (AFM) und Björn (QCM),

bei allen gegenwärtigen und vergangenen Laborkollegen: Alla, Anja, Beate, Christoph, Dagmar, Evelyn, Frank, Jens, Joe, Mairin, Markus, Muffin, Ruth, Susanne, Patrick, Tanja, Thanh, und Ulf, sowie dem ganzen AK Galla (BHS und Lipidis) für eine nette Zusammenarbeit während der 3 Jahre. (Hier sei besonders Anja und Markus für ihre Teilzeit-Mitbewohnerschaft der WG Zwipp und Jens für lange Diskussionen über Klonierungen und Moorhühner gedankt),

bei T., Schachi und Lübbe für die unterstützende Bereitstellung von Fachwissen und Ablenkungen im Laboralltag und darüber hinaus,

bei Anne, Antje, Freddy, Hedda, Lydia, Sandra, Silke, Steffi, Wolfgang und Walter für die Unterstützung in allen Instituts-Lebenslagen,

beim ganzen Institut für die kollegiale Atmosphäre,

bei meinen Freunden innerhalb und ausserhalb Münsters, besonders bei Ansgar, Claudia, Frauke, Gesine, Hennes, Jan, Kristina, Matthias, Markus, Melanie Muffin, Ruth und Volker,

bei meinen Eltern und Geschwistern für die immerwährende Unterstützung

und ganz besonders bei Alla (geb. Zozulya) für ihre Zusammenarbeit im Institut und Zuhause!!! Я тебе кохаю! Дякую!!!

| | | |
|----------|--|----|
| 1 | Summary | 1 |
| 2 | Introduction | 3 |
| 2.1 | Barriers of the central nervous system | 3 |
| 2.1.1 | Historical background | 4 |
| 2.1.2 | Barrier systems in the mammalian brain | 5 |
| 2.2 | Organization of the blood-brain barrier | 6 |
| 2.2.1 | Cell-cell contacts between brain capillary endothelial cells | 8 |
| 2.2.2 | Selective transport functions of capillary endothelial cells | 9 |
| 2.2.3 | Metabolic elements of the blood-brain barrier | 11 |
| 2.3 | <i>In vitro</i> models of the blood-brain barrier | 11 |
| 2.3.1 | Primary cultures of brain capillary endothelial cells | 13 |
| 2.3.2 | Cell lines as <i>in vitro</i> models of the blood-brain barrier | 14 |
| 2.4 | Regulation of blood brain barrier properties: Hormones | 16 |
| 2.5 | Objectives of the project | 20 |
| 3 | Experimental | 21 |
| 3.1 | Cell biology | 21 |
| 3.1.1 | Primary culture of murine brain capillary endothelial cells (MBCEC) .. | 21 |
| 3.1.2 | Transfection of cells with small interfering RNA | 26 |
| 3.1.3 | Immunocytochemistry | 27 |
| 3.1.4 | Atomic force microscopy | 29 |
| 3.1.5 | Transmission electron microscopy | 30 |
| 3.1.6 | Measurement of electrical properties of primary cultured murine brain capillary endothelial cells | 31 |
| 3.1.7 | Quartz Crystal Microbalance | 33 |
| 3.1.8 | Permeability studies | 36 |
| 3.2 | Molecular biology | 37 |
| 3.2.1 | Quantification of nucleic acids | 37 |
| 3.2.2 | Agarose gel electrophoresis | 38 |
| 3.2.3 | Isolation of DNA from agarose gels | 39 |
| 3.2.4 | Isolation of plasmid DNA | 39 |
| 3.2.5 | Isolation of RNA | 40 |
| 3.2.6 | cDNA synthesis | 40 |

| | | |
|----------|--|-----------|
| 3.2.7 | Polymerase chain reaction methods | 41 |
| 3.2.8 | Nucleic acid blotting and hybridisation | 44 |
| 3.2.9 | Cloning and ligation..... | 47 |
| 3.3 | Microbiology | 49 |
| 3.3.1 | Preparation of competent <i>E. coli</i> cells | 49 |
| 3.3.2 | Transformation of <i>E. coli</i> cells | 50 |
| 3.3.3 | Cultures of <i>E. coli</i> cells | 50 |
| 3.3.4 | Storage of <i>E. coli</i> cells..... | 50 |
| 3.4 | Protein biochemistry | 50 |
| 3.4.1 | Isolation of proteins from cultured cells | 51 |
| 3.4.2 | Determination of protein concentration | 51 |
| 3.4.3 | SDS-polyacrylamide gel electrophoresis..... | 51 |
| 3.4.4 | Coomassie Blue staining..... | 53 |
| 3.4.5 | Protein blotting and immunodetection | 53 |
| 4 | Results | 55 |
| 4.1 | Establishment of the primary culture of mouse brain capillary endothelial cells..... | 55 |
| 4.2 | Characterisation of murine brain capillary endothelial cells..... | 56 |
| 4.2.1 | Morphological characterisation of MBCEC..... | 56 |
| 4.3 | Identification of blood-brain barrier related proteins on RNA-level | 62 |
| 4.4 | Functional effects of hydrocortisone on MBCEC | 64 |
| 4.4.1 | Electrical properties of MBCEC..... | 64 |
| 4.4.2 | Sucrose permeability of MBCEC..... | 69 |
| 4.4.3 | Influence of hydrocortisone and serum on morphology of MBCEC and localisation of tight junction proteins..... | 70 |
| 4.4.4 | Influence of hydrocortisone on cell-cell contacts and cell surface | 75 |
| 4.4.5 | Transmission electron microscopy | 78 |
| 4.4.6 | Influence of hydrocortisone on expression of blood brain-barrier related proteins on RNA-level | 81 |
| 4.4.7 | Influence of hydrocortisone on protein expression of tight junction proteins | 83 |
| 4.5 | Gene silencing at primary cultures of brain capillary endothelial cells..... | 84 |
| 4.5.1 | Immunofluorescence staining of siRNA-transfected cells | 84 |

| | | |
|----------|--|------------|
| 4.5.2 | Western blot with siRNA transfected cells..... | 85 |
| 5 | Discussion | 87 |
| 5.1 | <i>In vitro</i> model of murine brain capillary endothelial cells | 87 |
| 5.2 | Influence of hydrocortisone on electrical properties of MBCEC | 88 |
| 5.3 | Influence of hydrocortisone and serum on morphology and mechanical properties of MBCEC | 92 |
| 5.4 | Influence of hydrocortisone on RNA- and protein expression | 97 |
| 5.5 | Application of RNA interference method on primary cultures of microvascular endothelial cells..... | 99 |
| 6 | Conclusion | 101 |
| 7 | Materials and devices | 103 |
| 7.1 | Materials..... | 103 |
| 7.2 | Devices | 105 |
| 8 | References | 107 |
| | Appendix A: Abbreviations..... | 124 |
| | Appendix B: WWW links | 126 |
| | Appendix C: Genotypes of <i>Escherichia coli</i> K12 strains | 127 |
| | Appendix D: Sequences | 128 |
| | Primer sequences: PCR..... | 128 |
| | Primer sequences: QRT-PCR | 128 |
| | siRNA sequences | 129 |
| | Appendix E: Clone charts | 130 |
| | Appendix F: List of table and figure captions | 132 |
| | Table captions | 132 |
| | Figure captions..... | 132 |

1 Summary

The blood-brain barrier (BBB) controls the passage of toxic and xenobiotic substances from the blood to the interstitial fluid of the brain. The transcellular pathway to the brain is strictly controlled by the morphological base of the BBB, the microvascular endothelial cells. These cells are linked with well developed tight junctions building up close connections between adjacent cells and prevent paracellular diffusion for various hydrophilic substances. Furthermore, these cells are equipped with a variety of transporters which actively extrude possibly harmful compounds from the cells back to the blood. Many *in vitro* models for the BBB are available but it is controversially discussed which model best approaches the *in vivo* situation. An *in vitro*-model of microvascular endothelial cells approves an investigation of mobility for pharmaceuticals across the BBB and thus, allows prognoses for effective drug-treatment of the brain. Furthermore, it allows investigations on the regulatory pathways controlling the tightness of cell-cell contacts. Many existing models are based on endothelial cell lines, like the endothelioma cell line bEnd5 from mouse brain capillaries. These cells are immortalised and not comparable to the *in vivo* situation. Other models are not even based on brain-derived cells like human umbilical vein endothelial cells (HUVEC) or peripheral microvessel endothelial cells¹.

To complete the investigations of a well established porcine primary capillary endothelial cell culture model of the blood-brain barrier, a new model was established based in mouse-derived brain microvascular endothelial cells. After the characterisation of this model the effect of the glucocorticoid hormone hydrocortisone on the blood-brain barrier properties of the cultured cells was investigated. By determination of the transendothelial electrical resistance it could be shown that hydrocortisone leads to altered barrier properties of the cells cultured in serum-free medium. This finding is accompanied by a change in the cell shape and redistribution of actin filaments. The advantages of a murine based model of the bbb are the availability of murine-specific antibodies, the known genomic data and the possibility to use knock out animals for further relevant studies. Together with the primary culture of porcine microvascular endothelial cells, two reliable *in vitro* models are now available to mimic the blood-brain barrier phenotype *in vitro*. The murine system facilitates application of modern

¹ Nakagawa, S., Dohgu, S., Yamauchi, A., Shirabe, S., Kataoka, Y., Niwa, M.; An *in vitro* model of the blood brain barrier with human peripheral microvessel endothelial cells; poster on the "Sixth Symposium on Signal Transduction on the Blood-Brain Barrier" Szeged, Hungary, 2003

molecular biological methods using the advantages of this model while the porcine system with its high electrical resistance and low sucrose permeability corresponding to the *in vivo* situation allows determination of permeability for pharmaceuticals. Both systems give a good basis for further physiological studies and the investigation of the pharmacokinetical background.

2 Introduction

The blood-brain barrier (BBB) provides both, anatomical and physiological protection for the central nervous system (CNS). The barrier strictly regulates the entry of substances, proteins and blood borne cells into the nervous tissue. Pharmacological treatment remains difficult for disorders of the central nervous system like Kreuzfeld-Jakob-Syndrom, Alzheimer and Multiple Scleroses due to poor drug passage across the blood-brain and the blood-cerebrospinal fluid barriers (Frick, 1965; Gardner, 1968; Spector and Johanson; 1989). The blood-brain barrier builds up a boundary between the blood and the brain interstitium and is morphologically based on endothelial cells lining the microvascular capillaries in the brain. The blood-cerebrospinal fluid barrier is mainly located in the choroid plexus separating the blood in the choroid plexus capillaries from the cerebrospinal fluid that fills the ventricles and cushions external surfaces of the brain. Both barriers provide a defined ionic environment for the brain and control strictly the passage of substances by restricted passive diffusion and by various transport phenomena like facilitated diffusion, active transport mechanisms, receptor mediated endocytosis and metabolism. On one hand these features provide the brain with nutrients and keep the homeostasis of the brain interstitium and on the other hand they prohibit the treatment of brain disorders with drugs. Thus, it is important to understand the regulation of the blood-brain barrier permeability as well as the transport mechanisms.

2.1 Barriers of the central nervous system

The brain, especially the neuronal signal transduction, is sensitive against infinitesimal changes in composition of the interstitial fluid. The signal transduction of neurons is mediated in two ways: the rapid propagation of electrical activity along the neuronal axons by modulation of the membrane potential mediated by voltage-gated Na^+ -channels and the transmission across the synaptic cleft with neurotransmitters regulated by voltage-gated Ca^{++} -channels (Alberts et al., 1998). Both processes require a stable chemical milieu of the interstitial fluid because changing its chemical composition would disturb the well regulated signal transduction (Bradbury, 1993). Furthermore, an unhindered entry of neurotoxic substances into the interstitial fluid would influence the chemical signal transduction within

the synaptic cleft (Abbott, 1992). Thus, the chemical environment of the brain parenchyma needs to be separated from the blood-stream. Furthermore, neurotoxins must be hindered from entering the brain, as neurons have to last a lifetime without replacement because they are terminally differentiated and are unable to divide (Alberts et al., 1994). The chemical composition of the blood, respectively, hormones, amino acids and ions fluctuates in the body especially after meals or bouts of exercises. If the brain is exposed to such fluctuations, the result might be uncontrolled nervous activity, since some hormones and amino acids serve as neurotransmitters. Especially potassium ions influence the threshold for the firing of nerve cells.

2.1.1 Historical background

The concept of a barrier system in the brain arose in the late 19th century. The bacteriologist Paul Ehrlich observed that certain dyes, administered intravenously to small animals, stained all of the organs except the brain tissue (Ehrlich, 1885). Ehrlich's interpretation of this observation was that the brain has a lower affinity for the applied dyes. Somewhat later, in 1898, Roux and Borrel observed that tetanus toxin injected into cerebrospinal fluid caused marked cerebral symptoms but when administered intravenously, produced no discernible cerebral effect in these animals (Roux, 1889). In 1913, Goldman injected the dye trypan blue directly into the cerebrospinal fluid of rabbits and dogs and found that the dye readily stained the whole brain but did not enter the bloodstream to stain the other organs. Thus, Goldman showed that the central nervous system is separated somehow from the blood by a barrier of some kind (Goldmann, 1913). His findings correlated with the other researchers (Roux, 1889, Lewandowsky, 1900) and these three investigators attributed their results to special permeability properties of small blood vessels in the brain. But the hypotheses that capillaries provide the anatomical base of the barrier properties was not confirmable in the early 20th century as no method was available to investigate the small ultrastructure of the blood vessels in the brain. With the development of electron microscopy, in the 1950's insights into the anatomical structures of the brain were provided. Today, detailed information about the cellular organization of the different permeability barriers of the central nervous system are available (Saunders et al., 1999).

2.1.2 Barrier systems in the mammalian brain

There are different structures in the brain which maintain the homeostasis of the brain interstitium: A large network of cerebral capillaries, which separates the bloodstream from the brain interstitial fluid and which is defined as the blood-brain barrier (BBB), an arachnoid membrane that covers the brain's outer surface and a highly vascularized choroid plexus (figure 2-1). The latter structures act as barriers between the blood and the cerebrospinal fluid (CSF) and are named blood-cerebrospinal-fluid barrier (BCSFB). While these two systems protect the central nervous system at its macroscopic border areas, the BBB controls the entry and exit of compounds within the brain and is mainly responsible for providing the brain with necessary nutrients. The choroid plexus produces the cerebrospinal fluid, which contains nutrients, ions and other essential molecules and which flows through the ventricular system, around the spinal chord, into the subarachnoid space surrounding the brain and drains back into the blood. Finally, the cerebrospinal fluid forms a protecting fluid layer around the brain that cushions bumps against the skull during abrupt movements and it provides the brain with nutrients and ions. As the cerebrospinal fluid freely exchanges substances with the interstitial fluid which surrounds the brain's neurons, the BCSFB must also keep toxic compounds out of the brain.

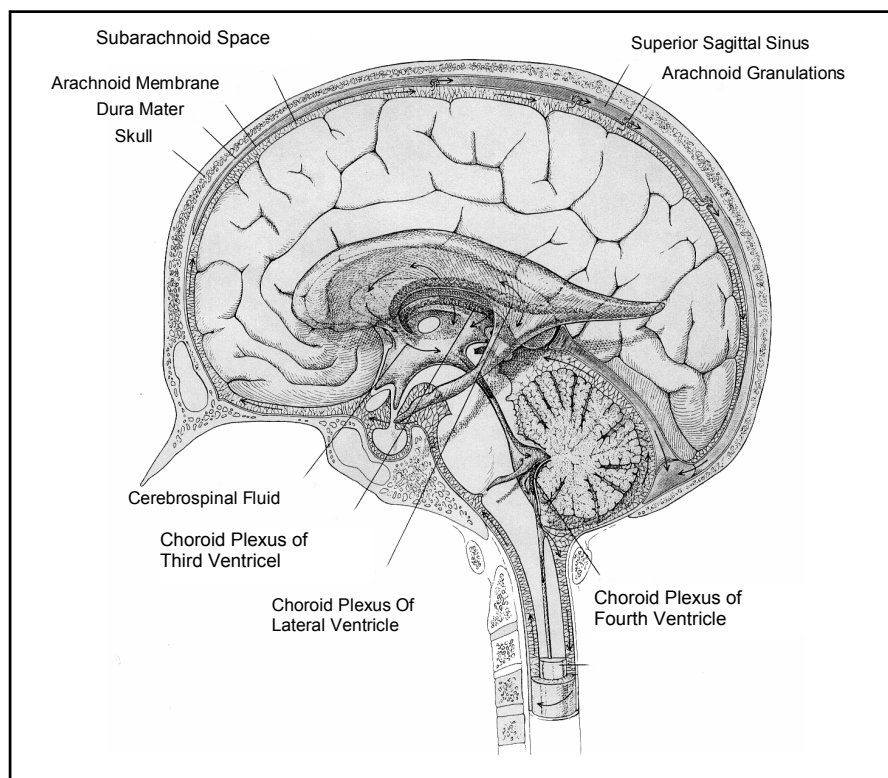


Figure 2-1: Schematic view of the mammalian brain. Overview about the ventricles of the choroid plexus. (Spector and Johanson, 1989)

While the subarachnoidal membrane is generally impermeable for water-soluble substances and its role in forming the BCSFB is largely passive, the choroid plexus, however, actively regulates concentrations of molecules in the CSF. According to that, the BCSFB-barrier is an active barrier. Different from the BBB the capillary epithelial cells in the choroid plexus are fenestrated (Keep and Jones, 1990). Here the surrounding epithelial cells are sealed together by intercellular junctions that impede the passage of even small water-soluble molecules between the blood and the CSF. Active transport systems provide an ion gradient across the epithelial cell layer which results in a net transport of NaCl and thereby induces an osmotically driven water flow into ventricles forming the CSF. Additionally, the CSF is enriched by active transport systems with substances derived from the blood which are essential for the brain, but only in a small amount, like vitamin C, folates, vitamin B6 and desoxiribonucleosides (Spector and Johanson, 1989).

2.2 Organization of the blood-brain barrier

Brightman and Reese (1969) were the first, who showed by electron microscopy, that the capillary endothelial cells are the anatomic structures of the blood-brain barrier. After injecting horseradish peroxidase into the blood stream, in most organs the enzyme penetrated the capillary wall through channels and gaps between adjacent endothelial cells or it was engulfed in pinocytotic vesicles. In the brain, the infiltration of peroxidase was stopped by the tight connection between adjacent endothelial cells. Later, Brightman and Reese injected horseradish peroxidase into one of the cerebral ventricles and observed that the enzyme was distributed in the extracellular space of the brain, but it was prevented from leaving the brain by the tightly joined endothelial cells (Brightman and Reese, 1969).

Figure 2-2 shows a micrograph of a cross-section of a brain capillary and adjacent glia cells. The capillary lumen (1) is completely surrounded by endothelial cells, which are inter- and intracellular connected with tight junctions. These junctions seal off the intercellular cleft against smallest molecules and actually convert the endothelial cell layer into a closed interface between the blood and the brain interstitium. At the abluminal (basolateral) side the cells are surrounded by a 100 – 150 nm thick basement membrane built up by extracellular matrix molecules (2). The main molecules are laminin A and B, fibronectins, collagen IV and proteoglycans (Krause et al., 1991). Embedded within this basement membrane the pericytes

are localized (3). Different from smooth muscle cells of the larger vessels, the pericytes are not assembled in capillaries but their cell bodies are orientated parallel to the capillary while its long processes extend around the capillary (Shepro and Morel, 1993). Their exact function is unclear, but experimental evidence indicates that they influence cell proliferation (Balabanov and Dore-Duffy, 1998; Orlidge and D'amee, 1987) and play a role in phagocytotic procedures of neuronal immune defence (Balabanov and Dore-Duffy, 1998) or other transport processes (Krause et al., 1991; Sims, 1986). And finally they participate in endothelial differentiation (Balabanov and Dore-Duffy, 1998). The brain capillary is separated from the surrounding tissue by the so-called *Membrana limitans gliae perivascularis*, which consists of the astrocytic end feet (4). The astrocytic end feet cover 99% of the surface of the capillaries and form cell-cell contacts to the surrounding neurons (Pardridge, 1993). They ensure a rapid recovery of the resting membrane potential of the neurons by uptake of potassium ions directly after an action potential was triggered (Hertz, 1989). Furthermore, it is controversially discussed, if astrocytes play an important role in the induction of the blood-brain barrier phenotype (Holash et al., 1993; Minakawa et al., 1991; Stewart and Wiley, 1981; Svendgaard et al., 1975).

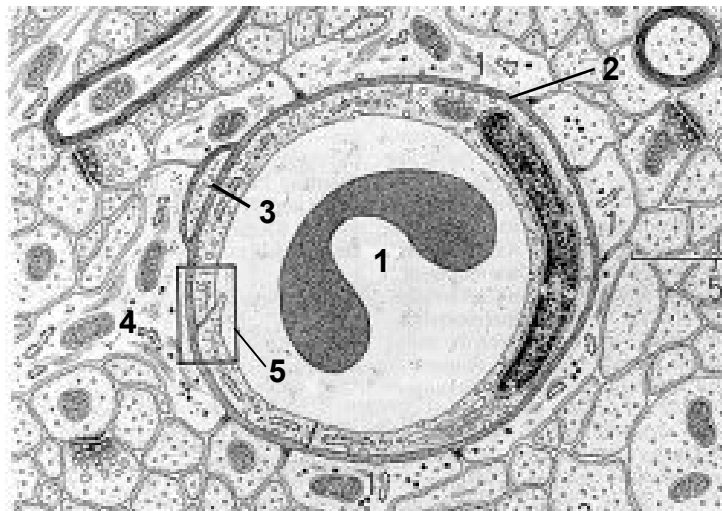


Figure 2-2: Micrograph of a cross-section of a brain capillary (Krstic, 1988).
(1) lumen with erythrocyte; (2) basal lamina; (3) pericyte; (4) astrocytic end foot; (5) tight junctions.

2.2.1 Cell-cell contacts between brain capillary endothelial cells

The brain capillary endothelial cells form a single layer and a continuous interface between the blood and the interstitial fluid. So they form a “belt-like” structure that inhibits passive diffusion and unspecific passage of compounds to the brain. The structural features of the cells are responsible for these properties of the whole capillary. The single cells form neither pores nor fenestrations. Additionally, the number of vesicles is much lower than in other capillaries like for instance in muscles (Betz, 1886). Three major functions are implicated in the term blood-brain barrier: First, the protection of the brain from the blood milieu as achieved by complex *tight junctions*. Second, the selective transport by specialised transport systems either to provide the brain with necessary nutrients or to remove metabolites and finally, the metabolism or modification of blood- or brain-borne substances.

The apparently most interesting structural attribute of the blood-brain barrier are the so called tight junctional complexes (figure 2-3). They are the molecular basis of the blood-brain barrier and form a continuous belt around the cells and seal the paracellular cleft between the cells (Reese and Karnovsky, 1967). In electron micrographs of freeze fracture replicas, the tight junctions appear as a network of small ridges on one side, and complementary grooves on the opposite side (Dermietzel, 1975; Nico et al., 1992). The molecular structure of the tight junctions is still not completely clarified, but there is unequivocal evidence for a lipidic and proteinaceous nature of these structures.

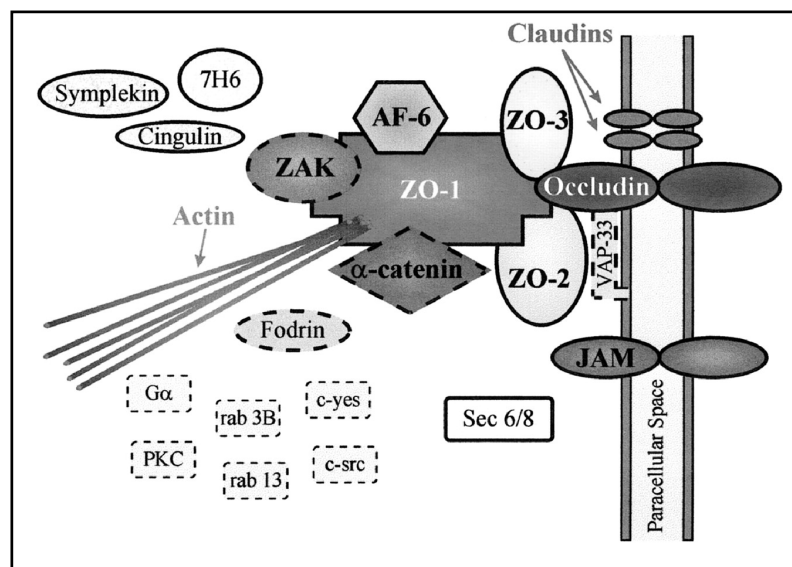


Figure 2-3: Molecular structure of the tight junctions. The cellular cleft is sealed with the transmembrane proteins occludin and different claudins. Directly associated is ZO-1 which belongs to the family of membrane-associated guanylate kinases (MAGUK). The tight junctional zone is linked to the cytoskeletal elements (actin stress fibres). Figure taken from (Fanning et al., 1999).

Following the lipidic model of Kachar and Reese, the exoplasmatic membrane-domains of the lipid bilayer of two adjacent cells fuse. As a consequence of this, a continuous lipid-layer at the apical part of the junctions is formed. The tight junction strands are formed by lipidic cylinders in which lipids are arranged in inverted micelles (Grebenkamper and Galla, 1994; Hein et al., 1992; Kachar and Reese, 1982). The protein model is based on transmembrane proteins located at the cell-cell contacts. The proteins span the intercellular cleft and are connected extracellularly by non-covalent protein-protein interactions (van Meer et al., 1986; van Meer and Simons, 1986). The participation of the transmembrane proteins occludin (Furuse et al., 1993), different transmembrane proteins from the family of claudins (Furuse et al., 1998) as well as the cytosolic peripheral membrane proteins Zonula Occludens-protein-1 (ZO-1) (Stevenson et al., 1986), ZO-2 (Jesaitis and Goodenough, 1994) and ZO-3 (p130) (Anderson et al., 1993; Haskins et al., 1998) is generally expected. The proteins cingulin (Citi et al., 1989) and 7H6 antigen (Zhong et al., 1993) seem to be associated to the *tight junctions* as well. One model which proposes a combined lipid and protein model was published by Wegener and Galla (Wegener and Galla, 1996). In this model the proteins are responsible for the formation of inverse micellar structures within the tight junction strands. Wolburg (2000) has suggested that the P-face association of tight junction particles in electron micrographs from freeze fracture micrographs is an indicator of a functional barrier (Kniesel and Wolburg 2000; Wolburg et al., 1994). Besides these morphological investigations, substantial data implies that the phosphorylation state of the junctional proteins is involved in the restricted permeability characteristics in brain capillary endothelial cells rather than the quantity of the proteins (Kniesel and Wolburg, 2000; Rubin and Staddon, 1999).

2.2.2 Selective transport functions of capillary endothelial cells

As the tight junctions seal the paracellular cleft of adjacent brain capillary endothelial cells, each transfer of compounds across the brain endothelium has to be transcellular. There are several essential transfer mechanisms which stabilise the interstitial brain environment as well as supply the brain with adequate important nutrients. The most decisive factor for passive diffusion across the blood-brain barrier is the lipophilic solubility, which enables the molecules to dissolve into and pass through the lipidic core of the cell membranes. What happens inside of the predominantly aqueous interior of the cell is unclear but presumably such lipid-soluble molecules are able to leave the cytoplasm at the other side of the cell along

the concentration gradient to reach the interior of the brain. Several studies have shown a clear correlation between the octanol/water partition coefficient and penetration into the brain, as long as the regarded compound is not a substrate for any specific transport system (Levin, 1980; Lohmann et al., 2002; Pardridge, 1993). Apart from the lipid solubility, the molecular size is another key factor that determines the penetration of a molecule into the CNS (Abraham et al., 1994; Habgood et al., 2000; Habgood et al., 1999).

D-glucose, the main source of energy for the brain, enters the brain via facilitated diffusion. In the brain the glucose transport via the GLUT-1 protein (Crone, 1965) is highly stereospecific for D-glucose (Johansson, 1990) and directed from a region of high concentration (blood) to a lower concentration (brain). In such movement, the gradient provides the energy source for transport and the carriers merely facilitate the diffusion. Without the carriers, transport would occur more slowly. The stereospecific transport of large amino acids, required for the synthesis of neurotransmitters and proteins, occurs the same way with specific transporters (Oldendorf and Szabo, 1976).

Other systems transport substances actively against their concentration gradient across the blood-brain barrier endothelium. These transport processes require external energy. For instance the small neutral amino acid transporter is distributed in the abluminal membrane to ensure that those acids can be transported out of the brain into the endothelial cell (Goldstein and Betz, 1986). These transporters protect the CNS from glycine or GABA, for instance, which act as neurotransmitters (Dermietzel and Krause, 1991). In the case of glycine, the inward movement is coupled to the sodium gradient to provide the needed energy.

Some substances are transported from the blood to the brain interstitium by receptor-mediated endocytoses. Brightman (1989) found receptors for insulin present in the luminal membrane of brain capillaries, but it is still unclear whether insulin is degraded within the endothelial cells or transported into the brain (Brightman, 1989). Another active carrier system is the receptor mediated transport protein transferrin which ensures the supply with ferrum. The luminal membrane localised transferrin receptor presumably releases ferrum after internalising transferrin as Fe^{2+} or a low molecular complex across the abluminal membrane to the brain interstitium (Bradbury, 1993).

Another system of protection is a transport system which carries lipophilic substances out of the endothelial cells and is incorporated into the plasma membrane. This system, called the Multi-Drug Resistance-System, consists of different transport proteins like P-glycoprotein

(Pgp) (Cordon-Cardo et al., 1989; Schinkel et al., 1994) and the brain multidrug resistance protein (BMDP) (Eisenblatter and Galla, 2002). These proteins belong to a group of ABC-transporters protecting the brain by active transport of toxic substances provided with energy by ATP.

2.2.3 Metabolic elements of the blood-brain barrier

The combination of permeable barriers and selective transport mechanisms is not the only means of the blood-brain barrier to prevent the brain from uncontrolled chemical fluctuations within the interstitial fluid. Compounds that enter the endothelial cells either due to their lipophilic nature or to their affinity to one of the transport proteins can be converted by metabolic processes into a chemical compound incapable of traversing the abluminal membrane. For example, 4-hydroxy-tryptophane and L-dopa are carried by the L-system of amino acid transporters to the cytosol of the endothelial cells. An uncontrolled passage across the abluminal membrane would be dangerous because these compounds are precursors of the neurotransmitter serotonin and dopamine. Once in the endothelium, these substances are converted to dopamine and dihydroxyphenylacetic acid (DOPAC) and cannot cross the luminal membrane into the brain. This phenomenon, which is found for a lot of compounds (Goldstein and Betz, 1986; Greig 1992; Johansson, 1990; Vorbrodt, 1988) is called the metabolic blood-brain barrier.

2.3 *In vitro* models of the blood-brain barrier

There has been considerable interest in establishing blood-brain barrier cell culture models. The original reason was to set up an assay system for pharmacological studies to predict drug penetration across the blood-brain barrier. Examinations on cell cultures are better represented and more reproducible. Larger quantities of cell populations are accessible in *in vitro* studies as well as working with cell culture models avoids animal experimentation. Another major reason has been to understand the modulation of barrier properties and the phenotypical characteristics of isolated capillary endothelial cells. In culture, numerous structural and functional properties of capillary endothelial cells, including junctional tightness, rate of

endocytosis and presence of specific transporters, can be assayed reproducibly. Cell culture is also an excellent tool to investigate pathological disorders affiliated to the blood-brain barrier, such as brain tumours, Alzheimer's disease, Multiple Sclerosis and AIDS-associated syndromes. Using the cell culture also gives an advantage in analysing transmigration processes in inflammatory states of the endothelial cells or blood-brain barrier dysfunction caused by the Malaria pathogen *Plasmodium falciparum* (Brown et al., 1999). Information from pharmacological, physiological and pathological investigations could accelerate the development of new pharmaceuticals and novel drug delivery strategies. The major goal is the derivation of microvascular endothelial cell-cultures which express the blood-brain barrier phenotype. Therefore, it is necessary to identify common features of endothelial cells from large vessels and of cerebral microvascular endothelium to clarify, to what extent cultured cells are differentiated. Common endothelial features are listed in table 2-1.

Table 2-1: Common Features of Endothelial Cells (Deli and Joo, 1996)

| Characteristics | Authors |
|--|--|
| Presence of General Endothelial Markers | |
| Factor VII-related antigene | (Phillips et al., 1979a) |
| Alkaline phosphatase | (Bowman et al., 1981a; Karnushina et al., 1980b) |
| Specific binding of lectins | (Diglio et al., 1982) |
| Uptake of acetylated LDL | (Krause et al., 1982; Tontsch and Bauer, 1989) |
| Active Arachidonic Acid Metabolism | |
| Presence of cyclooxygenase | (Gecse et al., 1982; Gerritsen et al., 1980; Gesce et al., 1981; Goehlert et al., 1981; Maurer et al., 1980) |
| Presence of lipooxygenase | (Moore et al.; 1988a; Moore et al., 1988b) |
| Prostacycline synthesis | (Chamoux et al.; 1991; Marceau et al., 1989; Rosenthal and Jones, 1988) |
| Reactive Second Messenger Systems | |
| Adenylate cyclase | (Baranczyk-Kuzma et al., 1992; Joo et al., 1975; Joo and Toth, 1975; Palmer et al., 1980a; Palmer et al., 1980b) |
| Guanylate cyclase | (Homayoun et al., 1989; Joo et al., 1983; Karnushina et al., 1980a; Nakane et al., 1983) |
| Protein kinase C | (Catalan et al., 1989; Hanson-Painton et al., 1993; Krizbai et al., 1995; Markovac and Goldstein, 1988) |
| Calcium/calmodulin-dependent protein kinase II | |
| Synthesis and Secretion of Vasoactive Substances | (Deli et al., 1993) |
| Nitric oxide | (Durieu-Trautmann et al. 1993; Morin and Stanboli 1993) |
| Endothelin | (Bacic et al., 1992) |
| Angiotensin II | (Gimbrone et al., 1979) |

The distinguishable features of cerebral microvascular endothelial cells from other endothelium are the presence of tight interendothelial junctions, the paucity of pinocytotic activity (Brightman and Reese 1969, Joo 1971), high number of mitochondria (Oldendorf et

al., 1977), the absence of fenestrations (Stewart et al., 1994) and expression of specific marker enzymes like transferrin receptors (Jefferies et al., 1984) and γ -glutamyltranspeptidase (Orlowski et al., 1974). However, among the variety of specialised properties, the most important one is an efficient endothelial barrier function with a low paracellular permeability, which can easily be probed by monitoring the passage of small solutes (e.g. sucrose or inulin) across the cellular monolayer. Often used tracer methods, however, have a rather limited time resolution and tight junction complexity and barrier function is most sensitively and readily quantified by the measurement of the transendothelial electrical resistance (Schneeberger and Lynch, 1992).

2.3.1 Primary cultures of brain capillary endothelial cells

In 1978, Panula and coworker demonstrated that isolated rat brain microvessel endothelial cells could be kept in culture (Panula et al., 1978). Today, most research groups use a primary culture of brain capillary endothelial cells (Audus et al., 1996) derived from rat (Abbott et al., 1992a, Barrand et al., 1995), dog (Speth and Harik 1985) cow (Audus and Borchardt 1987, Cecchelli et al., 1999, Dehouck et al., 1990; Meresse et al., 1989, Rubin et al., 1991), pig (Mischek et al., 1989; Hoheisel, 1998), primate (Shi and Audus, 1994) or human brain (Stanimirovic et al., 1996) (see also table 2-2). In general, the brain tissue is either enzymatically or mechanically dispersed followed by filtration and centrifugation steps. The cultured cells evince the typical properties of microvascular endothelial cells which include the typical protein pattern, attenuated pinocytosis, lack of fenestrations and tight junctions (Audus and Borchardt, 1986; Audus and Borchardt, 1987; Bowman et al., 1983). However, the isolation of pure endothelial cells, as a blood-brain barrier model, is fraught with a number of problems. Even though there have been improvements in techniques for isolation and growth of the cells, the process is still time consuming, labour intense and expensive. Isolating primary endothelial cells is prone to preparation variations, the cells are fastidious in their growth requirements and they have a limited life and utility span. Furthermore, very often cells de-differentiate *in vitro*. These facts lead to the difficulties in comparing results from experiments with different cell preparations or passages.

2.3.2 Cell lines as *in vitro* models of the blood-brain barrier

An alternative approach is the cultivation and investigation of immortalised brain capillary endothelial cells which would represent a significant progress in this area as long as they can be shown to maintain their barrier properties and characteristics. Higher reproducibility, more homogeneity, the ease of propagation, a short population doubling time and the lack of exogenous growth requirements motivate researchers to develop cell lines derived from rat (Durieu-Trautmann et al., 1991; Greenwood et al., 1996, Lechardeur et al., 1995, Roux et al., 1994, Tan et al., 2001; Trautmann et al., 1993) bovine (t-BBEC-117; (Sobue et al., 1999); (Stins et al., 1997), porcine (PBMEC/C1-2; (Teifel and Friedl, 1996) and human brain microvessels (SV-HCEC) (Muruganandam et al., 1997). There are several alternatives to immortalise the isolated endothelial cells. Exposing to radiation causes random modification in the genome which can lead to an immortalisation of cells. Culturing these clones followed by a characterisation of the cell's properties can lead to a blood-brain barrier related cell line. Other prevalent methods are transfection with SV40 thermosensitive large T gene (Lechardeur et al., 1995), viral oncogenic immortalization with polyoma virus early genes (Robinson et al., 1986), Rous sarcoma virus E1A gene (Roux et al., 1994) or SV40 early genes (Durieu-Trautmann et al., 1991; Tatsuta et al., 1992). However, to date, none of these immortalised cell lines express all of the features necessary for an entirely useful blood-brain barrier model in a consistent fashion. There have been attempts to induce the blood-brain barrier differentiation in endothelial cell lines (Lechardeur et al., 1995) but no cell line expresses all features of a reliable blood-brain barrier *in vitro* model. This is particularly evident for measuring the barrier function and integrity by transendothelial resistance. Some cerebral endothelial cell lines have been shown to restrict the passage of macromolecules and have been used in studies of paracellular permeability. None of them have been shown to consistently express a transendothelial resistance that is comparable to blood brain barrier *in vivo* situation.

To overcome this problem several attempts have been made to reinduce blood-brain barrier properties in endothelial cells (cell lines and primary cultures of endothelial cells) by co-culturing them with astrocytes or glioma cells (Gaillard et al., 2000; Gaillard et al., 2001; Hurst and Fritz, 1996; Rubin et al., 1991) or brain-derived factors (table 2-2). There is substantial evidence that the establishment and maintenance of the unique cerebral endothelial cell phenotype results from the neuronal milieu especially specific interactions provided by astrocytic foot processes which surround the brain microvessels (Dermietzel and Krause,

1991; Janzer and Raff, 1987; Stewart and Wiley, 1981). Furthermore, numerous studies have utilised conditioned medium generated from cultures of rat brain astrocytes or C6-glioma cells and found that induction does not require direct cell-cell interactions (Cancilla et al., 1993; Dehouck et al., 1994; Hurst and Fritz, 1996; Igarashi et al., 1999; Ramsohoye and Fritz, 1998; Raub, 1996; Rist et al., 1997; Rubin et al., 1991). However, neither cocultures with astrocytes, nor addition of astrocytic conditioned medium provide endothelial cell monolayers with such low sucrose permeability properties found *in vivo*.

Table 2-2: Effects of compounds on different blood-brain barrier models *in vitro* (modified from Beuckmann and Galla, 1998)

| Species and cell type | Influencing factor | Effects on |
|--------------------------------|--|--|
| Bovine bcec subcultured | A | Tight junctions |
| Bovine bcec | ACM, cAMP | TEER, P ^{sucrose} |
| Bovine bcec | Forskolin, phorbol esters, A, ACM | Tight junctions, TEER, P ^{inulin} |
| Bovine bcec 3. passage | A-CCM | TEER, GGT, P ^{sucrose} , P ^{inulin} |
| Human umbilical vein EC | A-CCM, ACM | ALP, tight junctions |
| Bovine bcec | C6, astrocytoma-CM | TEER, P ^{sucrose} , P ^{dextran} , P ^{peg} , GGT |
| Bovine bcec cloned | C6-PM | GGT, NaK-ATPase |
| Bovine bcec cloned | C6, C6-PM, neuron PM | GGT, NaK-ATPase |
| Bovine bcec primary | A, C6 | ALP, GGT |
| Bovine bcec primary | ACM, C6-CM | GLUT-1 |
| Human bcec | A | Butury-choline esterase |
| Porcine bcec primary | HC | TEER, P ^{sucrose} , protein patterns, P-glycoprotein, capillary-like structures |
| Porcine bcec primary | A, C6 | ALP, GGT |
| Porcine and murine bcec cloned | Heparin, ECGF | Protein patterns |
| Canine bcec | - | GLUT-I |
| Bovine bcec cell line | Bovine brain homogenate, TNF- α | GLUT-I, actin |
| Bovine bcec cloned | A-CCM | LDL-binding |
| Porcine bcec primary | A, C6, NB, PE | ALP |
| Calf artery EC | ACM, interleukin-6 | ALP |
| RAT bcec immortal | All- <i>trans</i> -retinoic acid | GGT, P-glycoprotein |
| Porcine bcec primary | cAMP | ALP |
| Rat bcec immortal | APM, C6-PM, C6-CM, A-CCM | Capillary-like structures |
| Mouse bcec immortal | C6 | |
| Mouse bcec | ACM | Glucose uptake |
| Bovine retinal capillary EC | A, C6 | Capillary-like structures |
| Bovine retinal capillary EC | Steroids, C6 | Capillary-like structures |

Abbreviations: A, astrocyte; ALP, alkaline phosphatase; bcec, brain capillary endothelial cells; C6, C6-glioma; CCM, continuously conditioned medium; CM, conditioned medium; EC, endothelial cells, GF, growth factor; GGT, γ -glutamyltranspeptidase; HC, hydrocortisone; NB, neuroblastome; PE, plexus epithelium; peg, polyethyleneglycol; PM, plasma membranes; TEER, transendothelial electrical resistance; TNF, tumor necrosis factor.

Therefore, other approaches have been made to achieve high transendothelial electrical resistance within the cell culture. Cyclic Adenosin-3',5'-monophosphate (cAMP) is a compound commonly discussed in correlation with modulation of tight junctional complexes. It influences cell-proliferation (Davison and Karasek, 1981) and morphology (Antonov et al., 1986) of endothelial cells. cAMP is a second messenger and is produced by adenylatcyclase from adenosintriphosphate (ATP). Proteinkinase A is induced by cAMP and is able to induce a signal transduction cascade by phosphorylation of serin- or threonin residues of catalytic subunits of different proteins. For instance, (Rubin et al., 1991) found that elevation levels in the brain endothelial cells produce a striking increase in tight junction resistance and structural changes consistent with inducing high-resistance junctional complexes. Supplementation of the medium with physiological amounts of the glucocorticoid steroid hydrocortisone (550nM) and the withdrawal of serum, Franke et al., have established a cell culture model of porcine capillary endothelial cells (Franke et al., 2000; Franke et al., 1999; Hoheisel et al., 1998c) that closely mimics the *in vivo* blood-brain barrier phenotype. For the first time, a cell culture model was available with transendothelial resistance of more than $1000 \Omega\text{cm}^2$ and up to $2000 \Omega\text{cm}^2$ measured in brain capillaries *in vivo* (Crone and Olesen, 1982).

The paracellular permeability of ^{14}C -sucrose, $5 \cdot 10^{-7} \text{ cm/s}$, has also been shown to be similar to the measured *in vivo* value (Levin, 1980). The expression of tight junction proteins was confirmed by both, northern blot analysis and immunocytochemistry (Eisenblätter et al., 2001; Nitz et al., 2001). Even P-glycoprotein has been proven to be expressed (Ferber, 2000). Thus, a cell culture model has been developed with fully differentiated brain capillary endothelial cells well suited to study physiology, pharmacology and pathology of the blood brain barrier (Franke et al., 2000; Hoheisel et al., 1998a).

2.4 Regulation of blood brain barrier properties: Hormones

Regulation of the tight junctions is a dynamic process determined by several cellular and metabolic factors (Anderson et al., 1993; Citi, 1993; Madara, 1988) including calcium, phorbolic esters, members of the insulin-like growth factor-I family (Buse et al., 1995a) and glucocorticoids. As mentioned in section 2.3.2 glucocorticoids influence the barrier properties of cultured brain microvessel endothelial cells derived from pig. Buse et al (Buse et al.,

1995b) determined that the synthetic glucocorticoid dexamethasone effects the formation of *tight junctions*. Singer et al. (1994) have shown that dexamethasone increases the ZO-1 expression but the effects that cause a drastic increase of transendothelial resistance are still unknown (Singer et al., 1994). Hydrocortisone does not influence tight junction proteins on RNA-, nor on protein-level. While it is known that extracellular matrix compounds play an important role during formation of the blood-brain barrier properties, newer results imply that MMPs are involved in barrier-forming processes (Alexander and Elrod, 2002; Lohmann, 2003).

During evolution, three major systems were established to control and adjust the function of the organs, tissues and cells of organisms: the nervous system, the immune system and the hormonal system. While the neuronal information is very fast and able to transfer information within parts of a second, the hormonal communication last between a few seconds and several minutes. The latter is mainly responsible for adjustment of the whole organism. Hormones are chemically very diverse compounds which are produced usually from specific anatomically defined cells and tissues assembled in so called glands. They are secreted to the blood and cause specific metabolic processes in their effector organs.

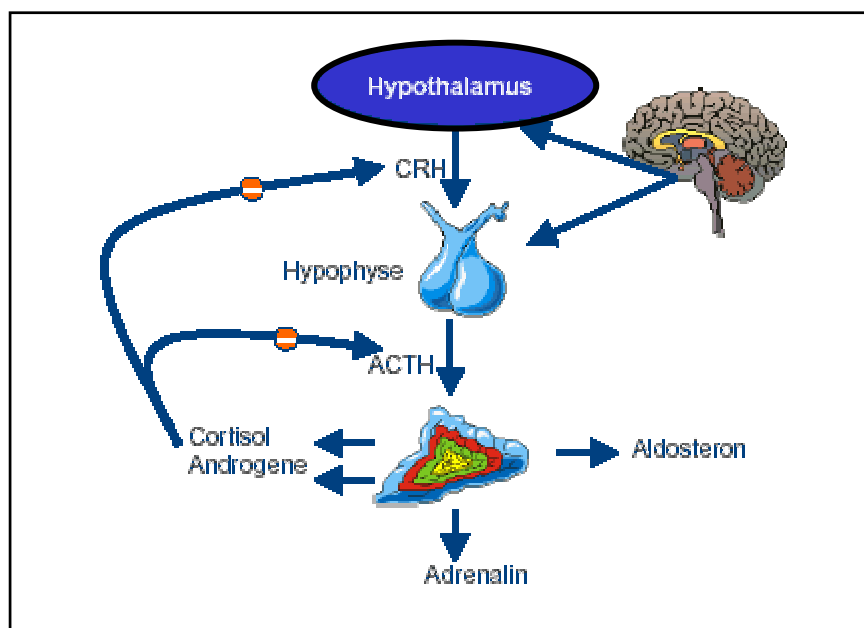


Figure 2-4: Regulation of glucocorticoid secretion. The Hypothalamus is not only addicted from the information of the CNS but underlies a feedback-control by HC. After processing all incoming data, the neuronal cells in the hypothalamus release neurosecretoric hormones, either corticoliberin (activating) or corticostatin (inactivating). These hormones are affecting an appropriate signal in the hypophysis and either inhibit or elevate the secretion of glandiotrope hormones within the hypophysis. The glandiotrope hormones attain the adrenal cortex via blood-stream and stimulate the biosyntheses and secretion of glucocorticoids respectively mineralcorticoids. The glucocorticoid hydrocortisone regulates the hierarchical upstream lying glands by feedback-inhibition. This leads to a sensitive regulation of hydrocortisone concentration and is influenced at the same time by several factors. CRH: corticotrophin-releasing hormone; ACTH: adrenocorticotropic hormone

Classifying hormone action is very difficult due to their varying chemical structures and functions. Most of them cause a signal transduction cascade within the cell mediated by specific receptors beginning with a *second messenger* signal or act like a transcription factor by binding to an intracellular receptor. Although the concentration of hormones is frequently low, it fluctuates depending on physical state, intrinsic rhythm and physiological conditions. It is strictly controlled within the organism and can be effected by the rate of secretion and activation. The activity of several glands is regulated by hormonal control mechanisms, which are shown for the hypophyses-hypothalamus system in figure 2-4.

Hydrocortisone is the main glucocorticoid hormone and belongs to a group of lipophilic C_{21} -steroidhormones. It is synthesised in the adrenal cortex from the hormone progesterone (Stryer, 1996). The concentration in the blood is strictly controlled by the hypophysis-hypothalamus system and varies between 70 and 550 nM. Hydrocortisone enters the cells by passing from the blood across the cell membrane to the cytoplasm. There it binds to glucocorticoid receptors (GR) and constitutes a receptor-hormone complex. The receptor is expressed in two isoforms called GR α and GR β . The correlated 95 and 90 kDa proteins are encoded by one gene (Encio and Detera-Wadleigh, 1991) and are generated by alternative splicing from exon 9 (figure 2-5). The 5' terminal part of the gene encodes the specific sequence

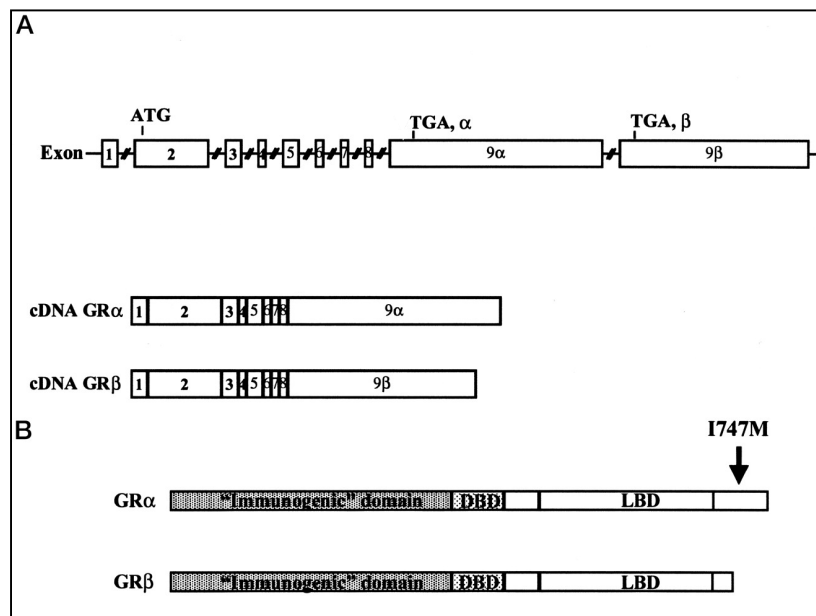


Figure 2-5: A: Schematic representation of the human GR gene and the alternatively spliced cDNAs encoding the α and β isoforms of this receptor. B: Functional domains of the GR. Functional domains and subdomains are indicated. *DBD*: DNA-binding domain (Encio and Detera-Wadleigh, 1991).

for the α -isoform while the 3'-terminal part contains the information for the β -isoform (Oakley et al., 1999). The glucocorticoid receptors are associated with heat-shock proteins (HSP 90 and HSP 59) (Gehring 1993; Rexin et al., 1988). After binding, the heat shock proteins are released by the glucocorticoid receptors and the cytoplasmic glucocorticoid-receptor complex dimerises (figure 2-6). The proteins then translocate to the nucleus where it regulates transcription by binding to glucocorticoid response elements. The zinc-finger-motive mediated interaction with the glucocorticoid-response elements of an enhancer-region of a gene either enhances or reduces the gene-expression (Eggert et al., 1995). The response to the signal can vary and depends on the affected organ. The primary cause is an induction of tissue-specific enzyme expression. The second effect is determined by the induced enzymes. A common effect of hydrocortisone is an influence on the glucose metabolism, which is directed to gluconeogenesis. Furthermore, it inhibits the peripheral utilisation of glucose and has a catabolic effect on the protein metabolism, which entails an immunosuppressive effect caused by the reduced production of antibodies.

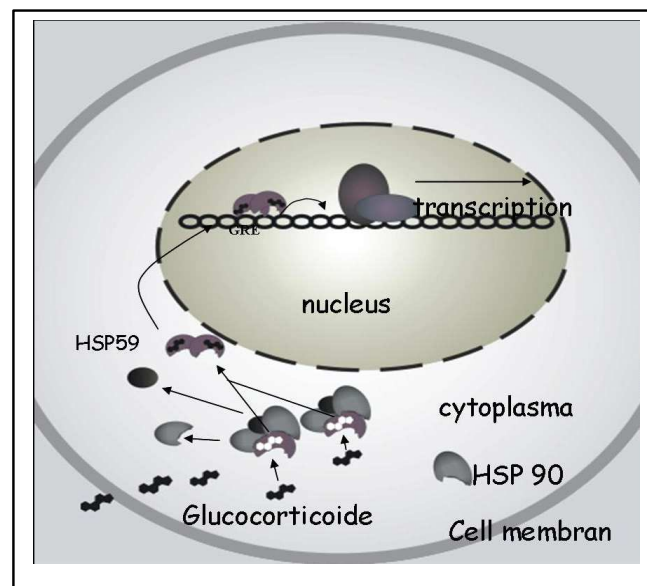


Figure 2-6: Signal transduction pathway of glucocorticoids. The lipophilic molecules penetrate the membrane and bind to cytoplasmic localised GR associated with heat-shock proteins (HSP). After release of the HSP two receptor-ligand complexes dimerise and translocates to the nucleus.

2.5 Objectives of the project

Many attempts have been made to establish *in vitro* blood-brain barrier model systems that closely mimic the *in vivo* situation (section 2.3.1). Primary cultures of brain capillary endothelial cells are reliable models to investigate blood-brain barrier phenomena. In our group a culture system of porcine derived endothelial cells was established which is defined by high TEER and low sucrose permeability (Hoheisel et al., 1998b). This model is well characterised and based on serum-free medium supplemented with hydrocortisone in a physiological concentration. In order to investigate if hydrocortisone is able to induce similar effects in other mammalian cell systems, the main goal of this work was to establish a murine brain capillary endothelial cell (MBCEC) culture system comparable to the porcine system. After characterisation of this MBCEC primary culture, effects of hydrocortisone should be investigated. Furthermore, a blood-brain barrier model system based on murine derived cells gives better access to molecular biological works due to access to the mouse genome data. This allows using sequence data to apply modern methods like small interfering RNA-methods or the investigation of knock-out mice for further experiments. Furthermore, antibodies against mouse-proteins are easily available and finally, a lot of groups work with murine model systems. For this reason, received data can be compared to results within the same species. A murine *in vitro* model of the blood-brain barrier is thus highly demanded.

3 Experimental

3.1 Cell biology

All working procedures concerning the cell culture experiments including the handling and sterilisation of pipettes and buffers were applied as described by Freshney to minimize the risk of contaminations (Freshney, 2000).

Cell culture work was exclusively performed in a laminar-flow hood with sterile equipment, solutions and media. For cell plating, culture flasks (75 cm²), petri dishes (10 cm² and 28 cm²), 8-well electrodes and 8-well plates were used. The cells were cultured at 37°C in a water saturated atmosphere with 5% (v/v) CO₂.

3.1.1 Primary culture of murine brain capillary endothelial cells (MBCEC)

Preparation: The isolation of murine brain capillary endothelial cells from 6-10 weeks old mice (C57BL6/J) was performed as described by (Deli et al., 2003) and modified in our lab.

The mice were sacrificed with cervical dislocation. The head was rinsed in 70% (v/v) ethanol and the mice were decapitated with a pair of scissors. After fixing the head, the skin was cut from the neck to the forehead. The cranium was opened with a sagittal incision and the forebrain removed with forceps. The forebrain was transferred into ice-cold PBS containing the antibiotics penicillin (200 U/ml) and streptomycin (200 U/ml). Fresh storage buffer was applied under the laminar-flow hood. Secretoric and non-cortical parts of the brain were removed and the brains were cut into halves. The meninges were removed by spreading and gently rolling the hemispheres on Whatman paper. Visible vessels were removed and the brain was stored until usage in ice-cold DMEM. The grey and white matter consisting of the cerebral tissue was then cut with scalpels, the pieces were homogenised with forceps and transferred into a tube and supplemented with 13.5 ml DMEM. After mechanical homogenization by pipetting up and down at least 25 times until complete homogenization 1.0 ml Collagenase (CLS2 10 mg/ml) and 200 µl DNase I (1 mg/ml) were added. The homogenate was mixed thoroughly and incubated in a shaker for 1 h at 37°C. To isolate the released capillaries the suspension was mixed with 10 ml DMEM and centrifuged (20°C,

1000 x g, 10 min). The supernatant was discarded and the pellet was thoroughly resuspended in 25 ml 25% (w/v) BSA/DMEM. This suspension was centrifuged (4°C, 1000 x g, 20 min, swing-out bucket rotor). Both supernatant phases were discarded and the pellet containing the capillaries was resuspended in 9 ml DMEM. The second digest with 1 ml collagenase/dispase (10 mg/ml) and 100 µl DNaseI (1 mg/ml) was performed like the first digestion step. After complete digest the cell suspension was mixed with 10 ml DMEM and the mixture was centrifuged (20°C, 700 x g, 8 min). The supernatant was discarded and the pellet thoroughly resuspended in 2 ml DMEM. The suspension was carefully applied on the top of a percoll-gradient and centrifuged (4°C, 1000 x g, 10 min, swing-out bucket rotor). The white-colored interphase containing the digested capillaries was aspirated with a syringe-attached long needle and diluted in 10 ml DMEM avoiding contact with the red-colored interphase containing red blood cells, pericytes and astrocytes. After the following centrifugation (20°C, 1000 x g, 10 min) the pellet was resuspended in DMEM, again centrifuged (20°C, 700 x g, 8 min) and resuspended in mouse plating medium. The isolated capillaries were plated on a total of 3 to 4 cm²/brain in plating medium on collagenIV/fibronectin-coated petri dishes.

Culturing. One day after the isolation of capillaries the medium was substituted with fresh plating medium. Two days after the preparation the plating medium was removed and the cells were cultivated in mouse culture medium.

Passage of cells. After reaching 80% of confluence the cells were subcultured. First, cells were washed twice with PBS and detached from their substrate with trypsin solution (0.25% w/v) at room temperature. For complete detachment of cells the trypsin solution was carefully pipetted over the cell layer. The displacement of the cells was followed by inverse microscopy and trypsin digestion was stopped by addition of serum-containing medium as soon as cell-detachment was completed. The cell suspension was centrifuged (20°C, 140 x g, 10 min). Cells were resuspended in plating medium and plated on either collagen-G coated 8-well ECIS-electrodes (*AP-Biophysics*), 8-well chamber slides (*LabTeq, NUNC*) or alternatively on rat tail collagen coated microporous polycarbonate filter membranes (0.4 µm pore size, 1.13 cm² or 0.33 cm² growth area; TranswellTM No. 3401 and 4312, Costar[®]) with a density of 220,000 cells/cm².

Exchange of media. Two days after the passage the medium was replaced by serum-free medium supplemented either with or without hydrocortisone. Alternatively, cells were

cultured in serum-containing medium. The cells were cultured for one or two more days to assure that they had reached confluence until they were used for histological investigations, TEER determination or permeability studies.

| | | |
|----------------------|----------|--------------------------------------|
| PBS | 140 mM | NaCl |
| | 2.7 mM | KCl |
| | 8.1 mM | Na ₂ HPO ₄ |
| | 1.5 mM | KH ₂ PO ₄ |
| PBS ⁺⁺ | | PBS |
| | 0.5 mM | MgCl ₂ |
| | 0.9 mM | CaCl ₂ |
| mouse culutre medium | 20 ml | plasma derived serum (PDS) |
| | 1 ng/ml | bFGF |
| | 80 ml | DMEM |
| | 1 µg/ml | heparin |
| | 1% (v/v) | gentamycin |
| | 0.7 mM | L-glutamine |
| mouse plating medium | | mouse culture medium |
| | | 4 (µg/ml) puromycin |
| percoll-gradient | 19 ml | PBS |
| | 1 ml | PBS (10 fold concentration) |
| | 1 ml | PDS |
| | 10 ml | percoll |
| | | centrifugation (4°C, 30,000 x g, 1h) |

3.1.1.1 Primary culture of porcine brain capillary endothelial cells (PBCEC)

Preparation. The isolation of porcine brain capillary endothelial cells (PBCEC) from 6 month old pigs was performed as described by (Tewes et al., 1996).

The hemispheres of porcine brains were taken from freshly slaughtered pigs and collected in ice-cold 70% (v/v) ethanol. For transport, ethanol was replaced by ice-cold PBS containing the antibiotics penicillin (200 U/ml) and streptomycin (200 U/ml). The storage buffer was refreshed once again in the laminar-flow hood. After shortly flaming the hemispheres, the meninges and adhering larger vessels were carefully removed. Secretory brain areas were dissected, and the grey and white matter consisting of cerebral tissue was then mechanically homogenized using scalpels and a sterile cutter with rolling blades. The homogenate was supplemented with preparation medium (37°C) to a final volume of 100 ml per brain. After addition of 1.6% (w/v) dry powdered unspecific protease/dispase II the suspension was stirred at 37°C for 2 h. To isolate the released capillaries, 100 ml of the digested homogenate were mixed with 150 ml of a 18% (w/v) dextran solution (4°C, MW ~ 160 kDa) and centrifuged (4°C, 6800 x g, 10 min). Both supernatant phases were discarded and the pellet containing the capillaries was resuspended in 9 ml plating medium per brain. This suspension was filtered through a nylon mesh (180 µm pore size) to remove larger blood vessels. In order to improve the separation of the capillaries, the filtered suspension was triturated up and down 5 times in a 10 ml sized pipette with the pipette tip placed directly onto the bottom of a petri dish, This mechanical disruption of capillary fragments to small pieces allows a shorter incubation time of the second digestion: A mix of collagenase/dispase II (0.1% (w/v)) was added to remove the mainly collagen containing basement membrane and to release the endothelial cells. This digestion was performed at 37°C for 30 min in a flask with a hanging magnetic stirrer to avoid any cell damage. State of digestion was controlled by inverse microscopy. The isolated endothelial cells were collected by centrifugation (20°C, 140 x g, 10 min) and resuspended in 10 ml plating medium per percoll gradient. This discontinuous percoll gradient was prepared from 15 ml percoll solution of a density of $\rho = 1.07$ g/ml and 20 ml percoll solution of $\rho = 1.03$ g/ml. 10 ml of the cell suspension were carefully placed onto the top of the gradient and centrifuged in a swing-out bucket rotor (4°C, 1300 x g, 10 min). The cell load of each gradient was adjusted to correspond to 1-2 brains. The red-stained, sharp interface containing the endothelial cells was aspirated from the lower middle of the gradient and diluted in plating medium. After a final centrifugation (20°C, 140 x g, 10 min), the pellet was gently

resuspended in plating medium and the cell yield of one brain was plated on a total of 6 x 75 cm² collagen-G coated culture substrates.

Culturing. One day after preparation the cells were washed twice with PBS⁺⁺ buffer to remove cell debris and non-adherent cell bodies and afterwards supplied with fresh culture medium afterwards.

Passage of cells. To reduce contamination with other cells from the brain parenchyma, the cells were subcultured two days after preparation. First, cells were washed twice with PBS and detached with trypsin solution (0.25% w/v). The displacement of endothelial cells was followed by inverse microscopy and trypsin digestion was stopped by addition of serum as soon as the majority of endothelial cells had lifted off the culture surface. The cell suspension was centrifuged (20°C, 140 x g, 10 min), the cell pellet was resuspended in plating medium and plated on either collagen-G coated flasks, glass cover slips or alternatively on rat tail collagen coated microporous polycarbonate filter membranes (0.4 µm pore size, 1 cm² growth area, TranswellTM No.3401, Costar[®]) with a density of 220,000 cells/cm².

Exchange of media. Two days after passage the plating medium was replaced by hydrocortisone containing serum-free medium without further washing. The cells were cultured for two more days until they were used for immunocytochemistry, permeability- and TEER studies or RNA- and protein-isolation.

| | | |
|-------------------------|----------|------------------------------------|
| preparation medium | | Earle's Medium 199 |
| | 0.7 mM | L-glutamine |
| | 1% (v/v) | penicillin/streptomycin (10 mg/ml) |
| | 1% | gentamicin (10 mg/ml) |
| pig plating medium | | preparation medium |
| | 10% | newborn calf serum (NCS) |
| pig culture medium | | plating medium without gentamicin |
| serum-free medium (SFM) | | DMEM/Ham's F12-Medium |
| | 0.7 mM | L-glutamine |
| | 1% (v/v) | penicillin/streptomycin (10 mg/ml) |
| | 1% (v/v) | gentamicin (10 mg/ml) |

| | | |
|------------------------------|------------------------------------|--|
| SFM + hydrocortisone | 550 nM | SFM hydrocortisone |
| dextran solution | 200 ml 4.4 g 360 g ad 2 l | Earle's buffer (10 x) containing phenol red NaHCO ₃ dextran (~ 162 kDa/mol) ddH ₂ O |
| percoll solutions | | |
| $\rho = 1.03 \text{ g/cm}^3$ | 400 ml 90 ml 10 l | PBS percoll Earle's Medium M199 (10 x) |
| $\rho = 1.07 \text{ g/cm}^3$ | 200 ml 270 ml 30 l | PBS percoll Earle's Medium M199 (10 x) |

3.1.2 Transfection of cells with small interfering RNA

Inhibiting the expression of specific target proteins is a powerful tool to investigate the function of these proteins *in vitro*. Many techniques were developed to induce knock-down or knock-out of targets including knock-out animals or *in vitro* techniques like the transfection with antisense DNA oligonucleotides and plasmids, respectively expressing antisense DNA inside the cells. Elbashir (Elbashir et al., 2001) described an application of RNA interference in mammalian cells, which was used until then for non-mammalian systems like plants and *C.elegans* (Bosher et al., 1999; Fagard et al., 2000). The basis of this method is the introduction of small interfering double-stranded RNA with sequence homology to a target mRNA. During transfection with small interfering RNA, specific double-stranded RNA is introduced into the cells and interrupts the translation of target genes by complementary binding and degradation of mRNA targets within the cytoplasm.

This method was sought to apply to primary cultures of brain capillary endothelial cell cultures.

The transfection with small interfering RNA (siRNA) was performed either before passage in 75 cm² flasks and 10 cm² petri dishes or after passage in 24-well plates. To transfect the

double-stranded RNA into either MBCEC or PBCEC the cationic lipid reagent *Oligofectamin*TM (*Invitrogene*) was used. The positively charged lipids interact with the negatively charged RNA and the lipid-RNA-complex is able to penetrate the cell membrane and reach the cytoplasm of the cell. Transfection was performed according the manufacturer's instructions. First, *Oligofectamin*TM was mixed with Opti-MEM[®] I *reduced serum medium* and incubated for 10 min at room temperature (solution I). In parallel, siRNA (20 μ M) was diluted in Opti-MEM I (solution II), mixed, combined with solution I and incubated for 15-20 min at room temperature. In between, the cells were washed with Opti-MEM and medium was applied (table 3-1) The transfection mixture was added to the cells and incubated for 4 h (37°C, water-saturated atmosphere, 5% (v/v) CO₂). Finally, growth medium with 3-fold concentration of antibiotics and serum were applied and cells were cultured until used for experiments in the incubator. For concentrations and amount of solutions used, see table 3-1.

Table 3-1: Overview of amounts and concentrations of used solutions during transfection with siRNA

| Reagent | Solution I | | Solution II | | Opti-MEM | Growth-medium |
|----------------------------------|--------------------|--------------|-------------|----------------|----------|---------------|
| | siRNA (20 μ M) | Opti-MEM I | Opti-MEM I | Oligofectamine | | |
| Flask (75 cm ²) | 39 μ l | 1484 μ l | 30 μ l | 10 μ l | 6.25 ml | 3.9 ml |
| Petri dish (10 cm ²) | 24 μ l | 420 μ l | 18 μ l | 4.5 μ l | 1.39 ml | 1.2 ml |

Growth medium

plating medium

30 % (v/v) FCS

3 % (v/v) penicillin/streptomycin (10 mg/ml)

2.1 mM L-glutamine

3.1.3 Immunocytochemistry

For immunofluorescence studies, murine and porcine brain capillary endothelial cells were plated on either collagen-G coated coverslips placed into 24 well-plates or alternatively on rat tail collagen coated microporous polycarbonate filter membranes. In the latter case, all experimental steps until the embedding were performed on the filter-inserts placed in 12-well plates. The cells were washed twice with PBS before fixation was performed by adding 250 μ l 4% (v/v) paraformaldehyde (PFA) followed by an incubation period of 10 min at 20°C. Before incubation with the primary antibody, fixed cells were washed 5 times with PBS and non-specific binding-sites were blocked for 20 min at room temperature supplemented with 3% (v/v) NGS and 0.1% (v/v) TRITON-X-100 in PBS. Afterwards the primary antibody,

diluted in PBS supplemented with 0.3% (v/v) NGS and 0.1% (v/v) TRITON-X-100, was added and the specimen were incubated for 1 h at room temperature (RT). For the dilution of the primary antibodies see table 3-2. Both antibodies were centrifuged at 15,000 rpm for 5 min to avoid antibody precipitations. After incubation, probes were washed with PBS and blocked with 10% (v/v) NGS (in PBS) again, before the secondary antibody (table 3-3) was applied in a 1:1000 dilution in PBS containing 3% NGS followed by a 30 min incubation at 20°C. After further washing (2x with PBS) cells were postfixed with 4% (v/v) PFA for 10 min at room temperature. The fixative was removed by washing 5 times with PBS and cover slips or filters were then shortly treated with ddH₂O and dried on Kimwipes[®]. For embedding, one drop of Paramount (*Polysciences*) was placed onto an optical slide and the coverslip was then put face down onto the slide. Filters membranes were excised from the inserts, transferred to the optical slide and allowed to settle. The samples were stored at 4°C in darkness to prevent bleaching of the fluorophores. Normally, the detection was performed 48 h after embedding of the cells, either by epifluorescence or laser scanning microscopy. Otherwise samples were stored at 4°C.

Table 3-2: Primary antibodies used in immunofluorescence staining

| Antibody | dilution (in PBS, 0.3% (v/v) NGS, 0.1% (v/v) TRITON-X-100) |
|--|---|
| Rabbit anti-Occludin (Zymed) | 1:200 (1.25 µg/ml) |
| Mouse anti-Occludin (Zymed) | 1:200 (2.50 µg/ml) |
| Rabbit anti-Claudin 5 | 1:100 (2.5 µg/ml) |
| Rabbit anti-ZO1 (Zymed) | 1:100 (2.5 µg/ml) |
| Rat anti-ZO1 (Chemicon) | 1:100 (2.3 µg/ml) |
| Rabbit anti-GFAP (Sigma) | 1:80 (1.25 µg/ml) |
| BMDP (AB 391 ²) | 1:100 (not available) |
| Mouse anti- α -sm-Actin (Zymed) | 1:100 (81 µg/ml) |
| Lamin A/C (Santa Cruz) | 1:100 (1.13 µg/ml) |

Table 3-3: Secondary antibodies used in immunofluorescence staining

| Antibody | Antibody dilution |
|----------------------------|--------------------------|
| Anti-mouse FITC (Mobitec) | 1:1000 (20 ng/ml) |
| Anti-mouse TRITC (Mobitec) | 1:1000 (20 ng/ml) |
| Anti-rat TRITC (Mobitec) | 1:1000 (20 ng/ml) |
| Anti-rabbit FITC (Sigma) | 1:1000 (20 ng/ml) |
| Anti-rabbit TRITC (Sigma) | 1:1000 (20 ng/ml) |

² From Susan E. Bates, Rockville Pike, Bethesda (MD), USA

| | | |
|------------------------------|-------------|--|
| Fixing | 4% (w/v) | paraformaldehyde (in ddH ₂ O) |
| blocking solution | 10% (w/v) | new-born goat serum |
| | 0.5% (v/v) | Triton X-100 |
| | 1% (w/v) | bovine serum albumine |
| antibody incubation solution | 3% (w/v) | new-born goat serum |
| | 0.5% (v/v) | Triton X-100 |
| | 0.1 % (w/v) | NaAzid |
| | 1% (w/v) | bovine serum albumine |

3.1.4 Atomic force microscopy

In contrast to electron microscopy techniques, atomic force microscopy (AFM) allows imaging the surface of living cells under physiological conditions with high resolution (Drake et al., 1989, Schar-Zammaretti et al., 2002; Yamane et al., 2000). The fixing and contrasting procedures during the preparation of biological samples for electron microscopy often causes artefacts. The surface imaging of living cells is less error-prone concerning artefacts than electron microscopy techniques. The use of phase imaging techniques enables the discrimination between different cell membrane components and offers detailed high resolution information about cell-cell contacts or cytoskeletal elements (stress fibres) (Chasan et al., 2002; Zhang et al., 2003). In addition to these topographic measurements, the AFM can be used to measure the long range attractive or repulsive forces between the probe tip and the sample surface, elucidating local chemical and mechanical properties like adhesion and elasticity. These two features of AFM, force mapping and imaging, were applied for studying MBCEC *in vitro*.

Experimental setup. For atomic force microscopy the cells were cultured as described in 3.1.1 and 3.1.1.1 and after passage seeded on collagen-G coated 8-well Lab-Tek[®] chamber-slides[™] (Nalgene) (45,000 – 90,000 cells/cm²) and cultured until confluence. After reaching confluence, the medium was replaced by incubation medium (either SFM with and without hydrocortisone or in serum-containing medium). After 24 or 48 hours in culture, the medium was removed and cells were washed (PBS⁺⁺, 37°C) to remove proteins from the cell surface. The chambers were shifted. The slide with the cells was transferred into a petri dish, fixed and

covered with PBS⁺⁺. The experiments were performed with a Bioscope equipped with a NanoscopeIIIa controller (*Digital Instruments*) employing gold-coated V-shaped cantilevers (*Veeco Instruments*) with a spring constant of 0.01 N/m. The spring constant was determined exactly by thermal noise measurements (*National Instruments*, NI5411). The cells layer surface was scanned in contact mode processed by the manufacturer's software (version 4.43.R6). Subsequently, the force mappings were accomplished with a trigger of 50 nm at 750 nm long force curves (lateral resolution: 64 x 64 per image).

The determination of the Young's modulus was based on the Hertz model. For the analysis of the force curve, the cantilever tip is presumed to be conical and the contact area to be spherical. Following Sneddon's modification of the Hertz model the incision of elastically bodies can be solved geometrically (Domke, 1998, Hertz, 1881; Sneddon, 1965).

3.1.5 Transmission electron microscopy

While the resolution of light microscopy is restricted by the wavelength of visible light (400-700 nm), transmission electron microscopy (TEM) permits to observe cellular structures within the range of the wavelength of electrons. Electrons can reach wavelengths as low as 1 pm. Practically the resolution in ultrathin sections of biological samples is around 1 nm.

Preparation of cell samples. For transmission electron microscopy the cells were subcultured after reaching 70% confluence (3.1.1) onto rat tail collagen coated microporous polycarbonate filter membranes. Fixation and embedding were performed as follows: The cells were washed twice with PBS⁺⁺ and fixed for a minimum of 1 h in sodium cacodylate buffer (0.1 M sodium cacodylate, 2.5% glutaraldehyde, 2 mM CaCl₂) at room-temperature. Afterwards, the specimen were washed with ddH₂O (30 min, shaker) and incubated for 45 min at room-temperature in 0.5 % (w/v) OsO₄ solution in sodium cacodylate buffer) followed by a second washing step for 30 min in ddH₂O. Subsequently, the samples were dehydrated by incubation in 75% (v/v) ethanol, 2 x 100% ethanol and finally propylene oxide for 5 min each. After incubation in a mixture of propylene/epon (1:1) for 30 min the specimen were incubated in pure epon for 15 min. Finally, the samples were embedded in a pure epon containing mold and dried for 24-48 h at 60°C. Ultrathin sections were examined and photographed using a Philips EM 201.

3.1.6 Measurement of electrical properties of primary cultured murine brain capillary endothelial cells

The determination of electrical properties of cells allows determining the barrier properties for small inorganic ions like Na^+ and Cl^- (Schneeberger and Lynch 1992). To determine the TEER of MBCEC, impedance spectroscopy has been applied. This method allows to extract the transendothelial resistance of the cell monolayer. The cells are not affected by this method. This enables the performance of long term measurements.

3.1.6.1 Determination of transendothelial electrical resistances of cells grown on filter membranes

The filters for TEER determination were coated with rat-tail collagen one day before cell inoculation and incubated over night at 37°C in a water saturated atmosphere. Afterwards the filters were dried in the laminar flow hood and stored at 4°C . The cells were cultivated on fibronectin/collagen IV coated petri dishes (3.1.1) and passaged after reaching 70-90% confluence. For measuring the TEER the cells were seeded on the coated filters in a density of $220,000 \text{ cells/cm}^2$. The medium was replaced by incubation medium (either serum-containing medium or SFM with or without hydrocortisone) after the cells had reached confluence on filters and the measurement was performed after one and two days in incubation medium. The filters containing the cultured cells were transferred into a chamber with a gold coated bottom. A platinum ring electrode was placed into the medium of the apical chamber (figure 3-1). A frequency generator (*Solartron*) applied alternating voltages (10-100 mV) in a frequency range from 1 to 10^5 Hz, measured the resulting current in a phase-sensitive fashion and calculated the impedance according to Ohm's law. The recorded impedance spectra were analysed by equivalent circuit modelling as described by (Wegener et al., 2000a). Alternatively, time dissolved measurements were performed using an automated apparatus reading 12 electrodes in parallel developed in our laboratory³.

³ Developed by Abrams, D., Janshoff, A., Willenbrinck, W., Wegener, J.

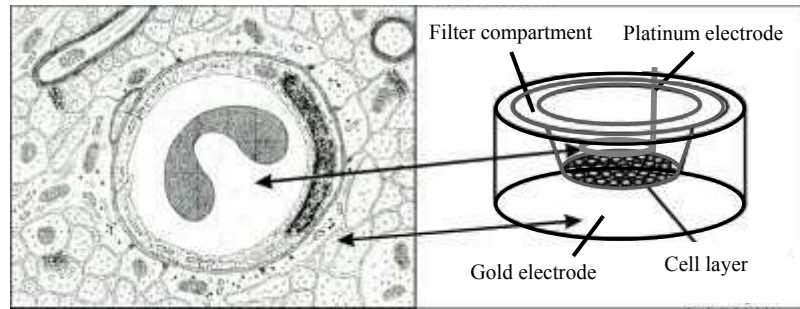


Figure 3-1: *In vitro* model of BBB and experimental setup for TEER measurement. The apical chamber represents the lumen of the vessel while the basolateral chamber simulates the brain side. The platinum ring electrode was placed into the apical chamber using the gold coated surface of the basolateral chamber as counter electrode.

3.1.6.2 Electric cell-substrate impedance sensing

Electric cell substrate sensing (ECIS) is an experimental method for investigating the electrical impedance as a function of the frequency of cell covered film electrodes. In contrast to the TEER measurement as described in section 3.1.6.1 cells are directly cultured on gold electrodes (figure 3-2 A). The analysis of the data allows conclusions about the resistance R_b between adjacent cells, which is a measure of the integrity and barrier function of the layer, the parameter α that describes the impedance contribution from the cell substrate adhesion zone and the capacitance of the cell membrane (C_M). Together, these parameters permit characterisation of the barrier and adhesion properties of cells in one experimental setup.

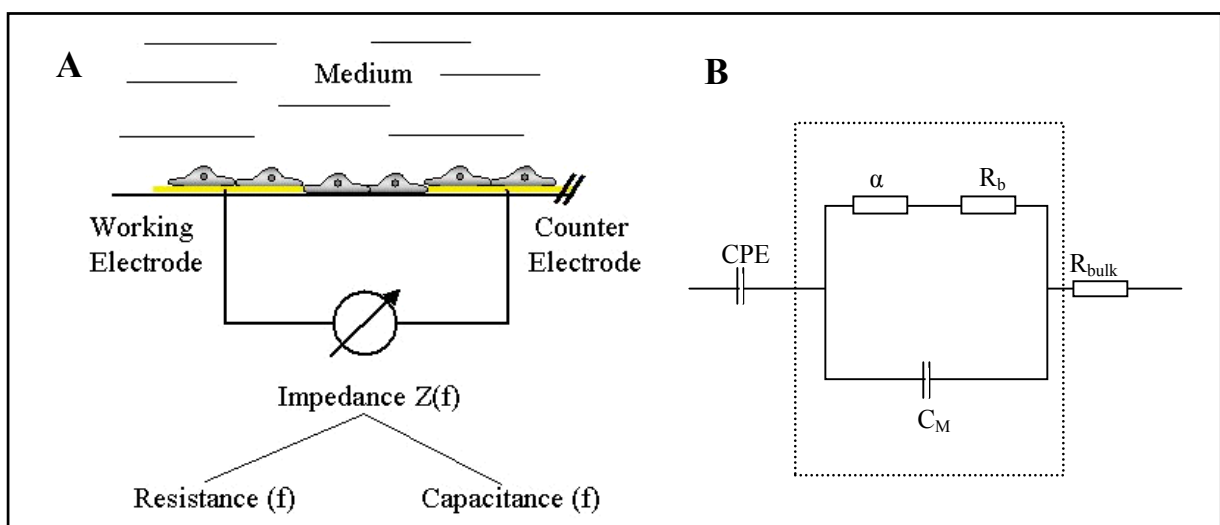


Figure 3-2: Setup for electric cell substrate sensing (ECIS). **A:** The cells are cultured directly onto gold electrodes. The working electrode is 300-fold smaller than the counter electrode. Thus, the working electrode becomes a bottle neck for the current and the electrical impedance of the system is dominated by the cells grown on the this electrode. **B:** Equivalent circuit (approximation). This model allows the determination of the parameters α , R_b and C_M .

Preparation of the electrodes. The ECIS device is based on AC impedance measurements using weak AC signals (Giaever and Keese, 1993; Lo et al., 1995, Mitra et al., 1991; Wegener et al., 2000b). An oscillator applies an AC signal of 70 mV amplitude to the two-electrode system using culture medium as the electrolyte. The data analysis had been described elsewhere (Wegener et al., 2000a).

For electrical cell-substrate impedance sensing (ECIS) 8-well arrays with 10 electrodes each (*Applied Biophysics*, figure 3-3) were used. Each well consists of 10 active electrodes at the bottom of the dish (each 250 μm diameter), electrically in parallel. Before cell culturing the arrays were cleaned for 5 min in an argon plasma cleaner (*Harrick*, New York) and the electrodes were immersed with an aqueous solution of L-cysteine (10 mM) to stabilise the interface impedance. Afterwards the electrodes were washed and coated with collagen-G. MBCEC were trypsinised as described in section 3.1.1. Cell density was monitored after centrifugation by using a standard hemacytometer and 300,000 cells were seeded into each chamber. Directly after seeding the arrays were placed into the array holder, electrical contact was established and the measurement was started.

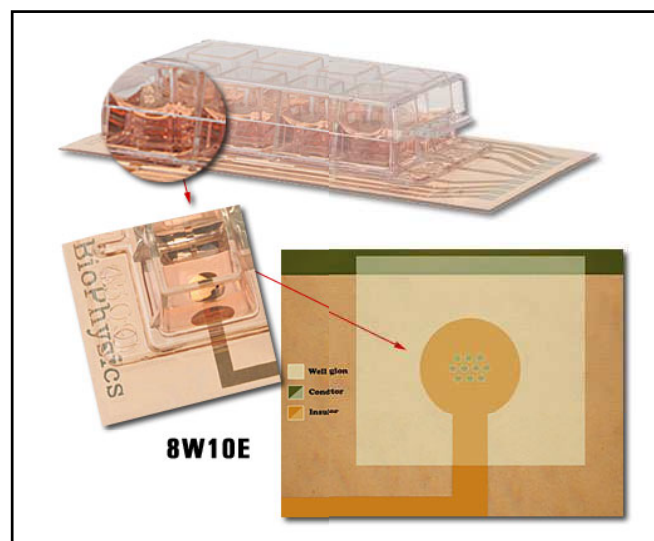


Figure 3-3: ECIS electrode in 8-well format (8W10E, *Applied BioPhysics*, Troy, NY). Each array consists of 8 wells with 10 electrodes per well in parallel.

3.1.7 Quartz Crystal Microbalance

The quartz crystal microbalance (QCM) is a sensitive technique to follow adsorption processes and adhesive properties of cells *in vitro* (Wegener et al., 1999, Wegener et al.,

2000c). The shifts in resonance frequency correlate with the number of cells attached to the resonator surface. This allows to investigate the adhesion kinetics of cells grown under different conditions and adhesion properties of cells after reaching confluence.

3.1.7.1 Preparation of quartz resonators for cell culture

Before cell culturing all quartz crystals were cleaned for 5 min in an argon plasma cleaner (Harrick, New York). For gelatine coating of quartzes gelatine was dissolved in ultrapure water (0.5% (w/v)) and the resonators were flooded with this solution for 90 min at room temperature. Subsequently, the gelatine solution was removed and glutaraldehyde (2.5% (w/v)) was applied for 15 min at room temperature to cross-link the gelatine. After incubation, the aldehyde was removed and chambers were incubated for 5 min in 70% ethanol for further sterilisation. Finally, the chambers were washed 5 times with sterile water and incubated overnight in ultrapure H₂O. The next day, the chambers were washed again 5 times with ultrapure H₂O to remove all traces of glutaraldehyde and ethanol which would inhibit cell growth. To perform quartz crystal microbalance (QCM) measurements the cells were cultured until 70-90% confluence as described in section 3.1.1 and then harvested and plated for QCM experiments onto gelatine-coated 5 MHz-AT-cut quartz resonators (figure 3-5 A).

3.1.7.2 Experimental setup for QCM measurement

For all QCM experiments plano-plano AT-cut quartz plates (14 mm in diameter) with a 5-MHz fundamental resonance frequency (*KVG*, Neckarbischofsheim) coated with gold electrodes on both sides, each exhibiting an area of 0.33 cm² were used (figure 3-5 A). For culturing cells on the quartz resonators small glass tubes were fixed onto their surface to allow direct culture of cells in chambers on the crystal's surface.

QCM measurements were performed in two different modes: The cell mode allows the determination of resistance values for the monolayer analogous to the ECIS measurement (cf. 3.1.6.2). It allows the electrical characterisation of the cell monolayer in a frequency range from 1-10⁵ Hz with determination of the parameters α , R_b and C_M by use of the low impedance platinum dipping electrode in combination with the gold electrode beneath the cells (figure 3-5 B).

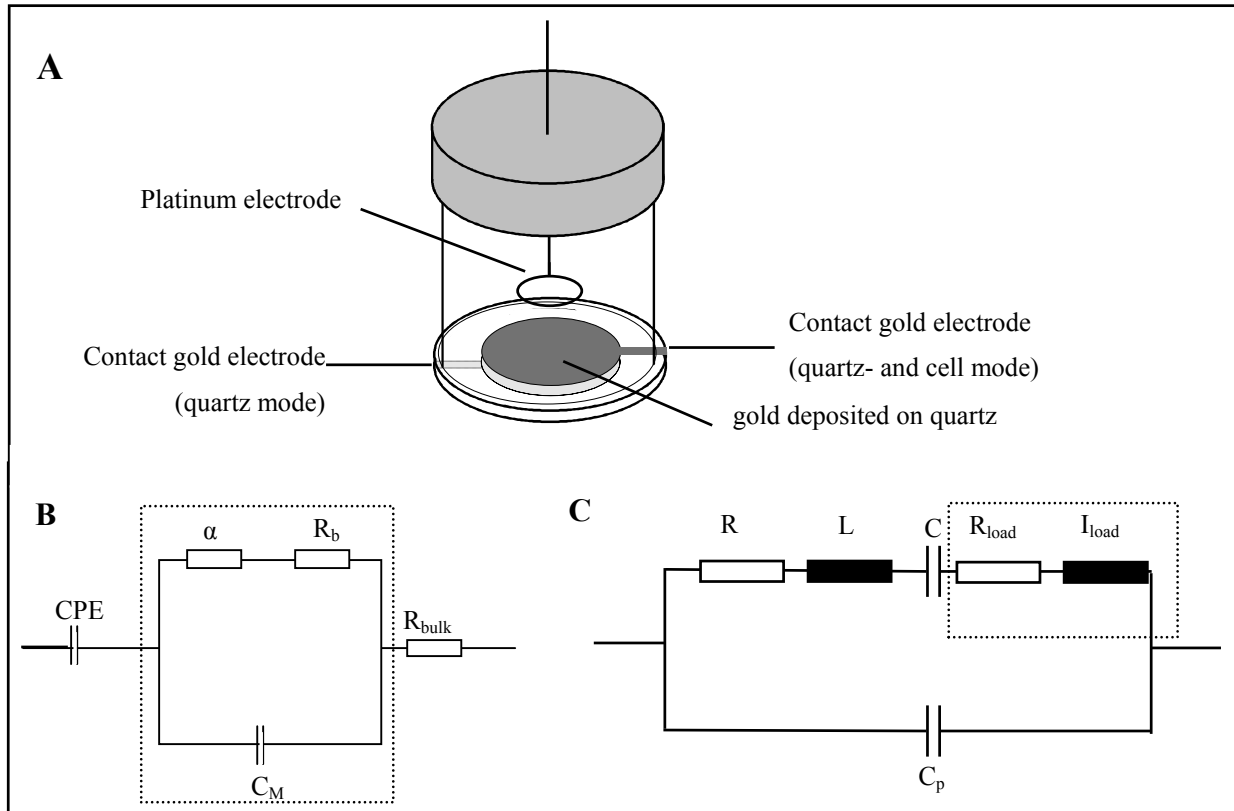


Figure 3-4: **A:** Experimental setup for QCM. Depicted is the chamber with the plano-plano AT-cut quartz at the bottom and the platinum ring electrode dipping in the culture medium from above. **B+C:** Equivalent circuits used for curve fitting of QCM experiments. **B:** Fitting of cell mode (ECIS). This model is an approximation. The dotted box represents the influence of the cell layer on the impedance spectrum. $R_{c,l}$ represents the transendothelial resistance arising from the formation of tight junctions between the cells. $C_{e,l}$ is the capacitance of the cell monolayer (cf. ECIS). **C:** Equivalent circuit non-linear curve fitting of the phase spectra recorded in quartz-mode measurements. R , L , C and C_p are the parameters of the unperturbed quartz crystal while the additional elements R_{load} and L_{load} representing the liquid loading and the cell monolayer, respectively, attached to the quartz surface (Wegener et al., 2001).

The quartz mode reads modifications of cell-substrate interactions via an electrical characterisation of changes in the quartz resonance (figure 3-4 C). Therefore, the electrical impedance of the oscillation is determined in a range of 4.96 to 5.04 MHz by using the electrodes on both sides of the quartz. A change in the adhesion of cells is detectable by a change of mechanical properties of the quartz which is mirrored in its electrical characteristics due to the piezoelectric coupling. After measurements in quartz and cell mode have been performed the cell layer was removed by cleaning the surface mechanically and the empty quartz resonator was measured again. The difference of the load resistance allows conclusions of cell-substrate interactions of cultured cells in quartz mode (Wegener et al., 2001).

3.1.8 Permeability studies

The permeability of murine brain microcapillary endothelial cells is, corresponding to the TEER, a measure for the integrity of the cell monolayer. To quantify endothelial permeability, hydrophilic marker substances with low molecular weight are used. Whereas lipophilic substances are able to penetrate the cell membrane and to pass the monolayer on transcellular pathways across the cells, small hydrophilic molecules only pass the layer through gaps between adjacent cells or (active) transport. These molecules are unable to penetrate and diffuse across the plasma membrane. To determine the paracellular permeability of the monolayer sucrose as a small hydrophilic molecule was used in all experiments as no transport systems for sucrose are known in brain capillary endothelial cells.

The experiments were performed as follows: cells were trypsinised, harvested and 90,000 cells were seeded on 0.33 cm² filters (*Costar 3401*). The cells were incubated for 2 days until reaching confluence. The medium was then replaced by incubation medium and cells were incubated for two more days. Which particular media were used for individual experiments is described in the results. ¹⁴C-sucrose (1 µCi/filter) was applied into the apical chamber and samples were taken after certain incubation times (5, 10, 15, 20, 40, 60 and 80 min) from the basolateral compartment.

3.1.8.1 Analysis of permeability data

The permeation rate of compounds across a cellular barrier is described by a permeability coefficient P (cm/s). This coefficient can be calculated following (Pardridge et al., 1990) or (Walter et al., 1995). In these models, the permeability coefficient (P_e) of cells on a filter membrane is corrected by the P_e of the filter membrane itself to obtain the P_c of the cells only (equation 2). The following steps were used to calculate the absolute permeability of the cell layer (equation 1).

$$P_e = \frac{n_{baso}}{C_0 \cdot t \cdot A} \quad [cm/s] \quad \text{Equation 1}$$

with n_{baso} equals the amount of permeated sucrose (Schinkel et al.); c_0 = concentration of sucrose in the apical chamber [mol/l]; t = permeation time [s] and A = permeation area [cm²].

$$\frac{1}{P_e(cells)} = \frac{1}{P_e(cells + filters)} + \frac{1}{P_e(filters)} \quad \text{Equation 2}$$

All values were normalised to the filter area and time. Thus P_e is given in units of cm/s.

3.2 Molecular biology

All devices, solutions, pipette tips and reaction tubes were sterilised by routine sterilisation techniques. Only chemicals of molecular biology grade were used. When working with RNA material, solutions were treated additionally with 0.1 % (v/v) dimethylpyrocarbonate (DMPC) to inactivate RNases. Glassware was treated at 200°C for at least 4 h and gloves worn during all RNA preparations and handlings.

3.2.1 Quantification of nucleic acids

3.2.1.1 Photometric determination of nucleic acid concentrations

Concentrations of nucleic acids were measured with an UV-VIS recording spectrophotometer (UV-2401PC, *Shimadzu*) at a wavelength of 260 nm which is most suited for RNA/DNA quantification due to the absorbance of purine and pyrimidine bases. Using a 1 cm cuvette an optical density at 260 nm (OD_{260}) corresponds to 40 $\mu\text{g/ml}$ of single stranded RNA and to 50 $\mu\text{g/ml}$ of double stranded DNA.

The purity of isolated nucleic acids was determined by measuring the optical density at 280 nm where the aromatic amino acids of proteins show highest absorbance. The ratio OD_{260}/OD_{280} is supposed to be between 1.8 and 2.1 for RNA dissolved in buffer with $\text{pH} > 7$ and about 1.8 for DNA.

3.2.1.2 Determination of concentrations by ethidiumbromide staining

The quantity of DNA, especially when used for cloning, was estimated on ethidiumbromide stained agarose gels with the help of commercially available DNA ladders from *Eurogentech*. The so called SMART-ladders contain definite amounts of DNA in each visible band to which the intensity of analysed DNA sample was visually compared and thus, the amount of DNA of the sample could be estimated.

3.2.2 Agarose gel electrophoresis

Nucleic acids can be separated according to their size in an agarose gel electrophoresis. The concentration of agarose was varied according to the expected size of the DNA fragments in order to obtain optimal separation results (table 3-4). To guarantee that nucleic acids move in the electrical field to the anode the electrophoresis must be performed at a pH close to neutral pH. Therefore, 1 x TAE-buffer for non-denaturing gels (DNA) and 1 x MEA-buffer for denaturing gels (RNA) were used. In case of DNA gels variable amounts of agarose were directly dissolved in 1 x TAE-buffer by heating in a microwave, whilst for RNA gels 1% (w/v) agarose was first dissolved in DMPC treated water. Afterwards 10 x MEA and formaldehyde (37%) were added to a final concentration of 1 x MEA and 6% (v/v) formaldehyde. Prior to electrophoresis the samples were diluted in DNA- or RNA-loading buffer. Furthermore, RNA samples were denatured for 10 min at 65°C and both formaldehyde and formamide present in the loading buffer inhibited further formation of RNA secondary structures. To determine the size of DNA fragments DNA ladders (*Life Technologies and Eurogentech*) were used. Gel electrophoresis was performed at 100 V. Nucleic acid fragments were visualised under UV-light (254 nm) using ethidiumbromid as dye. In case of DNA separation, gels were stained after electrophoresis in ethidiumbromid containing solution (0.5 mg/ml in 1 x TAE-buffer) while for RNA-visualisation 1 µl of an ethidiumbromid solution (1 mg/ml) was directly added to the samples prior loading.

Table 3-4: Concentrations of agarose gels

| Agarose concentration (% w/v) | 0.3 | 0.6 | 0.8 | 1.0 | 1.2 | 1.5 | 2.0 |
|-------------------------------|------|------|--------|-------|-------|-------|-------|
| nucleic acid range (kb) | 5-60 | 1-20 | 0.8-10 | 0.5-5 | 0.4-7 | 0.2-3 | 0.1-2 |

| | | |
|----------|--------------|----------------|
| 50 x TAE | 2 M | Tris |
| | 2 M | sodium acetate |
| | 0.5 | EDTA |
| | | pH 7.4-7.8 |
| 10 x MEA | 0.01 M, pH 8 | EDTA |
| | 0.2 M | MOPS |
| | 0.05 M | sodium acetate |
| | | pH 7.0 |

| | | |
|-------------------------|--------------|----------------------|
| 10 x DNA-loading buffer | 0.25 % (w/v) | bromophenol blue |
| | 0.25 % (w/v) | xylene cyanole |
| | 15 % (v/v) | Ficoll |
| 1 x RNA- loading buffer | 50 % (v/v) | formamide de-ionised |
| | 10 % (v/v) | 10 x MEA |
| | 16 % (v/v) | 37 % formaldehyde |
| | 5 % (v/v) | glycerol |
| | 0.25 % (w/v) | bromophenol blue |

3.2.3 Isolation of DNA from agarose gels

Gel extraction of DNA fragments was performed by using the QIAquick Gel Extraction Kit (*Qiagen*) according to the manufacturer's instructions. The DNA fragment was excised from agarose gel, weighed and dissolved in 3 gel volumes of Buffer QG at 50°C for 10 min (1 mg ~ 1 µl). Afterwards, one gel volume of isopropanol was added and DNA was purified by a QIAquick spin column. DNA adsorbs to the silica membrane in the presence of a high concentration of chaotropic salts at pH<7.5, while contaminants pass through the column and are efficiently washed away. The pure DNA was then eluted by 30-50 µl of 10 mM Tris/HCl and pH 8.5. Concentrations of purified DNA fragments were determined as described in 3.2.1.

3.2.4 Isolation of plasmid DNA

For different applications as PCR, restriction digest and sequencing, plasmid DNA was isolated from *E. coli*. The QIAprep Spin Miniprep (*Qiagen*) was used to isolate plasmid DNA from *E. coli* cultures grown overnight in LB-medium containing ampicillin. The isolation procedure is based on the principle of alkaline lyses of the cells, precipitation of genomic DNA, cell debris and proteins and adsorbance of plasmid-DNA onto silica in the presence of high salt concentrations. After removal of molecular contaminants plasmid-DNA was eluted by a low salt buffer at a pH between 7 and 8.5. The procedure was performed according the manufacturer's instructions given in the manual.

3.2.5 Isolation of RNA

Total RNA from cultured cells was isolated using commercial available kits. For the isolation of porcine and murine brain capillary endothelial cells, the High Pure RNA Isolation Kit[®] (Roche) was applied according to the instructions given in the manual.

3.2.5.1 Isolation of RNA from capillary endothelial cells

The cells were washed with PBS before lysis is carried out by incubating the sample with 400 μ l Triton[®] X-100 and guanidine hydrochloride containing lysis/binding buffer to inactivate RNases. Cells were detached with a rubber policeman and collected in a clean RNase-free tube. The cell suspension was applied to the filter tube where RNA binds to the surface of glass fibres in the presence of chaotropic salt. The binding process is specific for nucleic acids, and here optimized for RNA. The rest of the contaminating DNA were digested by DNase I, applied directly on the glass fibre fleece and incubated for 15 min at room-temperature. The bound RNA was then purified from salts, proteins and other cellular impurities by three washing steps and was finally eluted in 100 μ l RNase-free water. The purity of the RNA was checked by OD₂₆₀/OD₂₈₀-ratio (see section 1.2.1.1). RNA was quantified by measuring the OD₂₆₀ (section 3.2.1) and stored at -70°C.

3.2.6 cDNA synthesis

cDNA was transcribed from 5 μ g of total RNA using Superscript[™] II RNase H⁻ Reverse Transcriptase (Life Technologies[™]). The reaction mix was supplemented with accompanied 5 x First Strand Buffer and 0.1 M DTT as well as a primer mix. To synthesize cDNA for amplification of gene fragments for cloning oligo (dT)₁₂₋₁₈ (500 μ g/ml) and for TaqMan Realtime PCR random primer mix was applied. 1 μ l primer solution was added to the RNA sample to a final volume of 12 μ l, incubated in case of random primer first for 10 min at 25°C and afterwards for 20 min at 50°C. The first incubation was skipped when using oligo (dT) primer. Then the sample was denatured at 65°C to dissolve secondary structures and

immediately chilled on ice. 4 μ l First Strand Buffer, 2 μ l 0.1 M DTT and 1 μ l dNTP mix (10 mM each dATP, dCTP, dGTP, dTTP) were added and incubated at 42°C for 2 min before 1 μ l (100 units) of SuperScript II™ was added. cDNA synthesis was performed at 42 °C for 50 min and finished by inactivation of the enzyme at 70°C for 15 min. The cDNA pool was either used directly for Real-Time PCR or stored at -20°C.

3.2.7 Polymerase chain reaction methods

3.2.7.1 PCR

The polymerase chain reaction (PCR) was applied to amplify DNA fragments using two specific primers complementary to the ends of the desired DNA fragment. As templates either plasmid DNA or cDNA pools were used. All primers and their annealing temperatures are listed in appendix D. PCR with plasmid-DNA was performed to generate enough material for probing northern blots. In these cases the thermostable Taq DNA polymerase™ (*Life technologies*) and a reaction volume of 50 μ l was used as follows: 5 μ l 10 x PCR buffer and 1.5 μ l 50 mM MgCl₂ (both provided by the manufacturer), 2 μ l dNTP mix (10 mM each nucleotide), 0.5 μ l of 5'- and 3'-primer (10 μ M), 0.5 μ l plasmid DNA (approx. 0.2 μ g/ μ l), 40.5 μ l ddH₂O and finally 0.5 μ l of Taq DNA polymerase were gently mixed and incubated in the mastercycler gradient (*Eppendorf*). The PCR was performed according to the following program: 3 min initial denaturation at 95°C, 30 cycles of 30 sec denaturation at 95°C, 1 min annealing of the primers at specific temperatures (listed in appendix D) and 1.5 min elongation at 72°C. Afterwards the mixture was incubated for 5 min at 72°C for complete elongation of PCR fragments and finally stored at 4°C. PCR products were then analysed by agarose gel electrophoresis (section 3.2.2), purified from agarose gels (section 3.2.3) quantified (section 3.2.1) and used for probing either in northern blotting or cloning.

3.2.7.2 Quantitative real-time polymerase chain reaction (QRT-PCR)

TaqMan Real-time PCR was performed to determine the quantity of specific mRNA targets within isolated RNA (section 3.2.5.1). Comparable to northern blot analysis this method is used to quantify the mRNA expression of different RNA species of interest. This method is sensitive and the required amount of RNA is lower than in northern blot analysis. Real time PCR is a two step RT-PCR system. In the first step the RNA is transcribed by reverse transcriptase to complementary DNA (cDNA) by applying random primer mix as described in paragraph (3.2.6). The following second step is based on the polymerase chain reaction technology combined with a fluorescence detection system. Special dyes intercalate during the amplification of the targets and allow a determination of differences in the quantity during the exponential phase of amplification. Due to the fact that the applied dye intercalates unspecific into double stranded DNA it is mandatory to use primers with special standards. A reliable quantitative comparison of two independent sequences (target and house keeping gene) demands a similar efficiency of amplification in the exponential phase of amplification. Primers were chosen regarding the following criteria: The GC-content was between 40-60% and the length of oligonucleotides corresponded to 15 to 25 base pairs. For all primers the melting temperature constituted 60°C. Primers were chosen using the software Primer Express (version 2.0; *Applied Biosystems*).

3.2.7.2.1 TaqMan SYBR-Green PCR protocol

20 µl of the RT-product obtained as described in section 3.2.6 were diluted to a volume of 40 µl with DMPC-ddH₂O. 2.5 µl of this dilution were applied to the reaction mix containing 7.88 µl SYBR-Green universal PCR Master Mix™ (*PE Biosystems*), 3 µl of 5' - and 3' -primer (5 µM each) and 9.77 µl DMPC-ddH₂O (all primers are listed in appendix D). The SYBR-Green universal PCR Master Mix™ contains reaction buffer, dNTPs, MgCl₂, AmpliTaq Gold DNA-polymerase and two fluorescence dyes, the reporter dye SYBR-green which intercalates into DNA and a reference dye whose fluorescence properties are not influenced by amplification of DNA. The fluorescence of the reporter dye is normalized to the reference dye to avoid falsification of fluorescence fluctuation. The TaqMan-PCR was performed using a GeneAmp® 5700 (*PE Biosystems*®; software version 1.3) according to the following program: initial denaturation at 95°C for 10 min, 40 cycles of denaturation at 95°C for 15 sec followed by hybridisation and finally elongation at 60°C for 60 sec completed by a final elongation at

60°C for 15 min. To check the specificity of the obtained DNA fragment the amplification protocol was followed by dissociation at 95°C for 15 sec and hybridization at 60°C for 20 sec. The final slow heating from 60 to 90°C was detected by fluorescence and when a distinct signal is present the obtained amplification signals can be assumed to be specific estimated targets.

3.2.7.2.2 Analysis of quantitative Real-Time PCR data

To analyse real-time PCR data a relative quantification of target genes was performed by determining the amount of specific targets in one cDNA-population compared to another cDNA population. cDNA populations were transcribed from RNA from cells cultivated in SFM containing hydrocortisone in comparison to cells cultured in serum-containing medium without hydrocortisone. Fluorescence values are recorded during every cycle with a CCD camera and represent the amount of product amplified to that point in the amplification reaction by determination of the intensity of SYBR-green fluorescence. The fluorescence intensity of this dye increases by intercalation into the small groove of double-stranded DNA. The more templates present at the beginning of the reaction, the fewer number of cycles it takes to reach a point in which the signal is first recorded as statistically significant above background (Gibson et al., 1996). This point is defined as the threshold cycle (C_t) and will always appear during the exponential phase of amplification (figure 3-5). Therefore, quantification is not affected by any reaction components becoming limited in the plateau phase.

To correct for varying quality of applied nucleotides, the results of the target genes were compared with those of an internal reference gene. Moreover, the PCR buffer contains a fluorescence dye (ROX) which allows to normalise fluctuations of the fluorescence intensity of SYBR-green.

For preliminary analysis of the expression of target genes, the ΔC_t values of specific targets were compared. The latter are proportional to the normalised starting quantity of target genes. Higher values for ΔC_t correspond to lower expression level of target genes (X_N). The values were displayed inversely and normalise to the internal control ($Y_0 - \Delta C_T$) with Y_0 as the threshold cycle of the internal control ($Y_0 = 15$). Higher values now represent higher expression levels. The value 0 is corresponding to signals detected later than cycle 30. Those signals are not significantly higher than the background of the reaction.

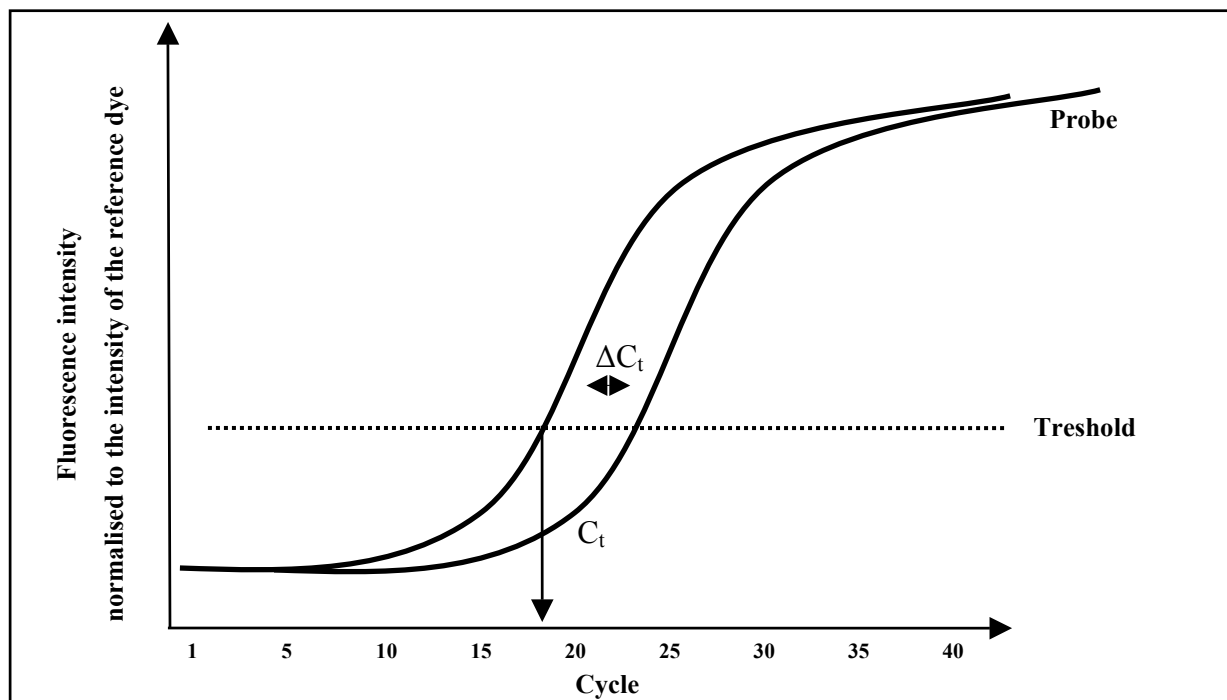


Figure 3-5: Semilog diagram of the fluorescence signal intensity versus cycle. C_t is the number of cycle where the fluorescence intensity is first recorded as significant above background in the exponential phase of amplification. ΔC_t gives the difference of fluorescence intensity corresponding to an internal reference gene (β -actin or GAPDH).

3.2.8 Nucleic acid blotting and hybridisation

3.2.8.1 Northern blotting

After separating RNA molecules in a denaturing gel (section 3.2.2), RNA was transferred from the gel onto a positively charged nylon membrane (Hybond, *Amersham Biotech*) by capillary transfer. The RNA of interest was then identified by hybridisation with radioactive, ^{32}P -labelled probes and visualisation by autoradiography as described in the following section (3.2.8.3). For the experimental setup a nylon membrane and Whatman™ filter papers were equilibrated in transfer buffer (20 x SSC) and the gel was soaked in RNase-free water immediately after gel electrophoresis. Capillary transfer proceeded for 12-18 h. Afterwards, the membrane was neutralised in 2 x SSC and transferred RNA was fixed to the membrane by UV-crosslinking (350 nm) for 100 sec and subsequent incubation (2 h, 80°C). Membranes

were stored between Whatman™ filter papers at room temperature until further use (Sambrook, 1989).

| | | |
|----------|-------|----------------|
| 20 x SSC | 3 M | NaCl |
| | 0.3 M | sodium citrate |

3.2.8.2 Preparation of α -³²P-labelled DNA probes

For probing northern blots radioactive labelled DNA samples were generated by using the Megaprime™ DNA labelling system (*Amersham Biotech*) according to the supplied protocol. After denaturation of purified DNA the Klenow fragment of *E. coli* DNA polymerase synthesises a second DNA strand and incorporates ³²P-labelled dCTP starting at the random primer present in the reaction mix. This primer mix contains nonanucleotides, which statistically bind every 80-100 nucleotides along the template.

To 25 ng DNA and 5 μ l random primer solution the appropriate volume of water was added to give a final volume of 50 μ l in the final Megaprime™ reaction. After 5 min denaturation at 100°C, 10 μ l labelling buffer, 5 μ l dCTP³² (10 μ Ci/ μ l) and 2 μ l enzyme were added and incubated for 15 min at 37°C. The reaction was stopped by applying 5 μ l EDTA (0.2 M) to chelate the bivalent cations, needed for the reaction. The radioactive probes were then purified from non-incorporated ³²P-labelled dCTP by size exclusion using MicroSpin™ G-50 Columns (*Amersham Biotech*) before the activity was measured by a scintillation counter (*Beckmann*).

3.2.8.3 Hybridisation

To identify and visualise specific mRNA molecules the radiolabelled probes were hybridised to the nucleic acid bound onto the nylon membrane. Before hybridisation the membranes were equilibrated with 10 mg/ml denatured herring sperm DNA-containing hybridisation solution at 42°C overnight to minimise unspecific binding of the probe to the membrane afterwards. For hybridisation the radiolabelled probe was denatured at 100°C for 10 min, chilled on ice and finally added to the hybridisation solution. Hybridisation was performed overnight at 42°C in a rotation incubator.

| | | |
|-------------------------|-----------------------|--|
| Hybridisation solution | 5 x | SSPE |
| | 50% (v/v) | formamide |
| | 5 x Denhardt solution | |
| | 1% (w/v) | SDS |
| | 10% (w/v) | dextrane sulphate sodium salt |
| 20 x SSPE | 3 M | NaCl |
| | 0.2 M | NaH ₂ PO ₄ ·H ₂ O |
| | 0.02 M | EDTA |
| | | pH 7.4 |
| 100 x Denhardt solution | 2% (w/v) | Ficoll |
| | 2% (w/v) | polyvinylpyrrolidone |
| | 2% (w/v) | bovine serum albumin |

3.2.8.4 Washing

Unspecifically bound radiolabelled probes were removed by separate washing. Membranes were washed twice with low stringent buffer (2 x SSPE) for 15 min at room temperature, then twice with medium stringent buffer (2 x SSPE, 2% (w/v) SDS) for 15 min at 65°C. After monitoring the radioactivity of the membrane high stringent buffer (0.1 x SSPE) was applied at room temperature as long as no further background activity could be monitored. For visualisation by autoradiography the membranes were exposed to Hyperfilms (*Amersham Biotech*) at -70°C for some hours up to some days depending on signal intensity.

| | | |
|-----------|--------|--|
| 20 x SSPE | 3 M | NaCl |
| | 0.2 M | NaH ₂ PO ₄ ·H ₂ O |
| | 0.02 M | EDTA |
| | | pH 7.4 |

3.2.8.5 Stripping

In order to normalise the RNA quantity transferred to the membrane, blots need to be stripped and probed with α -³²P-labelled GAPDH afterwards. Therefore, initially applied radioactive

labelled probes were removed by heating the membrane in stripping solution for 10 min at 100°C.

| | | |
|--------------------|----------|--|
| Stripping solution | 0.015 M | NaCl |
| | 0.1 x | SSC |
| | 1% (w/v) | SDS |
| 20 x SSC | 3 M | NaCl |
| | 0.3 M | Na ₃ citrate·H ₂ O |
| | | pH 7 |

3.2.9 Cloning and ligation

The construction of vectors was performed by two different ways. Either DNA was generated by PCR, purified by agarose gel electrophoresis and isolation from the gel, digested in the primer sites and cloned into a vector of choice which was linearised using the same restriction endonucleases. In case of single cut reaction the vector was dephosphorylated with shrimp alkaline phosphatase (0.1 U/μl) (*Roche*) before the ligation (30 min, 37°C). Or alternatively, DNA was generated by PCR and directly cloned into pT-Adv Vector (*Clontech*) by TA-cloning. In both cases ligation mixes were transformed into *E.coli* competent cells to amplify plasmids. Subsequently, plasmids were isolated, analysed by restriction digested and sequence analysis. The vectors are listed in appendix E.

3.2.9.1 Restriction

1 to 5 μg of DNA (either plasmids or PCR-fragments) were cut by 1 μl restriction endonucleases (10 U/μl, *New England Biolabs, NEB*) in the presence of 2 μl of the appropriate 10-fold concentrated reaction buffer in a final volume of 20 μl. The restriction mix was incubated for 90 min at 37°C. In case of plasmids the restriction reaction was controlled by gel electrophoresis and the linearised DNA or the insert were directly purified by the QIAquick Gel Extraction Kit (*Qiagen*) similar to the protocol given in section 3.2.3.

3.2.9.2 Ligation

Prior to ligation the concentration of purified and restricted DNA was estimated from agarose gel as described in section 3.2.1.2. The vector/insert-ratio was adjusted to 1:3 for best ligation efficiency. The ligation was carried out at 16°C overnight using 1 µl T4-DNA ligase (6 U/µl) (*NEB*), 2 µl 10 x ligation buffer (*NEB*), vector and insert DNA in the calculated ratio. ddH₂O was applied to a final volume of 20 µl. The ligation mix was stored until transformation into *E. coli* cells.

3.2.9.3 TA-cloning

TA-cloning was performed as described by *Clontech's* user manual. During PCR thermostable Taq polymerase adds a single desoxyadenosine (A) to the 3' ends and the pT-Adv Vector, with its 3'T-overhangs, enables to directly clone these products. Fresh PCR products and 50 ng pT-Adv Vector were added to 1 µl ligation buffer and 1 µl T4 DNA ligase (4U/µl) in a final volume of 10 µl. The ligation reaction was incubated at 14°C either for 4 h or overnight and finally transformation into *E. coli* cells was performed.

3.3 Microbiology

All microbiological procedures were done in a laminar flow hood (Flow BSB 4a) with sterile devices and solutions according to security level 1 conditions. Liquid cultures were carefully shaken and LB-plates were kept in an incubator. Both, liquid cultures and plates were incubated at 37°C.

3.3.1 Preparation of competent *E. coli* cells

To produce competent *E. coli* cells the bacteria were streaked out for a single colony on LB-plates. One colony was inoculated into 10 ml LB-medium and incubated in a shaker overnight at 37°C. The next day 100 ml LB-medium were inoculated with approximately 5 ml overnight culture to give a final optical density of $OD_{600} = 0.1$ and the bacterial suspension was grown to $OD_{600} = 0.7 - 1.0$ at 37°C. 50 ml of the culture was centrifuged (5 min, 4500 x g, 4°C), resuspended in 20 ml ice-cold 0.1 M $MgCl_2$ -solution and incubated for 10 min on ice. After a second centrifugation (5 min, 4500 x g, 4°C), the pellet was resuspended in 20 ml ice-cold 0.1 $CaCl_2$ -solution and kept on ice for further 25 min. Finally, the suspension was again centrifuged (5 min, 4500 x g, 4°C), the pellet resuspended in 2 ml ice-cold 0.1 M $CaCl_2$ -solution and 500 μ l glycerol (100%) were added to immediately freeze cells in liquid nitrogen in 100 μ l aliquots for storage. Competent cells were stored at -70°C.

| | | |
|-----------|------------|---------------|
| LB-medium | 1% (w/v) | peptone |
| | 0.5% (w/v) | yeast extract |
| | 1% (w/v) | NaCl |
| LB-plates | LB-medium | |
| | 1.5% (w/v) | agar |

3.3.2 Transformation of *E.coli* cells

For transformation, one aliquot (100 μ l) of competent *E.coli* cells was thawed on ice, either 10 μ l of ligation mix or 1 μ l of isolated plasmid-DNA was added and the mixture was incubated on ice for 30 min. To allow the DNA to permeate the cell membrane, cells were heat shocked at 42°C for 2 min. After 5 min on ice, 300 μ l LB-medium was added and the mixture was incubated at 37°C for 1 h. Cells were then plated onto LB plates containing the antibiotic ampicillin (50 μ g/ml) and incubated at 37°C until single colonies were grown. In case of blue/white screenings additionally 0.01% (w/v) X-Gal and 0.1 mM IPTG had been spread on the LB-plates before.

3.3.3 Cultures of *E. coli* cells

In order to isolate plasmid-DNA or to make glycerol stocks one single colony of choice was picked and inoculated in 3 ml LB-medium containing ampicillin (50 μ g/ml) overnight at 37°C until the culture was saturated.

3.3.4 Storage of *E. coli* cells

For long time conservation 700 μ l of a saturated bacterial suspension was mixed with 300 μ l of glycerol (100%) and stored at -70°C.

3.4 Protein biochemistry

For protein isolation the cells were cultured as described in 3.1.1 and 3.1.1.1. Cells were either passaged or protein isolation took part after reaching a confluent cell monolayer without subculturing the cells. The whole protein was isolated after two days in incubation medium.

3.4.1 Isolation of proteins from cultured cells

Cells were washed (3x) with PBS, covered with SPBS-solution, scratched with a rubber policeman and collected in a clean tube. All steps after washing were performed on ice to avoid proteinase activity. After centrifugating (4°C, 400 x g, 10 min) the supernatant was discarded and the pellet was resuspended in 100 µl SPBS buffer containing protease inhibitor. The cells were homogenised by pipetting up and down with a syringe, diluted in 100 µl SDS (2x) and denatured for 5 min at 95°C in order to destroy the nucleic acids present in the whole protein lysate. The protein-solutions were stored at -20°C.

| | | |
|------|---|---------------|
| SPBS | 50 mM | NaPi (pH 7.4) |
| | 150 mM | NaCl |
| | 0.32 M | Sucrose |
| | 1 mM | Na-EDTA, |
| | Protease Inhibitor Cocktail® (<i>Boehringer Mannheim</i>) | |

3.4.2 Determination of protein concentration

In order to determine the protein concentration of the isolated solubilised proteins the method developed by Bradford was used (citation). It involves addition of an acidic dye to protein solution and measured at 595 nm with a spectrophotometer. Comparison to a standard curve provides a relative measurement of protein concentration. Bio-Rad protein assay is a dye-binding assay in which a differential colour change of a dye occurs in response to various concentrations of protein. The absorbance maximum for Commassie Brilliant Blue G-250 dye shifts from 465 nm to 595 nm when binding to protein occurs.

3.4.3 SDS-polyacrylamide gel electrophoresis

Discontinuous polyacrylamid gel electrophoresis (SDS-PAGE) (Laemmli 1970) was performed in order to separate complex mixtures of proteins according to their size. Both the sample buffer, containing anionic detergent SDS, and heating to 100°C denatures the proteins

to give a so called random-coil conformation. SDS also masks the intrinsic protein charge and gives all proteins a net negative charge which is proportional to their molecular weight. When loaded onto a gel matrix and placed into an electric field, the negatively charged proteins migrate towards the anode and are separated by a molecular sieving effect. Discontinuous gels contain a short stacking gel with a low percentage of acrylamide to concentrate the sample followed by a resolving gel with a higher percentage of acrylamide. The degree of protein separation depends on the concentration of polyacrylamide, and so the concentration of the separating gel must be chosen according to the expected molecular weight of the sample proteins (table 3-5). Before gel electrophoresis protein samples were denatured for 10 min at 100°C in Laemmli sample buffer. For a 10 cm x 10 cm gel, electrophoresis was performed with 1 x electrophoresis buffer at 20 mA per gel. Experimental conditions for SDS-PAGE are listed in table 3-6.

Table 3-5: Acrylamide concentration for separation of proteins

| Resolving gel (% acrylamide) | 6 | 8 | 10 | 12 | 15 |
|-------------------------------------|--------|--------|--------|--------|------|
| Molecular weight range (kDa) | 30-200 | 20-175 | 15-150 | 10-100 | 6-50 |

Table 3-6: Compounds of SDS-gels.

| | Stacking gel 4.0% | Resolving gel 8% |
|--|----------------------|---------------------|
| ddH ₂ O | 1.85 ml | 2.9 ml |
| 0.4% (w/v) SDS, 1.5 M Tris/HCl, pH 8.8 | 0.75 ml | - |
| 0.4% (w/v) SDS, 0.5 M Tris/HCl, pH 8.8 | - | 1.5 ml |
| Acrylamid / bisacrylamid (37.5 /1) | 0.5 ml | 1.6 ml |
| TEMED | 20 µl | 20 µl |
| APS (10% (w/v)) | 12 µl | 12 µl |

| | | |
|-----------------------------|-------------|--|
| Laemmli sample buffer (3 x) | 30% (v/v) | glycerol |
| | 15% (v/v) | β-mercaptoethanol |
| | 6% (w/v) | SDS |
| | 37.5% (v/v) | 0.4% (w/v) SDS, 0.5 M Tris/HCl, pH 6.8 |
| | | small amounts of bromphenol blue |
| Electrophoresis buffer | 0.25 M | Tris/HCl |
| | 2 M | glycerol |
| | 10% (w/v) | SDS |

3.4.4 Coomassie Blue staining

The location of proteins in a gel was determined by Coomassie Blue staining. This detection method depends on non-specific binding of the dye Coomassie Brilliant Blue R to proteins. The detection limit is 0.3 to 1 µg per protein band. Proteins separated in a polyacrylamid gel precipitated using a fixing solution containing 25% (v/v) isopropanol, 10% (v/v) acetic acid and 0.05% (w/v) Coomassie Brilliant Blue for 30 min. For denstaining the gel was agitated in 10% acedic acid until the blue protein bands appeared against the clear background.

3.4.5 Protein blotting and immunodetection

The expression of proteins was detected by seperating the whole isolated protein by SDS-polyacrylamid-gel electrophoresis (section 3.4.3) and transferring it onto a positively charged nylon membrane (Hybond, *Amersham Biotech*) by semi-dry blotting. Thus, the proteins are immobilised and accessible for antibodies. The nylon membrane was pre wetted with transfer buffer and the gel was transferred onto the membrane. The gel and the membrane were positioned between the transfer-buffer pre-wetted Whatman™ paper and an electrical field (0.5 mA/cm²) was applied for 15 hours. Subsequently, the membrane was washed 3 times with H₂O and rests of the gel were removed. Afterwards, the membrane was pre-blocked with PVP (2% w/v) 3 times for 5 min. The primary antibody was applied in a dilution of 1:1000 in 0.1% PVP (w/v) for 1h (see table 3-7). The membrane was washed again in PVP (2%) and the secondary POD-labelled antibody was applied for 30 min in 0.1% PVP. The detection of the signal was performed by applying Amersham Biosciences Innovative ECL Kit™ (*Amersham*) and exposure to Hyperfilms (*Amersham Biotech*). The protein loading was determined by Protogold Detection Kit™. For this reason the membrane was washed in H₂O and incubated overnight in Protogold solution. Subsequently, the membrane was washed again with H₂O and the intensity of the staining was observed.

Transfer buffer:

| | |
|-----------|----------|
| 20 mM | Tris |
| 150 mM | Glycin |
| 0.1%(w/v) | SDS |
| 20% (v/v) | Methanol |

Table 3-7: Antibodies for western blotting

| Primary antibody | dilution (in 0.1% PVP (w/v); 0.05% TWEEN (v/v) in PBS) |
|---|--|
| Rabbit anti-Occludin (Zymed Laboratories) | 1: 1000 (0.25 mg/L) |
| Rabbit anti-Claudin 5 (Calbiochem) | 1: 1000 (0.25 mg/L) |
| Rabbit anti-ZO1 (Zymed Laboratories) | 1:1000 (0.25 mg/L) |
| Mouse anti-lamin A/C (Santa Cruz) | 1:1000 |
| Secondary antibody | dilution (in 0.1% PVP (w/v); 0.05% TWEEN (v/v) in PBS) |
| Goat anti-mouse (POD) (Sigma) | 1:3000 (0.35 µg/L) |
| Goat anti-rabbit (POD) (Chemicon) | 1:3000 (0.53 µg/L) |

4 Results

Hydrocortisone is known to induce the barrier forming phenotype in cultured porcine brain capillary endothelial cells (Hoheisel et al., 1998). The aim of the present work was to establish new primary culture system of murine derived brain capillary endothelial cells (MBCEC) and to investigate the effect of hydrocortisone on this culture system. After establishment of the murine based blood-brain barrier model *in vitro* the cells were characterised regarding their morphology, expression of common endothelial cell proteins and unique proteins of cerebral capillary endothelial cells. Subsequently, the barrier-forming effect of hydrocortisone was studied. Finally the porcine and the murine system were compared with respect to their barrier-forming properties.

4.1 Establishment of the primary culture of mouse brain capillary endothelial cells

Two alternative ways have been worked out to obtain microvascular endothelial cells from the brain for culturing. The cloning of endothelial cell islands emerging from identified capillaries plated *in vitro* (Dehouck, et al., 1990; Meresse et al., 1989) and the use of enzymatic digestion followed by a gradient centrifugation (Abbott et al., 1992; Franke et al., 2000). In this thesis a two-step digest was used to isolate the capillaries from the surrounding brain parenchyma and to open the basement membrane. Using this method, the cells are able to proliferate after seeding from the digested capillaries to a confluent monolayer.

The isolation was performed following a modified protocol from Maria Deli⁴ (section 3.1.1). After scarifying the mice, the brains were taken out and the meninges of the brains were removed. Subsequently, the brains were homogenised. In order to receive high yields several digestion times for the first digest with collagenase were observed. It was found that the best yields were reached after 1 h incubation with 750 µl collagenase CLS2 (10 mg/ml w/v). After centrifugation, the myelin could be removed and the second unspecific digest was performed. The optimal incubation time for the second digestion step was also 1 h applying 750 µl

⁴ Deli, M.A., Biological research centre Szeged, Hungary; personal communication

collagenase/dispase (10 mg/ml w/v). After the second digest, the cell-suspension was centrifuged, the pellet was resuspended in 2 ml DMEM and applied to a continuous percoll-gradient. The white microvessel-containing interphase was aspirated and the microvessels were obtained by centrifugation. Microvessels were seeded in different densities. To reach a confluent monolayer after 3-4 days *in vitro* the isolated capillaries were seeded in a total of 3 to 4 cm²/brain on collagen IV/fibronectin-coated petri dishes. For characterisation of the cells see section 4.2.

4.2 Characterisation of murine brain capillary endothelial cells

Cerebral capillary brain endothelial cells derived from 6-10 weeks old mice of either sex were isolated and cultured as described in section 3.1.1. Immunofluorescence-staining was performed to prove the localisation of endothelium specific markers like factor VIII-related antigen or blood-brain barrier-relevant proteins like tight junction-proteins. The expression level of tight junction proteins was investigated both, by western blot analysis and quantitative real-time PCR (QRT-PCR).

4.2.1 Morphological characterisation of MBCEC

Endothelial cells *in vitro* express a spindle-shaped morphology building up a confluent monolayer. Depending on the isolation procedure primary MBCEC cultures are more or less contaminated by glial cells. Thus, the first aim of this work was to establish a primary MBCEC culture system with low content of glial cells like astrocytes and pericytes. In order to receive reproducible data it was important to obtain monocultures of BCEC without contamination of astrocytes, pericytes or other cells from the brain parenchym.

4.2.1.1 Morphology of the MBCEC monolayer

Capillary endothelial cells can resist the damage caused by the isolation and enrichment procedures (Panula et al., 1978). Due to the fact that brain capillaries *in vivo* are tightly embedded in diverse glia cells like astrocytes and pericytes (figure 4-2), the isolation

procedure is not completely endothelial cell-specific but leads to co-cultivation with latter mentioned glial cells.

To ensure that only MBCEC were present in the cell culture, the cells were cultured the first two days *in vitro* in puromycin supplemented medium. Puromycin is an antibiotic with apoptosis inducing properties and allows to select specifically the endothelial cells in culture, while other cells die (Sanwal et al., 2001; Fernandez et al., 2001; Linnell et al., 2001; Francoise Roux & Maria Deli, personal communication).

One day after seeding freshly isolated MBCEC, groups of cells formed small islands expressing the so-called “fibroblast-like” morphology. After DIV 4 a confluent monolayer of cells was formed with a fusiform cell-shape with oval nucleus in the centre, neighbouring cells tightly apposed to each other. As shown in figure 4-1 *A*, this shape dominates the murine culture after reaching confluence. Cells cultured in absence of puromycin express also confluent monolayers with the same fusiform morphology but are visibly contaminated by other cell. In phase contrast images of these cultures cells with astrocytic and pericytic shape are visible within the cell-layer (figure 4-1 *B*).

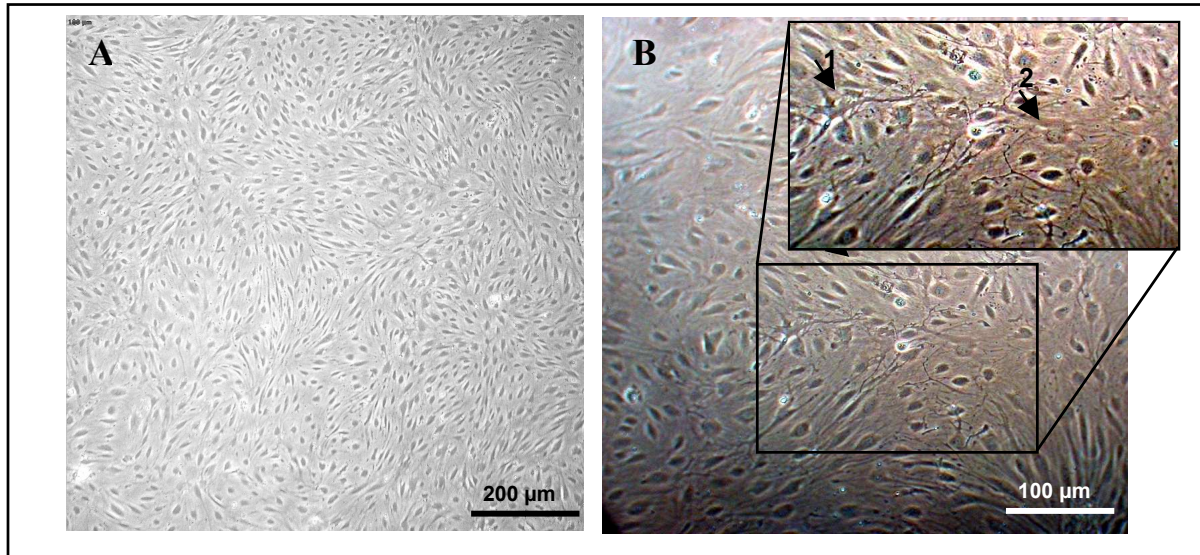


Figure 4-1 Endothelial cell morphology after 4 DIV determined by phase contrast microscopy. Panel *A* illustrates cells cultured in puromycin containing medium. The cells within the monolayer show the typical spindle-shaped morphology without gaps between cells. No contaminating cells are visible. Panel *B* images a cell layer of MBCEC cultured in absence of puromycin. In addition to the spindle-shaped morphology different structures are visible (arrows 1+2). The presence of contact inhibition is seen in both panels as no visible multilayers of cells can be detected.

Indirect immunofluorescence staining was performed with anti-*GFAP*-antibody against the astrocyte-specific *glial fibrillary acidic protein* (Pegram et al., 1985) and anti- α -*sm-actin*-antibody against smooth-muscle cell-actin for visualisation of pericytes (Skalli et al., 1989). Figure 4-2 indicates that no astrocytes were detectable in both, cultures supplemented with and without puromycin. In contrast, MBCEC cultured without puromycin are contaminated by pericytes (figure 4-2 C). No pericytes remain detectable in MBCEC cultured in puromycin-containing medium (figure 4-2 D).

Only these monocultures of MBCEC were chosen for further experiments concerning blood-brain barrier properties.

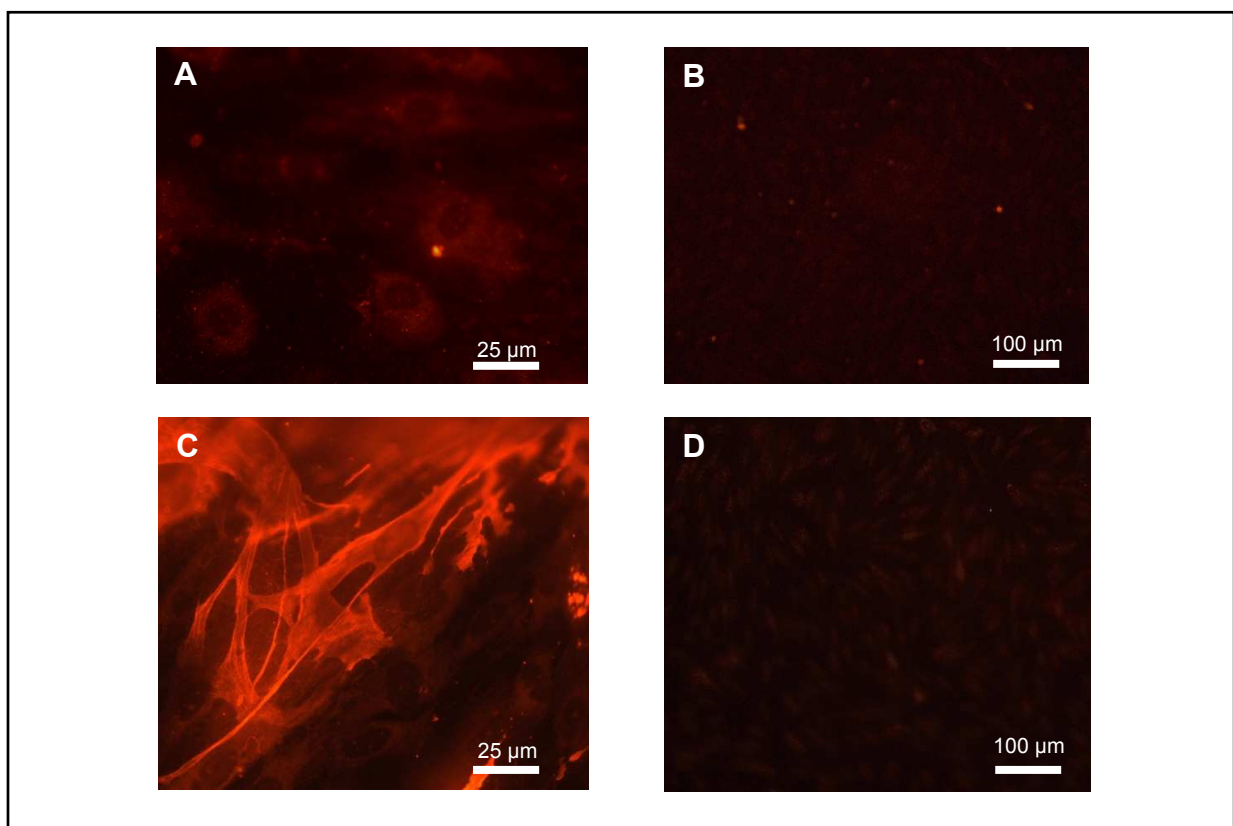


Figure 4-2: Immunofluorescence stain of MBCEC *in vitro*. A+B: Immunostaining against *glial fibrillary acidic protein* (GFAP). A: puromycin-free medium B: puromycin-supplemented medium. C+D: Immunofluorescence against α -smooth-muscle cell actin. C: puromycin-free medium D: puromycin-supplemented medium. While no astrocytes are detectable (A+B), cells cultured without puromycin are contaminated by pericytes (C).

4.2.1.2 Immunostaining of tight junction- and tight junction-associated proteins

One characteristic feature of cerebral capillary endothelial cells is the presence of well developed tight junctions. These tight cell-cell contacts are basically influenced by membrane localised proteins and form a belt between adjacent cells (section 2.2.1). The presence of tight junctions and tight junction-related proteins, such as ZO-1, was determined by indirect

immunofluorescence staining (3.1.3). The staining was performed either on permeable filters or on cover slips. On both substrates, MBCEC expressed the same staining pattern of investigated proteins. Thus, it was examined that the substrate has no effect on the immunofluorescence staining of cells. Due to the fact that no difference could be detected between the two culture conditions, only the data from MBCEC cultured on filter-substrates are shown. For investigation of tight junction expression, the tight junction-proteins occludin, claudins-1 and -5 and the tight junction-associated protein ZO-1 were chosen (figure 4-3).

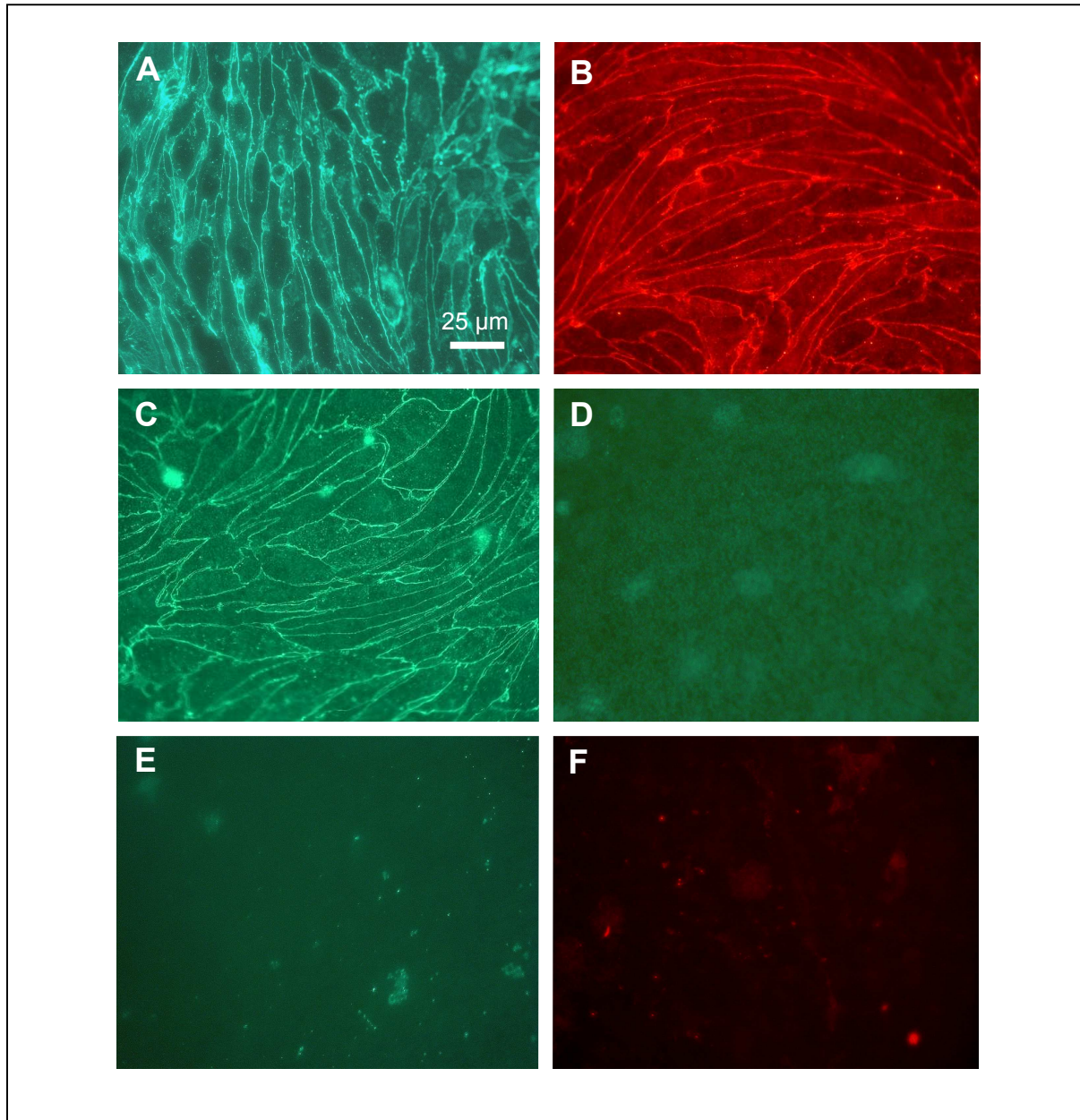


Figure 4-3: Tight junction expression in MBCEC. Micrographs show immunofluorescence labelling of cells after 6 DIV in serum-containing medium using antibodies against the tight junction proteins occludin, ZO-1, claudin-1 and -5. Panel A shows staining of occludin, panel B indicates ZO-1-staining. Panel C: Claudin-5; panel D: Claudin-1. Panel E: Secondary antibody control to A, C+E; F: secondary antibody control for B. Partial areas in the cell layer show cobble-stone cells while others express the fusiform morphology. Except claudin-1, the tight junction proteins occludin, claudin-5 and ZO-1 could be detected by immunofluorescence staining.

Figure 4-3 *A* reveals a specifically membrane-localised staining of occludin. The cell borders appear frayed. The cells express a heterogeneous morphology: Some of the cell bodies show the fusiform shape while others appear more cobble-stone-shaped. In contrast to ZO-1 and occludin, claudin-5 staining appears not as a distinct border between adjacent cells but shows a dotted line. The staining indicates only membrane-localisation while no staining can be detected at the nucleus. The same applies to claudin-5 and occludin (figure 4-3 *B, C*). The heterogeneous morphology of MBCEC is detectable by staining with anti-occludin and anti-claudin-5 antibody. Claudin-1 was not detectable in MBCEC by immunofluorescence staining (figure 4-4 *D*).

Double immunofluorescence staining was performed to investigate co-localisation of occludin, claudin-5 and ZO-1. Double staining against ZO-1 and occludin was performed as well as against ZO-1 and claudin-5. Data indicates a co-localisation of these three proteins at the cell borders between adjacent cells (figure 4-4).

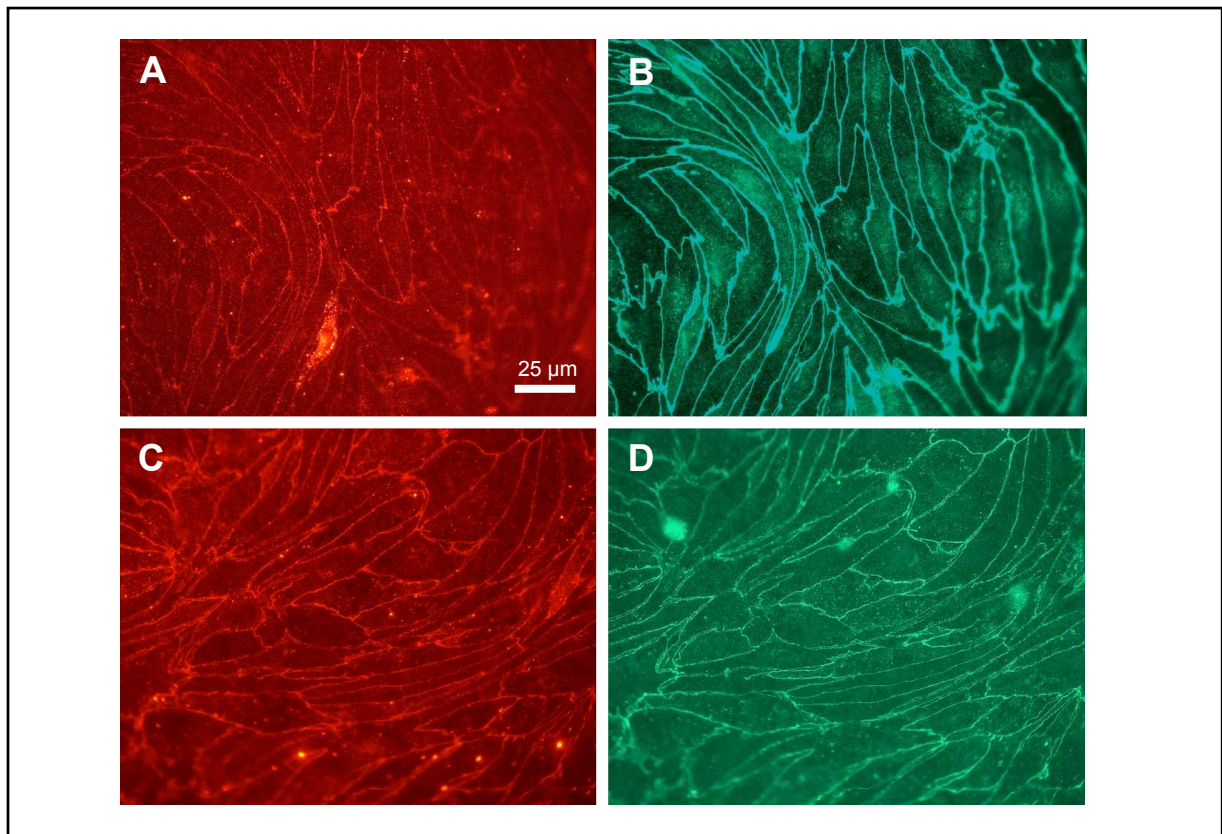


Figure 4-4: Immunofluorescence labelling of tight junction proteins in MBCEC. Double-immunofluorescence staining was performed at the 6. DIV. *A+B*: Immunostaining for ZO-1 (*A*) and occludin (*B*): *C+D*: co-localisation of ZO-1 (*C*) and claudin-5. The cells show both, a spindle-shaped morphology with distinct staining at the cell borders and a more cobble-stone shape with fuzzy staining. ZO-1 and the transmembrane proteins occludin and claudin-5 are co-localised.

4.2.1.3 Cellular localisation of brain multidrug resistance protein and factor VIII

Endothelial cells show expression of different membrane localised transporters as for instant P-glycoprotein or multi-drug resistance proteins of the family of ABC-transporters (Cordon-Cardo et al., 1989; Huai-Yun et al., 1998; McNamara and Lenox, 1998; Zhang et al., 2000). Brain Multidrug Resistance Protein (BMDP), a new multidrug resistance protein at the blood brain-brarrier, was detected in porcine capillary endothelial cells (Eisenblatter and Galla 2002). In order to observe, if this transporter is present in the isolated MBCEC as well, immunofluorescence staining against BMDP was performed. The MBCEC *in vitro* show a membrane-localised staining for BMDP (figure 4-5 A). The cells stained with antibodies against BMDP show the typical spindle-shaped morphology and are attached to each other. The protein is mainly located at the membrane and shows a weak cytoplasmic signal (see also figure 4-13). The expression of BMDP and P-glycoprotein was quantified on RNA- and protein level (section 4.3)

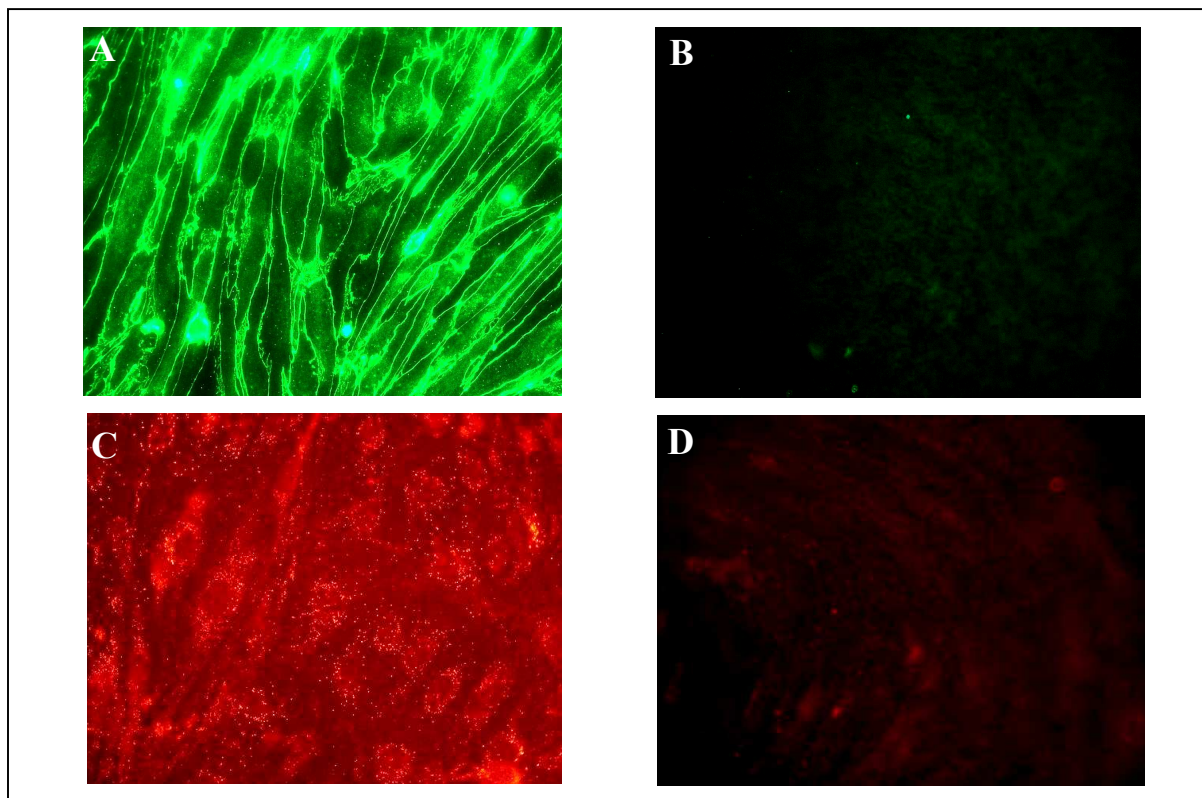


Figure 4-5: Localisation of brain multidrug resistance protein and factor VIII in MBCEC after 6 DIV. *A:* Anti-BXP 391 staining of BMDP. The protein is located at the membranes and shows weak cytoplasmic staining. *B:* MBCEC stained with secondary antibody to A. Panel C shows a micrograph of immunofluorescence staining against factor VIII. The protein is localised in the cytoplasm and indicates a granular pattern. Panel D shows the control stained with secondary antibody.

Another characteristic marker for endothelial cells is the expression of factor VIII (Bowman et al., 1981, Phillips et al., 1979). Figure 4-5 C renders the typical immunostaining pattern of this cytoplasmatic localised protein in MBCEC that is mainly accumulated in Weibel-Palladebodies (Wagner and Marder, 1984).

4.3 Identification of blood-brain barrier related proteins on RNA-level

Several methods were developed to detect RNA and to determine the RNA expression levels of specific genes. Northern blot analysis is the main tool used to identify genes quantitatively on the RNA level, but this technique requires large amounts of total RNA (25 µg). With PCR and its application to analyse RNA by reverse transcription (RT) and its ability to amplify the target genes by polymerase chain reaction, a new approach was found to quantify expression with small amounts of RNA (0.4 µg). While existing methods are generally time-consuming, the new method developed by (Higuchi et al., 1992; Higuchi et al., 1993) allowed the real-time detection of amplicons during the PCR (quantitative real-time polymerase chain reaction (QRT-PCR)). This method facilitates the detection of different expressed genes in RNA-species isolated from cultured cells or tissues. The expression pattern of proteins in a cell population is closely related to the function of the cells *in vivo*. Thus, it is possible to estimate the presence of proteins by determining their expression on the RNA-level. However, to quantify the expression of proteins, western blot analysis is necessary.

The application of QRT-PCR is beneficial to identify specific markers for microvascular brain endothelial cells on the RNA level. The reaction was performed and data was examined as described in section 3.2.7.2. Figure 4-6 presents the retrieved data of QRT-PCR. The typical marker enzymes for endothelial cells and blood-brain barrier phenotype are expressed on the RNA-level. The grade of expression of angiotensin converting enzyme and ferritintransferase is similar to the expression of GAPDH which was used as a house-keeping gene. γ -Glutamyltraspeptidase (GGT) and alkaline phosphatase (ALP) is lower expressed on the RNA-level but also detectable in MBCEC. Two other typical proteins could be detected: P-glycoprotein and BMDP. The RNA-expression level of these enzymes is comparable high in MBCEC.

Two well known marker enzymes for blood-brain barrier endothelial cells are alkaline phosphatase (ALP) and γ -glutamyltranspeptidase. Ferritin-transferase and angiotensin converting enzyme are known to be expressed in endothelial cells. As described above, the transporters P-glycoprotein and BMDP, were shown to be highly expressed at the blood brain-barrier. These enzymes were chosen to be investigated on expression pattern in the primary culture of MBCEC.

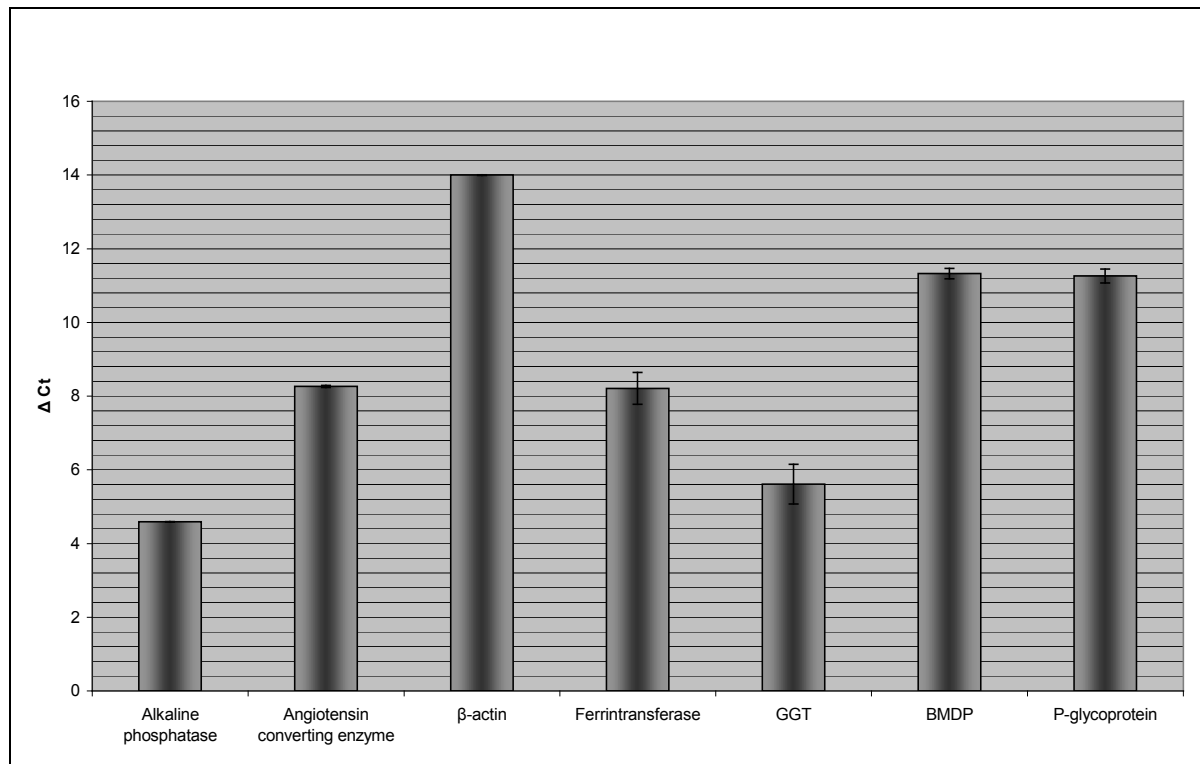


Figure 4-6: Expression of mRNA of blood-brain barrier related proteins and house-keeping genes. QRT-PCR was performed with 0.4 μ g total-RNA isolated from cells after DIV 5 in serum-containing medium. The reaction was executed with primers reported in appendix D. ΔC_T -values: alkaline phosphatase: 4.59; angiotensin-converting. enzyme: 8.27; β -actin: 14; ferritintransferase: 8.21; γ -glutamyltranspeptidase (GGT): 5.61; brain multidrug-resistance protein: 11.33; P-glycoprotein: 11.26. (standart deviation for n=3)

4.4 Functional effects of hydrocortisone on MBCEC

4.4.1 Electrical properties of MBCEC

It is well known that hydrocortisone strengthens the barrier function with respect to the electrical resistance and the permeability for sucrose of porcine brain capillary endothelial cells (Hoheisel et al., 1998a). The question arises, if this strengthening is a common effect in mammalian primary cultures of endothelial cells derived from brain capillaries.

4.4.1.1 Results of impedance spectroscopy and quartz microbalance on MBCEC

Impedance spectroscopy is, as described in section 3.1.6, a sensitive method to determine the transendothelial electrical resistance (TEER) across cell monolayers. As previously described, Hoheisel et al., (1998) found that porcine microvascular endothelial cells cultured in hydrocortisone-containing medium form a barrier with high electrical resistances and low sucrose permeability. Both, permeability and TEER mirror a degree of barrier formation similar to *in vivo* conditions. Following the assumption that murine derived endothelial cells behave similarly, MBCEC were isolated and cultured under similar conditions as PBCEC (section 3.1.1). These cells were subcultured for 2 days on rat tail collagen coated transwell filters (*Costar*) until they reached confluence. The TEER and permeability experiments were performed either 24 h or 48 h after the addition of the incubation medium (either serum-containing medium or SFM with hydrocortisone). Alternatively, long-term measurements were started directly after addition of hydrocortisone and serum, respectively.

Experiments show that hydrocortisone, in physiological concentration of 550 nM (Karlson, 1994), leads to a 5-fold higher electrical resistance than serum containing medium in MBCEC. The TEER rarely reached values higher than $500 \Omega \cdot \text{cm}^2$ after addition of hydrocortisone-supplemented medium. But usually the TEER amounted to $200 \Omega \cdot \text{cm}^2$ in hydrocortisone-containing medium while serum maintained the resistance at around $40 \Omega \cdot \text{cm}^2$ (figure 4-7). The withdrawal of serum and incubation of the cells in serum-free medium leads to a further decrease of TEER ($30 \Omega \cdot \text{cm}^2$). In comparison to the primary culture of porcine endothelial cells this is a contradictory result. The withdrawal of serum in PBCEC-culture leads to an increase in TEER (Hoheisel et al., 1998).

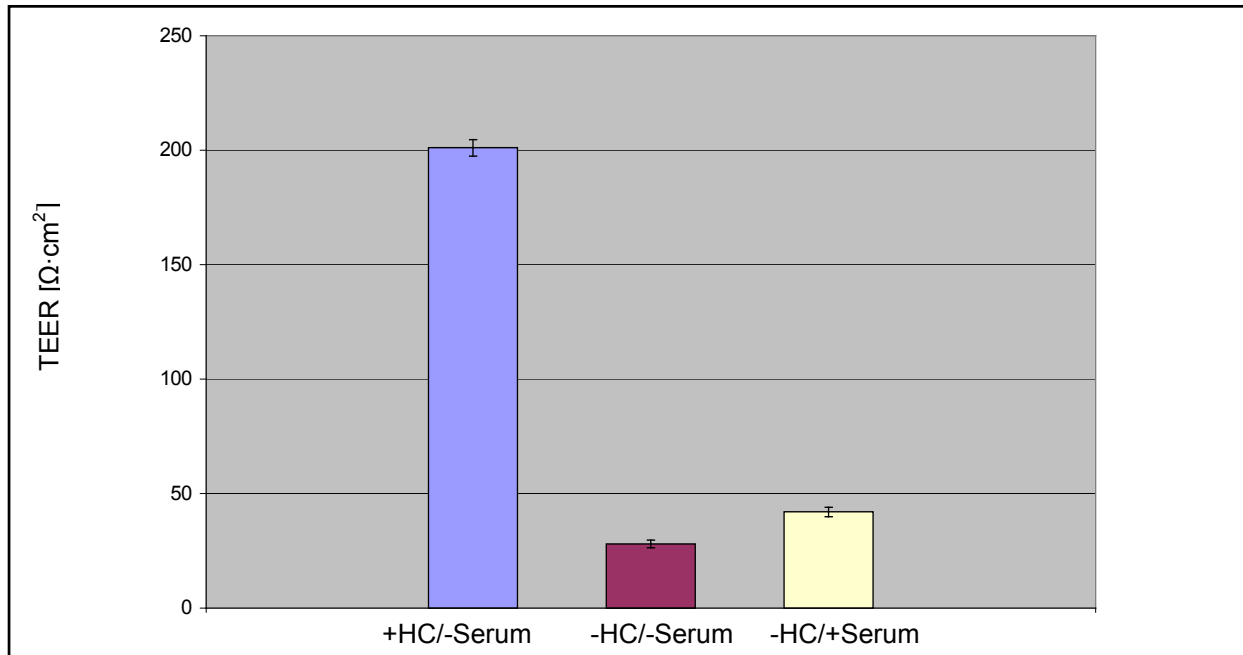


Figure 4-7: Influence of hydrocortisone on transendothelial resistance on MBCEC under different culture conditions. The cells were subcultured after DIV 3 and incubation medium was applied on the DIV 5. The measurement was performed after 2 more days. Cells cultured with hydrocortisone show a 5-fold higher TEER ($201 \Omega \cdot \text{cm}^2 \pm 3.6 \Omega \cdot \text{cm}^2$) than cells cultured in serum-containing medium $42 \Omega \cdot \text{cm}^2 (\pm 2.1 \Omega \cdot \text{cm}^2)$ while TEER of cells cultured without both supplements reach values of about $28 \Omega \cdot \text{cm}^2 (\pm 1.7 \Omega \cdot \text{cm}^2)$. (Standart deviation for $n=5$)

In order to investigate the time course of HC induced barrier strengthening the TEER was observed for 72 hours after addition of the incubation medium. Following the measurement (figure 4-8) the resistance starts to increase not directly but 2 hours after addition of hydrocortisone-containing medium. The resistance increase ($6 \Omega \cdot \text{cm}^2/\text{h}$) is almost linear until 15 hours after exchange of medium. The maximum value is reached after 40 hours. These results match the data received from PBCEC although these cells reach the highest resistance after 16 hours in hydrocortisone-containing medium (Nitz, 2001). MBCEC cultured under hydrocortisone conditions stay at high resistances for 20 hours and the decrease is recognisable after 55 hours in culture. In serum-containing medium the resistance increases slowly for 15 hours. Finally the cells remain at resistances around $40 \Omega \cdot \text{cm}^2$ for 40 hours. A following decrease is detectable after 40 hours and the measurement was stopped after 72 hours when the cells reached 80% of the maximum value. The cells cultured in serum-containing medium stay at low resistances during the observed 70 hours. The TEER reaches 30% of the maximum value of hydrocortisone-treated cells.

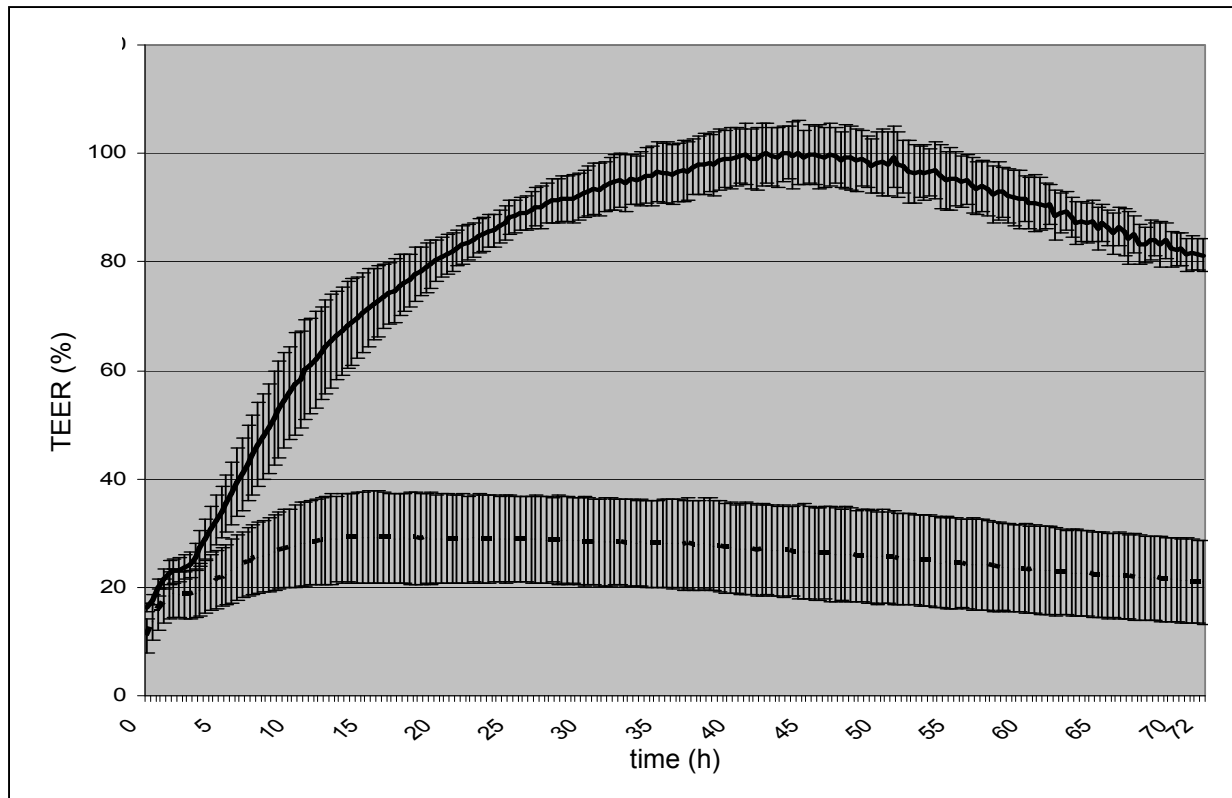


Figure 4-8: Time-dependent effect of hydrocortisone in MBCEC. The cells were subcultured after DIV 3 and the medium was exchanged after DIV 5. The measurement was started directly after application of incubation medium. The continuous line indicates the values for the hydrocortisone-supplemented cells, the broken line shows values for cells in serum-containing medium. The highest value for hydrocortisone was set as 100%. The measurement was performed on rat-tail collagen coated filters. All values were averaged (standard deviation for $n=3$).

4.4.1.2 Electric cell-substrate impedance sensing and quartz crystal microbalance measurements on MBCEC

As described in section 3.1.6.2 electrical cell-substrate sensing is a method to discriminate between three different morphological parameters. Whereas impedance spectroscopy on filters only gives the sum of resistances over the cell layer the application of ECIS allows distinguishing between more parameters. The parameter α describes the impedance contribution from the cell substrate adhesion zone and R_b indicates the resistance between the cells. Furthermore, it is possible to follow the capacitance of the system. The advantage in the separation of R_b and α is the opportunity to correlate changes in cell-substrate interaction and increase or decrease in paracellular resistance respectively.

In section 3.1.7 the applicability of QCM was described. This feature as well as ECIS to distinguish between α and R_b . Additionally, it is possible to measure the electrical parameter

in correlation with mechanical properties of the cells since a modulation in attachment to the quartz crystal would result in a difference in resonance parameters.

In quartz mode the cells were examined for their properties under different culture conditions (figure 4-9). MBCEC grown in serum-containing medium show no significant difference in motional resistance R but a trend to higher values is observed when cells are treated with hydrocortisone. The values for serum-treated cells reach $481 \Omega (\pm 16 \Omega)$ while hydrocortisone-treated cells are characterised by $512 \Omega (\pm 20 \Omega)$. The values for inductivity are also similar under both, serum- and hydrocortisone conditions. The difference between both culture conditions lay in range from $3.5 \mu\text{H} (\pm 4.6 \mu\text{H})$ for serum-treated cells to $4.3 \mu\text{H} (\pm 0.3 \mu\text{H})$ for hydrocortisone-treated cells.

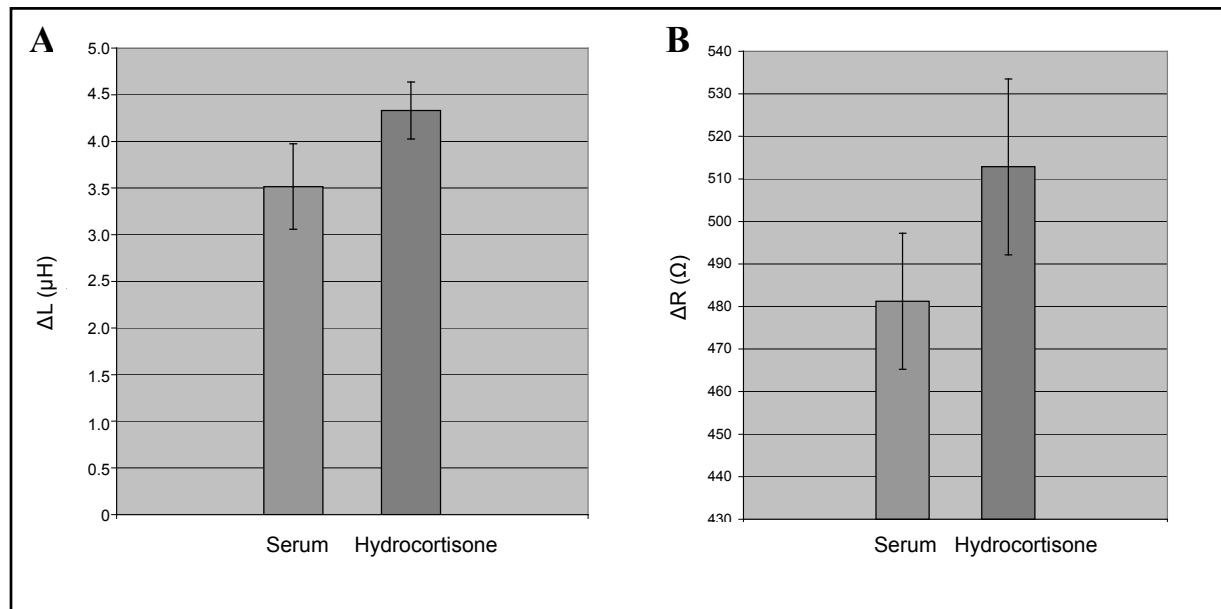


Figure 4-9: **A** the motional inductance ΔL and the **B** motional resistance ΔR of MBCEC cultured under two different conditions. The measurement was performed at room-temperature after an equilibration-time of 10 min. A total of $n=5$ resonators were investigated. A weighted average is presented.

The cell mode of the same measurements indicates a change in the electrical parameter. The parameters α and R_b show an increase from cells cultured in serum-containing medium compared to hydrocortisone-treated cells. The value of serum treated cells is around $13.5 \Omega^{1/2}\cdot\text{cm} (\pm 0.3 \Omega^{1/2}\cdot\text{cm})$ for α whereas R_b reaches $17.9 \Omega\cdot\text{cm}^2 (\pm 2.8 \Omega\cdot\text{cm}^2)$. There is a significant increase when the cells are cultured with 550 nM hydrocortisone ($\alpha = 23.5 \Omega^{1/2}\text{cm} \pm 0.9 \Omega^{1/2}\text{cm}$ and $R_b = 72.3 \Omega\cdot\text{cm}^2 \pm 8.4 \Omega\cdot\text{cm}^2$). This fact is a hint that hydrocortisone influences both, the cell-cell contacts (tight junctions) and the cell-substrate interactions.

It was interesting to find that hydrocortisone influences the capacitance of the cell layer. In PBCEC the membrane capacitance was quantified to $1 \mu\text{F}/\text{cm}^2$ for both culture conditions. MBCEC, however, reach values of $0.66 \mu\text{F}/\text{cm}^2$ (serum treated-cells) and $0.82 \mu\text{F}/\text{cm}^2$ (hydrocortisone-treated cells). Whereas the capacitance is governed by the structure of the membrane (microvilli, smooth surface) these findings implicate a change in membrane morphology. The ECIS-measurements performed on 8-well electrodes (data not shown) as described in section 3.1.6.2 correlated directly with the data shown in (figure 4-10).

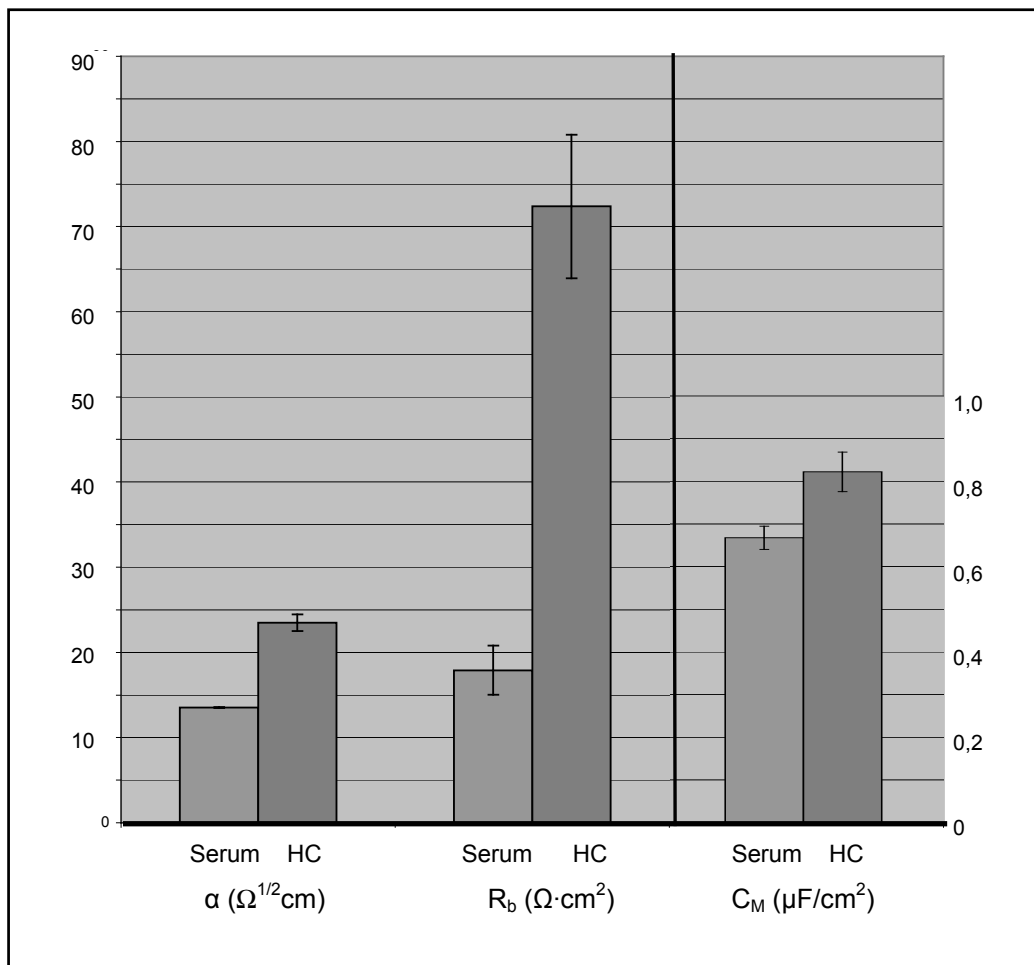


Figure 4-10: Results of ECIS. The same cells as in figure 4-9 were measured. α , R_b and C_M are presented as weighted average values for $n=5$. The measurement was performed at room-temperature after equilibrating the cells for 10 min. Hydrocortisone increases the parameter α indicating that the cell-substrate contact or the extracellular matrix is influenced by the glucocorticoid hormone. R_b indicates a strengthening of cell-cell contacts induced by hydrocortisone. The values for the membrane capacitance indicate a monolayer structure different from a layer of endothelial cells. Hydrocortisone influences this parameter as well as α and R_b .

4.4.2 Sucrose permeability of MBCEC

The intact microvasculature is an impermeable barrier for sucrose *in vivo*. This molecule diffuses neither passively across the barrier nor is it transported actively across the cell monolayer. This is also well known from *in vivo*-studies (Bowman et al., 1983; Gruenau et al., 1982; Neuhaus et al., 1991; Rubin et al., 1991). The fact that sucrose is a small hydrophilic molecule makes it suitable to quantify barrier properties of endothelial and epithelial cell-layers. Small lacks in the cell layer drastically increase the permeability for this marker. In this work sucrose permeability was studied to discover the barrier forming properties of MBCEC in correlation to the electrical resistances found as described in section 4.4.1.

Independent from the culture conditions the permeability of MBCEC is very high. While the permeability of PBCEC is in the range of $6 \cdot 10^{-7}$, MBCEC show a permeability in a range from $1.5 \cdot 10^{-5}$ up to $1 \cdot 10^{-4}$ cm/sec (figure 4-11). The latter value is already in the range of an empty filter without a cell layer. It is obvious that in presence of hydrocortisone the cells possess a lower permeability than cells cultured in serum free-medium. Hydrocortisone decreases the permeability down to $2.7 \cdot 10^{-5}$ cm/sec in comparison to serum-free medium. On the other hand the presence of serum reduces the permeability to values comparable with hydrocortisone. These results have to be interpreted carefully due to the systematic errors.

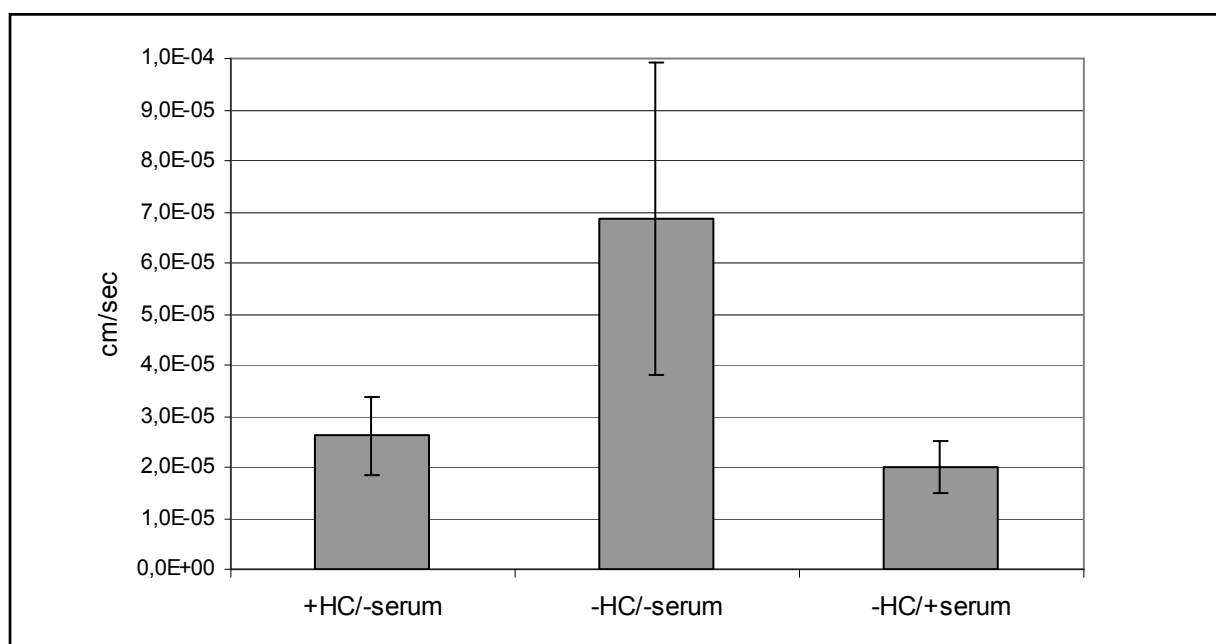


Figure 4-11: Permeability of MBCEC. Cells were cultured 3 DIV and subcultured for 2 DIV until exchange of medium. After the second day in incubation medium the permeability for 14 C-sucrose was determined for different incubation media (standart deviation n=5).

4.4.3 Influence of hydrocortisone and serum on morphology of MBCEC and localisation of tight junction proteins

To ascertain the influence of hydrocortisone on MBCEC initially on the morphology and localisation, expression and structure of tight junction proteins of the cells, MBCEC treated with hydrocortisone were examined in comparison to cells cultured in serum containing medium. Especially the increase in the electrical resistance of the parameter R_b (cell-cell contacts) leads to the assumption that the expression of tight junction proteins is altered. After the monolayer reached confluence, the medium was exchanged from culture medium to incubation medium (either serum-free medium supplemented with or without hydrocortisone) or serum-containing medium (foetal calf serum).

4.4.3.1 Cell morphology

Figure 4-12 (A+B) show phase contrast images of cells cultured in two culture-conditions. The cells were cultured in either serum containing medium or in medium without serum supplemented, with hydrocortisone. The cells were not subcultured, but grew in petri dishes until reaching confluence. As figure 4-12 indicates, both culture conditions have no influence on the visible integrity of the monolayer. The layers are confluent and neither hydrocortisone nor serum-containing medium interrupts or cause larger gaps in the layer. While under serum-content the cells confirm their spindle shaped morphology, cells under influence of hydrocortisone express both, a cobble-stone structure and spindle-shaped pads within the layer. In areas with spindle-shaped morphology lower contrast remain detectable. The change of morphology takes place after 8-10 hours following the exchange of the medium. Indirect immunostaining against the membrane localised tight junction protein occludin also illustrates this phenomenon (figure 4-12 C+D). The cells were cultured on permeable filters and analysed by impedance spectroscopy before fixing and providing the immunostaining procedures. The hydrocortisone treated MBCEC show a heterogenic morphology: Some cells are cobble-stone shaped while others, within the layer, form pads appearing in a spindle-shaped morphology. The staining at cell borders in areas with spindle-shaped cells is more distinct while the areas with different shape are characterised by a more diffuse structure of

cell-cell contacts. The ratio of spindle shaped cells is in a range of 50%. The serum-treated cells form a more homogenic layer with more or less cobble stoned morphology. Interestingly, the cells react different after subcultivation (figure 4-12 C+D). Before subculturing, the cells express spindle-shaped structures after serum-treatment, while the subcultured cells grown on filters and cultured in serum show the homogenic cobble-stone structure. Evidently the serum-treated cells show less distinct staining at the cell borders but more a diffuse cytoplasmic fluorescence (see also figure 4-13).

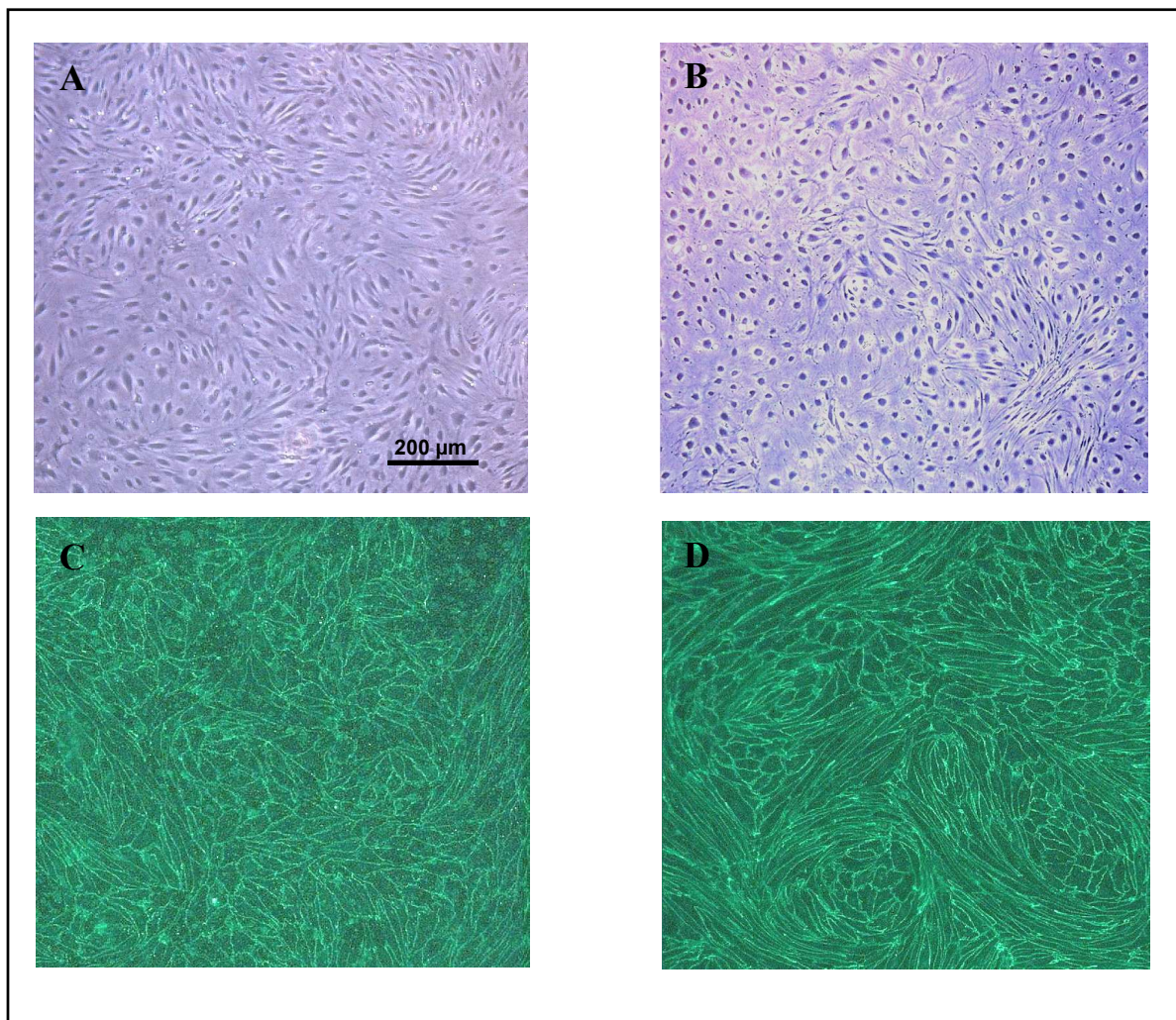


Figure 4-12: Morphology of cells treated either with serum- or with hydrocortisone-containing medium. A: Phase contrast of cells cultured until confluence without subculturing in serum-containing medium. Serum-treated cells show a fusiform cell-morphology. B: Phase contrast of cells treated with hydrocortisone containing medium. Hydrocortisone cells form a cobble-stone monolayer with pads of spindle-shaped cells. C+D: Cells after subculturing on rat-tail collagen coated filter-membranes. C: Anti-occludin staining of cells (serum). Serum-treated cells indicate a homogenic cobble-stone shaped cell-layer. D: anti-occludin staining of cells on filter membranes (hydrocortisone). These cells indicate a heterogenic morphology, either cobble stone- or fusiform shape.

4.4.3.2 Localisation of *tight junction-* and *tight junction* associated proteins

The identification and localisation of tight junction proteins occludin, claudins or occludin associated proteins like ZO-1 mirror the state of the tight junctions. As shown in figure 4-3, the tight junction proteins occludin and claudin-5 are expressed in MBCEC *in vitro*. The same applies to ZO-1. As described in section 4.4.1, hydrocortisone strengthens the electrical resistance from MBCEC. To observe if this is an effect of tight junction formation MBCEC were examined by immunofluorescence staining concerning the structure of tight junction proteins. Due to the fact that BMDP staining is membrane localised and similar to tight junction staining, the detection of this protein gives the advantage when comparing a non-tight junction specific change in the membrane morphology of the cells.

Figure 4-13 shows the results for indirect immunofluorescence of latter mentioned proteins. As referred to in section 4.4.3.1, hydrocortisone influences the structure of antibody-mediated staining of target proteins. The cells shown in figure 4-13 were cultured under three different conditions: They were either treated with serum-free medium with or without hydrocortisone or with serum-containing medium. As figure 4-13 indicates, withdrawing the serum already cause a redistribution of ZO-1. Serum-treated cells show a more diffuse staining of the membrane with partially fuzzy staining between adjacent cells, the serum withdrawal results in more distinct staining. Furthermore, several gaps appear between the tight junction strands of adjacent cells cultured in serum (figure 4-13 A+B). The frayed staining pattern disappears in culture with hydrocortisone. Additionally, the background stain and stain around the nucleus vanishes. The cell borders are more distinct and the cell morphology changes from cobble stone shape with serum to spindle shape when treated with hydrocortisone. The same applies to occludin. The change in morphology can be observed in figure 4-13 (D-E). The cells are lanker and the staining appears more distinct. Also gaps appear between cells under serum conditions while the membranes indicate a frayed morphology. Supplementing the culture medium with hydrocortisone leads to an increase in membrane staining when using anti-occludin primary antibody. The indirect immunofluorescence of BMDP, as a membrane standing, but not tight junction-associated protein gives the same appearance. In the presence of hydrocortisone the protein seems to be translocated to the membrane. Again the staining is more distinct while the background vanishes.

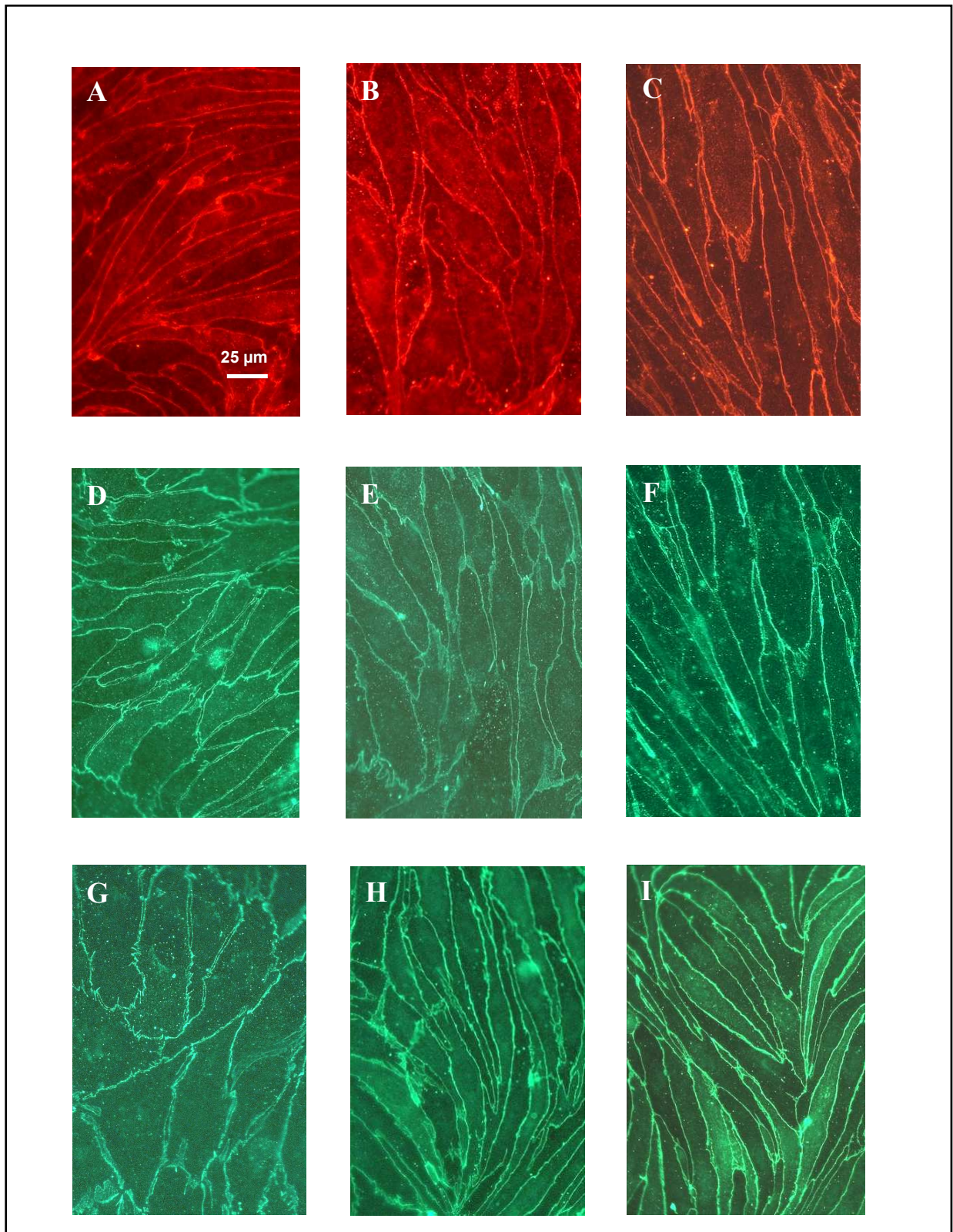


Figure 4-13: Effect of hydrocortisone on tight junctions. A, B, C: ZO-1; D, E, F: occludin; G, H, I: BMDP. Serum-containing medium: A, D and G; serum-free medium: B, E and H; hydrocortisone-containing medium: C, F and I. The cell-cell contacts appear more distinct when the MBCEC are cultured in hydrocortisone-supplemented medium. The cell-morphology changes to fusiform shape after hydrocortisone-treatment.

4.4.3.3 Influence of serum and hydrocortisone on the cytoskeleton

Actin is the most frequent protein in cells and occurs both, as soluble globular actin (G-actin) and as fibrous actin (F-actin). F-actin builds together with myosin the major compound of the cytoskeleton. Because of the contractile properties of f-actin and its linking to the tight junctions (figure 2-3), hydrocortisone may influence redistribution of actin filaments and therefore, may induce a morphological change of cells.

Figure 4-14 displays a staining with rhodamine-labelled phalloidin against actin filaments. The cells were cultured on microporous filter membranes, like the cells shown in previous images. Cells cultured in serum-containing medium indicate a lateral staining localised predominantly at the membranes with a high contrast to the cytoplasm (perijunctional staining). With removal of serum, actin redistributes within the cell body and evinces a filamentous distribution in the longitudinal direction of the cells. The addition of hydrocortisone enhances this effect and the intensity of distinct filamentous staining is increased (figure 4-14 *B*) in comparison to serum-free cultured cells (figure 4-14 *C*). Due to the fact that the tight junctions are linked to the cytoskeleton a change in the distribution of stress fibres may result in a morphological change of the distribution pattern of the membrane standing tight junction proteins.

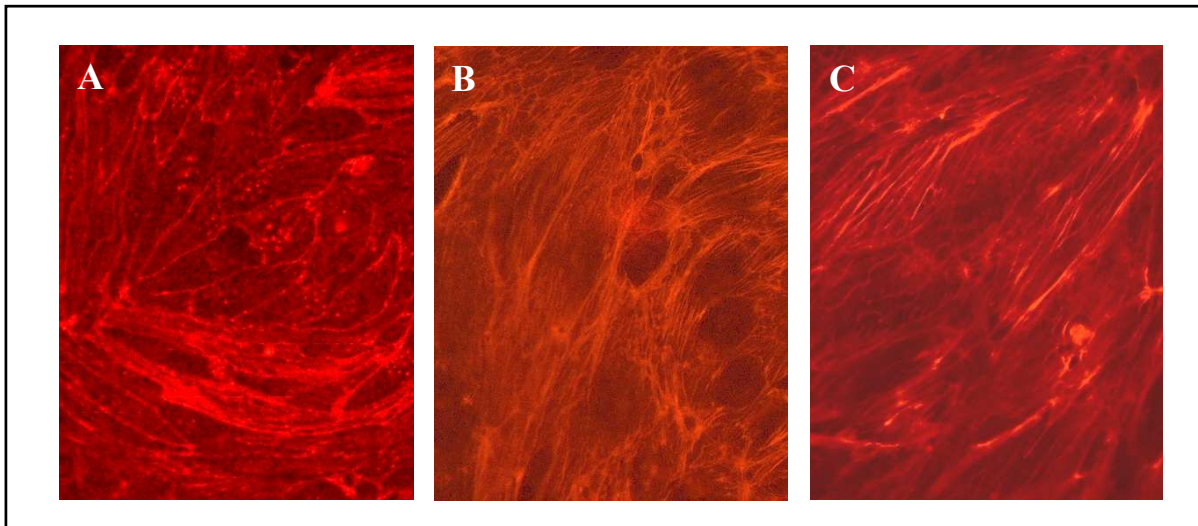


Figure 4-14: Direct phalloidin-staining of actin in MBCEC. A: serum-containing medium; B: serum-free medium; C: serum-free medium supplemented with hydrocortisone. The cells were cultured 2 days in incubation medium. The withdrawal of serum leads to a redistribution of actin within the cells. After addition of hydrocortisone, distinct actin-filaments appear in the longitudinal direction of the cell.

4.4.4 Influence of hydrocortisone on cell-cell contacts and cell surface

Phase contrast imaging and immunofluorescence staining give an idea of localisation and expression of individual proteins. To investigate the ultrastructure of the cells, other applications are necessary. Atomic force microscopy is a powerful tool for detection of ultrastructural characteristics of biological probes under physiological conditions.

4.4.4.1 Investigations of MBCEC by Atomic force microscopy

Phase contrast imaging and immunofluorescence staining of MBCEC indicates a morphological change after application of hydrocortisone. To investigate ultrastructural changes, atomic force microscopy was performed to explore changes in the surface morphology and the elasticity of cells cultured in different media. As mentioned in section 3.1.4, AFM allows obtaining information about changes in surface structures and enables the imaging of cell-cell contacts and stress fibres. The tight junction region between the cells was of special interest. Furthermore, it is possible to measure the elasticity by calculation of the Young's modulus. This information enables to draw conclusions about change in morphology as well as probable redistribution of actin filaments.

4.4.4.1.1 Investigation of topography profiles of MBCEC by AFM

Figure 4-15 presents topography profiles and deflection of cells cultured either with or without hydrocortisone⁵. The AFM images imply a hydrocortisone-induced structural reorganisation or formation of cytoskeleton elements and a change in the tight junction morphology. In correlation with immunofluorescence, cell-cell contact areas indicate frayed tight junction regions. The cells are cobble-stone shaped and the cytoskeleton elements are marginally seen. In hydrocortisone-treated cells the cell-cell contacts appear as distinct lines between adjacent cells and cytoskeletal elements are distributed in the longitudinal direction of the cells. The tight junctional region in hydrocortisone-treated cells indicates a cleft which can be seen in figure 4-15 *B*. In comparison, the structure of the cells cultured without

⁵ AFM investigations were performed in collaboration with Sebastian Schrot, Institut für Biochemie, WWU Münster, Germany.

hydrocortisone implies an increased altitude at the cell borders. This finding can be proven by analysing the profiles of the tight junction region (figure 4-16). After hydrocortisone-treatment, the average of altitude of tight junction regions indicates an increase. The data of cells cultured in serum-containing medium correspond to the findings in serum-free medium (data not shown).

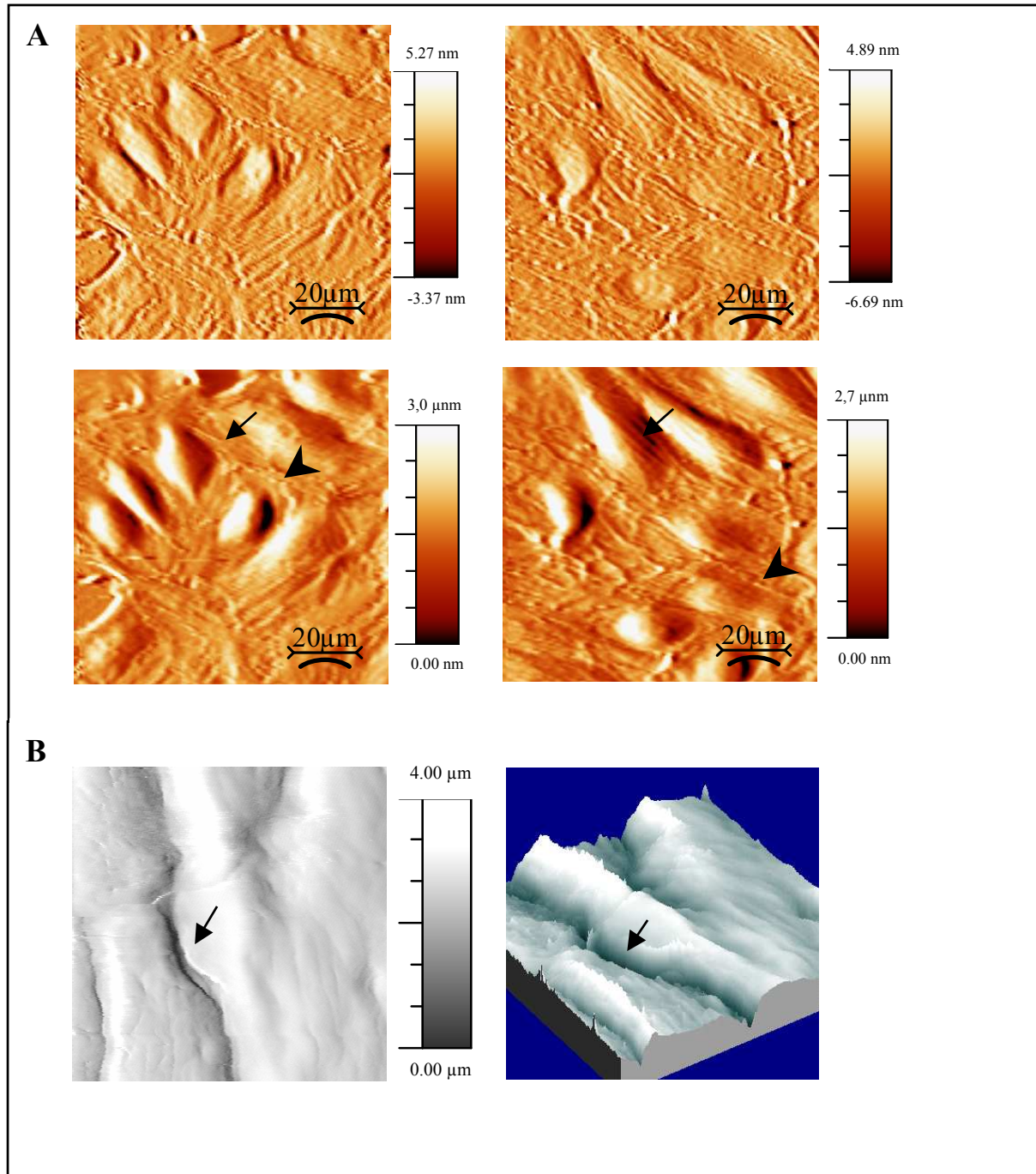


Figure 4-15: Topography images of MBCEC *in vitro*. A: Left images show the surface and deflection of cells cultured in serum-free medium. Cells on the right were treated with hydrocortisone. The serum-free cultured cells indicate frayed tight junctions (arrows) while the hydrocortisone-treated cells have distinct lines between adjacent cells (arrow-head). The arrow shows cable-like structures in longitudinal direction of the cell indicating stress fibres. B: 3D-image of cells cultured in hydrocortisone-containing medium. The cleft represents the contact-zone between adjacent cells. Arrows indicate the same region in both pictures.

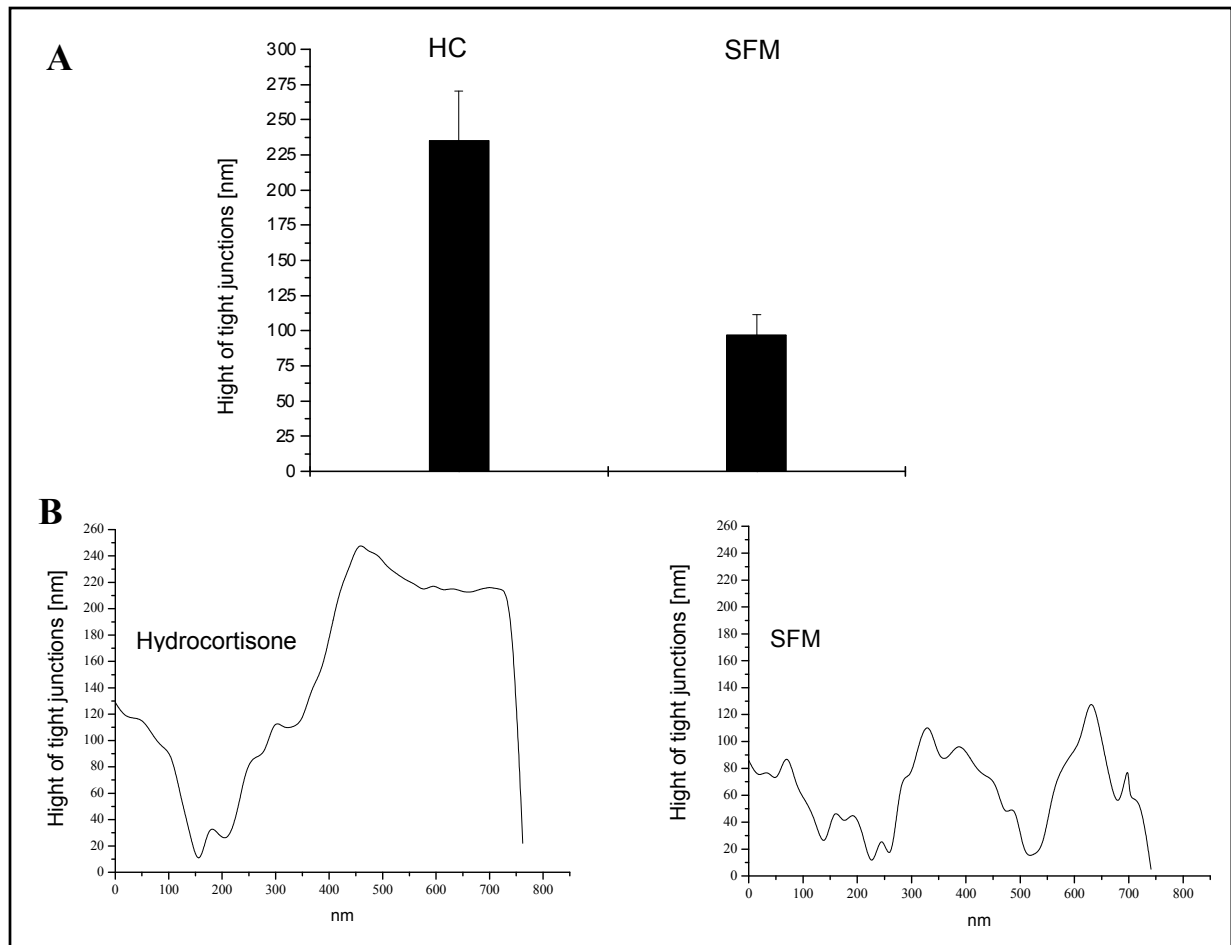


Figure 4-16: Height of tight junctions in different media. **A:** Average of the altitude within the tight junctional zone of cells culture with/without hydrocortisone. Cells cultured in HC show an increase of the altitude within the tight junctional zone. (standard deviation $n=8$) **B:** Cross section of the profile within a tight junction zone of cells cultured under different conditions.

4.4.4.1.2 Investigations of force curves of MBCEC by AFM

The force curves of AFM measurements give an idea about the elastic properties of the cell surface. These mechanical properties may play a major role in cellular processes as migration and cell division and can be brought in correlation with redistribution of cytoskeleton elements like stress fibres (Rademacher, 2002; Sackmann, 1994). The protein actin can form interconnected double-helical polymer fibres with a periodicity of 3.7 nm and is associated with a large number of proteins controlling the architecture of this network (Hartwig and Kwiatkowski, 1991). The investigation of mechanical properties was performed as described in section 3.1.4. As shown in figure 4-17 the cells treated with hydrocortisone possess a higher Young's modulus indicating a formation or redistribution of actin filaments (Rademacher, 2002).

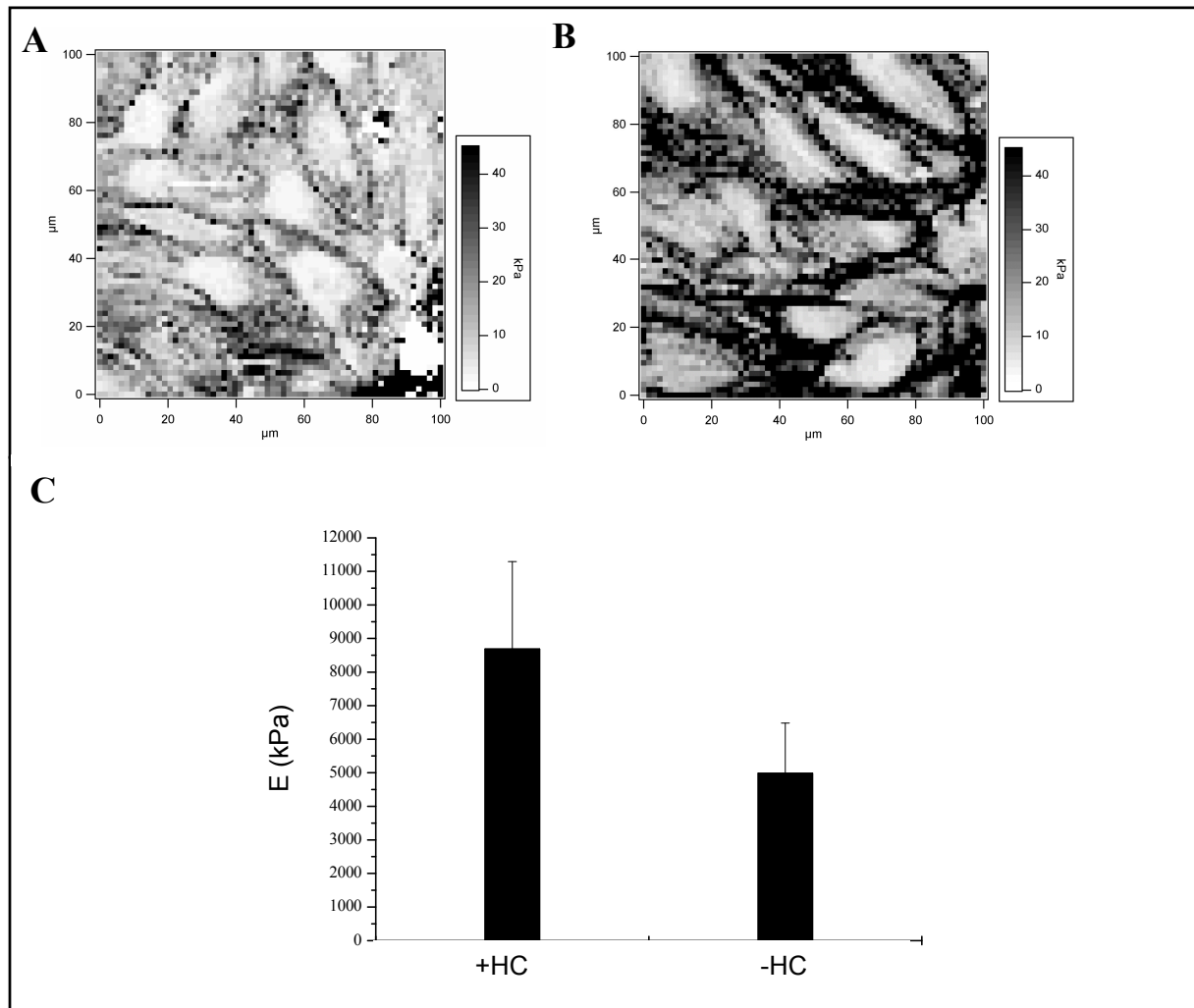


Figure 4-17: Force mapping of MBCEC under different conditions. **A:** Serum-free treated cells; **B:** Hydrocortisone-treated cells. The data implicate a change of mechanical properties of MBCEC under different culture conditions. **C:** Young's modulus of cells from different culture conditions. Cells treated with hydrocortisone possess higher elasticity. (+HC=8304 kPa \pm 2491 kPa; -HC= 5129 kPa \pm 1538 kPa; standard deviation n=6)

4.4.5 Transmission electron microscopy

As described in section 3.1.5, transmission electron microscopy gives the opportunity to investigate ultrathin sections of cells cultured on filter membranes. These specimen are contrasted with electron-dense heavy metal ions. At these electron-dense areas, the electron beam is refracted and thus, it is possible to image the probes and visualise subcellular details. To apply this technique, the cells were cultured on filter membranes as described in section 3.1.1 and after 2 days in incubation medium the TEER was determined in order to choose the cells with the highest transendothelial resistance of each culture condition.

TEM images of MBCEC indicate a flat morphology whereas hydrocortisone-treated cells are recognisably more flat than serum treated cells. As demonstrated in figure 4-19, all cells show vesicle-like structures, which could be glycogen reservoirs, indicating that the energy state of the cells is saturated. The cells cultured in presence of serum (A+B) are not as tightly attached to the substrate as hydrocortisone treated cells (C+D) especially at the cell-cell contact regions. In other regions of the cell layer, wide overlapping areas are expressed (figure 4-19 C) which correlates to the capacitance values of QCM-measurements (section 3.1.7). One of these areas is shown in figure 4-18. This image indicates a contact area of three adjacent cells cultured in serum. Two cells form blunt cell-cell contacts and overgrow a third cell. The differences between the culture conditions are mainly based on the cell-cell contact region. Most contact areas from serum-treated cells are blunt and marginal folds develop but do not attached to the adjacent cell (figure 4-19 B). The cells treated with hydrocortisone express electron dense tight junction regions with marginal folds attached to the adjacent cell (figure 4-19 D, E).

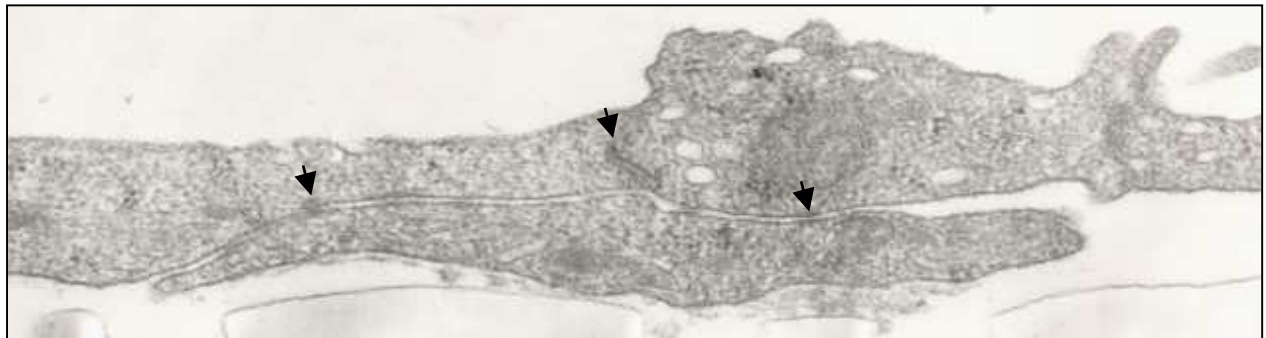


Figure 4-18: Micrograph of a TEM-image of MBCEC. Overlapping region of cells indicated by electron microscopy. The MBCEC were cultured in serum-containing medium. The image indicates a contact point between three adjacent cells. The tight junctions are indicated by arrows. As seen in all serum-treated cells the tight junctions are weak expressed.

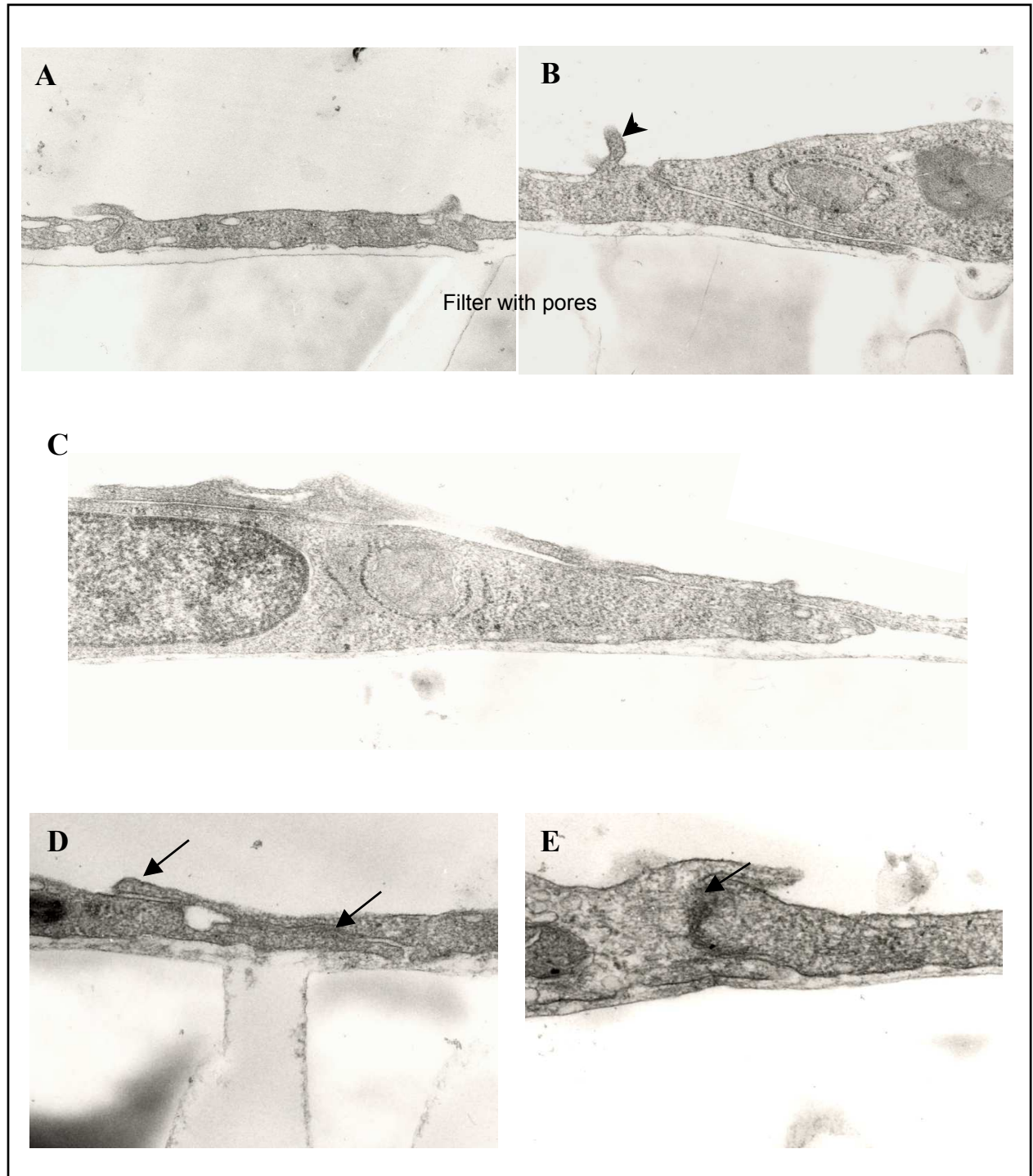


Figure 4-19: TEM images of MBCEC. A, B, C: MBCEC cultured under serum conditions DIV 2; D, E: hydrocortisone treated cells (DIV 2). A: Blunt cell-cell contacts without visible tight junctions. B: Cell-cell contact with marginal fold not attached to the adjacent cell (arrow-head). C: Overlapping area of adjacent cells. D: Cell-cell contact with attached marginal fold (left arrow) and electron dense tight junction area (right arrow). E: Cell-cell contact with electron dense tight junction area (arrow).

4.4.6 Influence of hydrocortisone on expression of blood brain-barrier related proteins on RNA-level

As described in section 2.4, hydrocortisone is a glucocorticoid hormone which regulates the expression of proteins on the RNA level by binding to glucocorticoid receptors and association to glucocorticoid response elements at DNA targets. This implicates that the change of MBCEC properties and the tight junction morphology may be the result of hydrocortisone-induced expression of different targets. In PBCEC the subtractive suppression hybridisation was applied to identify differentially expressed genes on the RNA level (Eisenblätter, 2002; Weidenfeller, 2000). Tight junction proteins were not affected by hydrocortisone-treatment but a new multidrug resistance protein (BMDP) was detected in PBCEC and identified as upregulated in the presence of hydrocortisone (Eisenblatter and Galla, 2002; Eisenblätter, 2002). In this work the tight junction-protein expression of MBCEC on RNA-level were investigated with QRT-PCR (3.2.7.2). Additionally, the expression of BMDP was checked in order to prove, if hydrocortisone also induces upregulation of this protein in MBCEC. Furthermore, the influence of different culture conditions on the RNA expression level of various blood-brain barrier marker proteins (4.3).

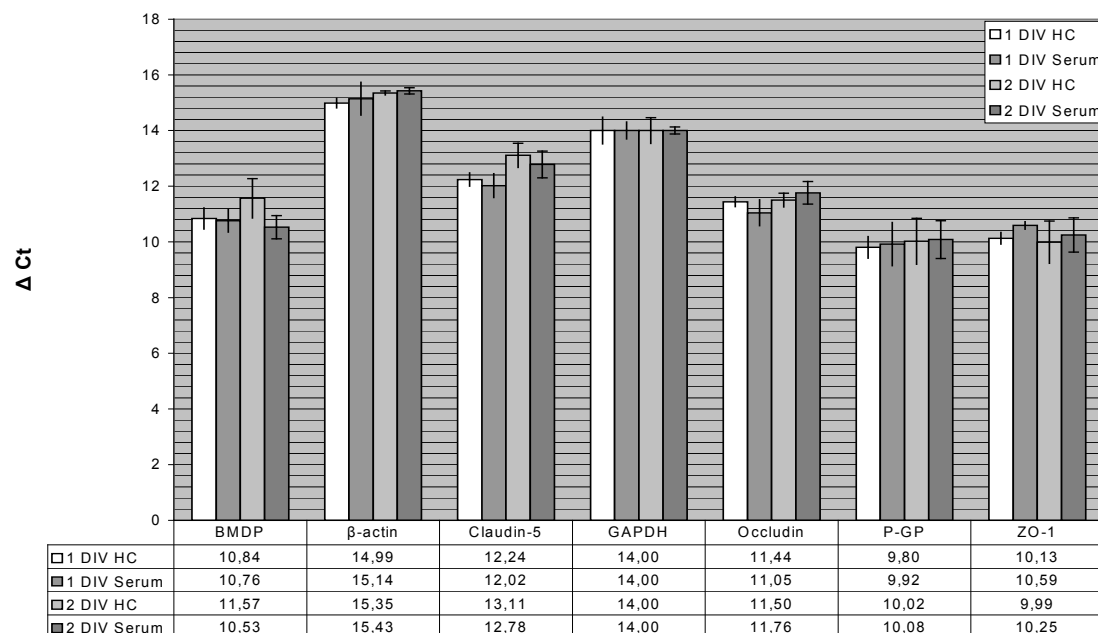


Figure 4-20: Results of QRT-PCR in MBCEC. Expression of RNA of different proteins and the house-keeping genes after one and two days in incubation medium. There are no significant differences on RNA-level of tight-junction protein expression on the same DIV. P-glycoprotein (PGP) and BMDP show higher expression in serum the first day whereas the expression at the second day indicates an increase with hydrocortisone. The values give the ΔC_T -values in relation to GAPDH. (standard deviation n=3)

Figure 4-20 shows the expression of tight junction proteins and transporters BMDP and P-glycoprotein after one and two days in incubation medium. When comparing the two culture conditions of MBCEC, the tight junction proteins occludin and claudin-5 show no significant change in their expression on the RNA-level. The same result was found for ZO-1 (data not shown). However, after two days in incubation medium the expression state is higher under both conditions. The same applies to the transporters BMDP and P-glycoprotein. But the expression state shows differences relating to the culture conditions. Serum-treated cells show a significantly increased expression of BMDP after one day in culture while the second day no significant changes can be detected (data with similar results not shown.). P-glycoprotein is not affected by hydrocortisone. The comparison of blood-brain barrier marker proteins shows also no significant change in the expression state of RNA-level of proteins in different culture conditions.

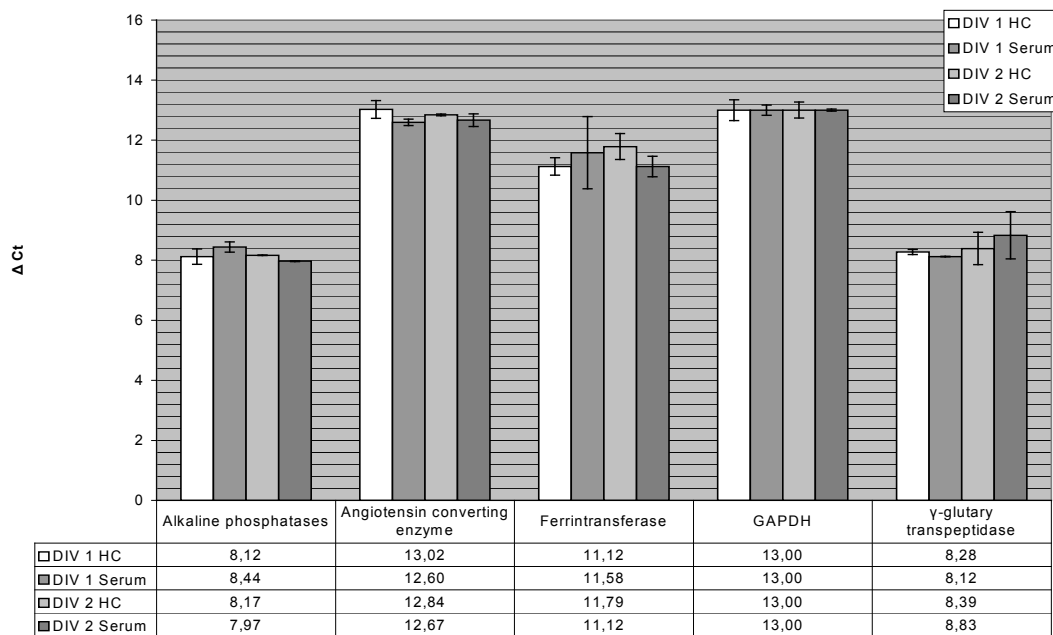


Figure 4-21: Expression pattern on RNA-level of blood-brain barrier markers in MBCEC after one and two days in incubation medium (either hydrocortisone containing medium or serum containing medium). The values give the ΔC_t -values in relation to GAPDH.

4.4.7 Influence of hydrocortisone on protein expression of tight junction proteins

Since there was no significant influence in expression among investigated tight junction proteins on the RNA-level, western blot analysis was performed to prove gene expression on protein level. The proteins were isolated as described in section 3.4.1 and visualised by incubation with POD-labelled 2nd antibody.

The expression of the tight junction protein occludin, claudin-5 and the tight junction-associated protein ZO-1 was determined to find possible differences between different culture conditions. The blots were stripped afterwards and the gel loading was controlled by staining the whole protein content by Protogold Detection KitTM (Amersham).

Figure 4-22 shows the results of western blot analysis. There are no detectable differences in the expression level of the investigated proteins. The signal intensity is the same in both, hydrocortisone and serum treated cells. The phosphorylation state of occludin is rather low indicated by the distinct signal. In contrast to this finding, occludin isolated from PBCEC is highly phosphorylated.

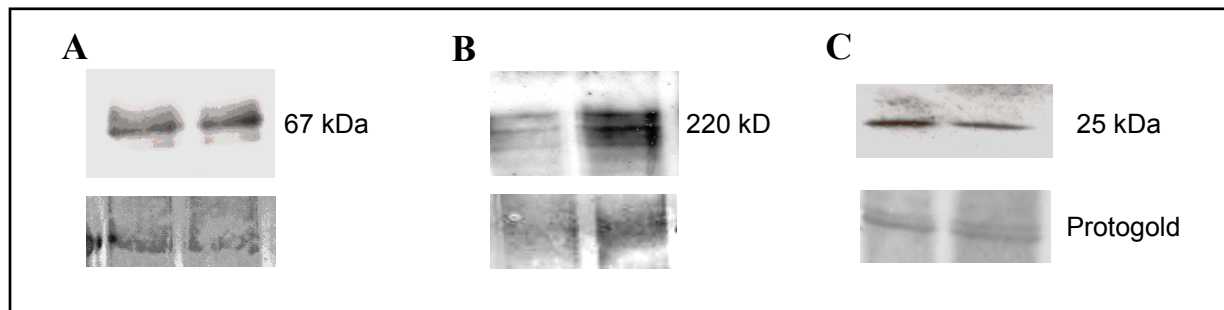


Figure 4-22: Western blot analysis of tight junction proteins. All cells were cultured until DIV 5. The incubation medium (either with hydrocortisone or serum) was added after a confluent monolayer was obtained. The protein isolation was performed after two further days in culture. A: occludin B: ZO-1, C: claudin-5. The first lane indicates the protein content of hydrocortisone-treated cells; the second lane shown the signal of cells cultured in serum-containing medium. For control of gel-loading staining with Protogold Detection KitTM (Amersham) is shown. No significantly change on protein-level of the proteins cultured under different culture conditions was observed.

4.5 Gene silencing at primary cultures of brain capillary endothelial cells

As described in section 3.1.2, RNA interference (RNAi) was investigated in this thesis on the application to primary blood-brain barrier culture systems. RNAi is a powerful method to investigate the effect of loss or down regulation of specific genes within a cell culture. Due to the fact that mammalian cells and especially brain endothelial cells are difficult to transfect with antisense plasmids, RNAi gives the opportunity to transfect small double-stranded RNA which can easily pass the membrane mediated by cationic lipids. Furthermore the targets of these RNA-species are the cytoplasmic localised mRNA. Thus, the transfection of nucleic acids into the nucleus is not necessary. It is known that RNA interference works in cultured mouse cells (Svoboda et al., 2001) and so the method was applied to the primary culture of MBCEC. After successful application RNAi was extended to PBCEC. These cells are available in higher quantity and thus, better suited for high throughput screening.

4.5.1 Immunofluorescence staining of siRNA-transfected cells

The cells were transfected with siRNA as described in section 3.1.2 and the result of silence inducing properties were investigated by indirect immunofluorescence. Afterwards, western blot analysis completed the investigation of the down regulation of the target proteins. The target protein was lamin A/C which is localised in the membrane of the nucleus. This protein was one of the first targets knocked down by RNAi in mammalian cell culture systems (Elbashir et al., 2001; Harborth et al., 2001; Tuschl et al., 2001). To get the same culture- and transfection conditions for cells cultured in petri dishes and on cover slips, the cover slips were placed into petri dishes and removed for immunofluorescence investigations before the isolation of proteins was performed. To estimate if the silencing-effect of transfected RNA depends on its concentration different amounts of siRNA were applied.

The cells were fixed and the immunofluorescence staining was performed as described in section 3.1.3. Figure 4-23 shows the result of indirect immunostaining against lamin A/C of siRNA-transfected and non transfected cells. As the images indicate the transfection with lamin A/C was successful and a significantly weaker signal could be detected in transfected

cells. While the minority of the cells seem to be unaffected by siRNA, nearly 60% of the cells show a significantly weaker signal.

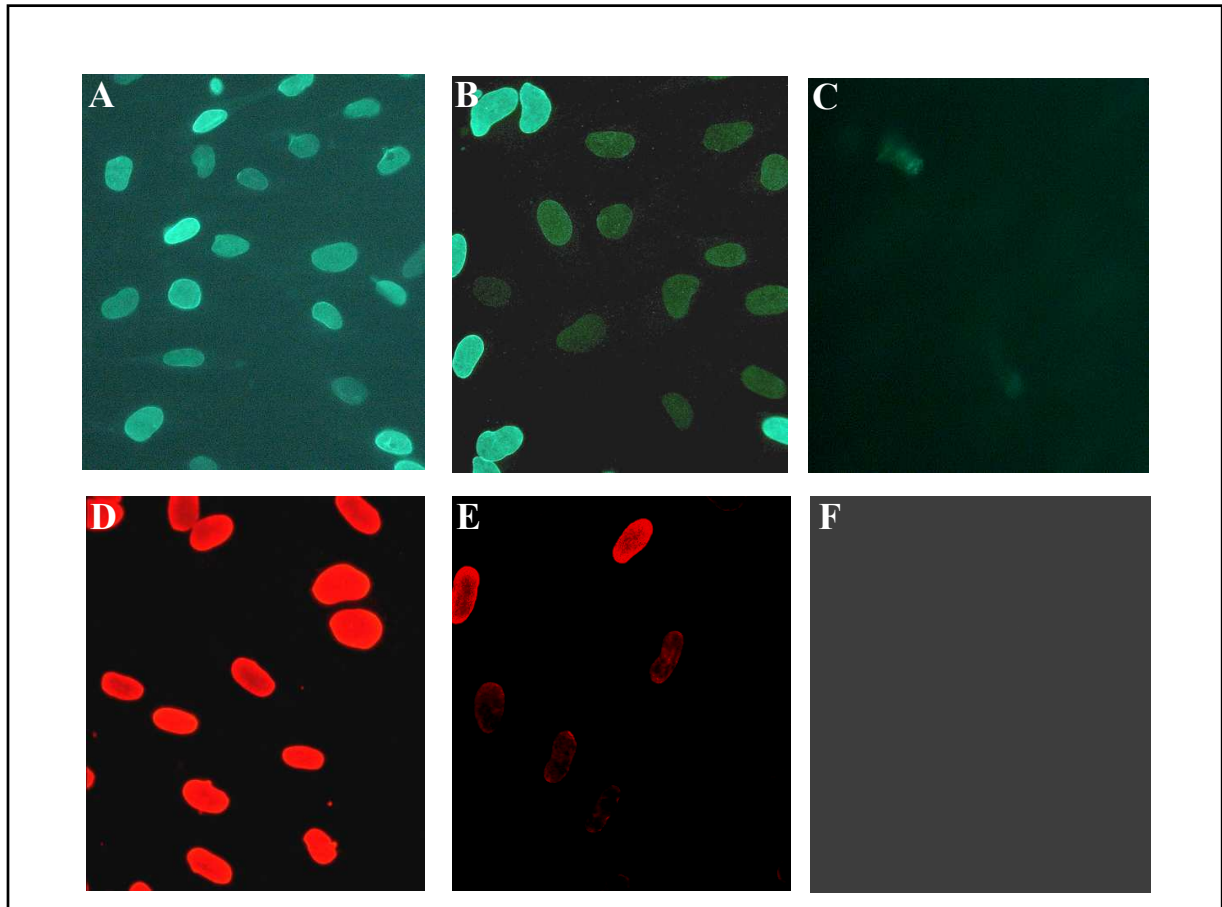


Figure 4-23: Immunodetection of lamin A/C in cultured murine and porcine brain capillary endothelial cells. The cells were transfected with a final concentration of 25 nM siRNA. A-C: MBCEC; D-F: PBCEC, A+D control without siRNA, B+E: transfected cells, C+F: secondary antibody-control.

4.5.2 Western blot with siRNA transfected cells

Western blot analysis was performed to quantify the efficiency of down-regulation. Figure 4-24 shows the result of the lamin detection of isolated proteins from porcine brain capillary endothelial cells. To find out if the efficiency is concentration dependent, cells were transfected with different amounts of siRNA. The immunoblot was performed with an anti-lamin A/C antibody (mouse) which recognizes both gene products of splice variants A and C. As indicated by figure 4-24, a down-regulation is visible in all concentrations of siRNA. Applying 100 nM siRNA results in an extensive loss of the signal (lane 3a) whereas 400 nM

is not as effective (lane 4). Protein loading is indicated by vimentine which was used as a marker protein.

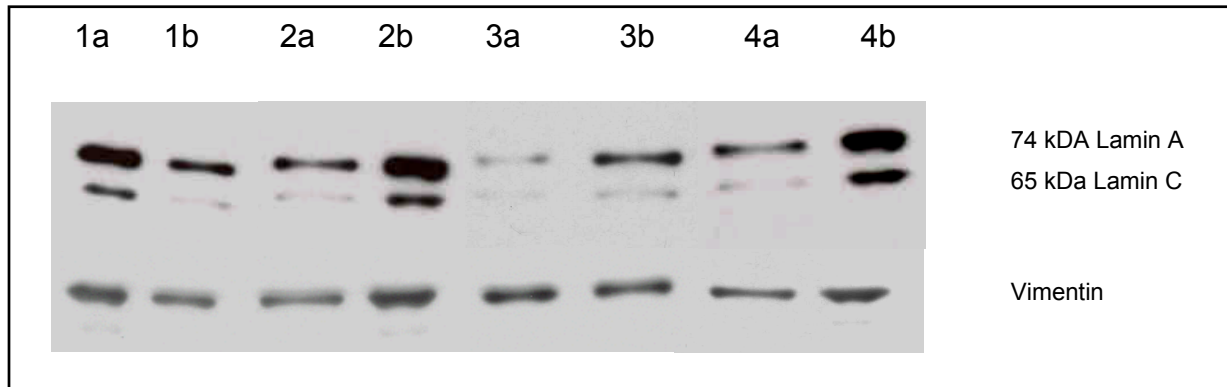


Figure 4-24: Change in expression of lamin A/C on protein level after transfection of cells with siRNA against lamin A/C. Lane a represents the protein isolated from transfected cells, b: control from not-transfected cells. Concentration of siRNA: 1: 25nM; 2: 50 nm, 3: 100 nM 4: 400 nM.

5 Discussion

5.1 *In vitro* model of murine brain capillary endothelial cells

Many *in vitro* models of the blood-brain barrier have been established to investigate the regulation of blood-brain barrier properties and the transport of compounds like pharmaka across the barrier. This thesis describes a new primary culture model based on murine-derived brain capillary endothelial cells. The model was characterised and compared to our well established serum-free porcine model of the blood brain barrier *in vitro* (Hoheisel et al., 1998b). The cells were isolated from brains of 6-10 weeks old mice (C57BL6/J) following a modified protocol of (Imaizumi et al., 1996) and cultivated for up to 8 days (section 3.1.1). Characterisation studies of the model indicate a well defined culture of primary endothelial cells after puromycin-treatment without almost any contaminating cells like astrocytes and pericytes. The cells are contact inhibited and form a confluent monolayer. Due to the fact that the culture contains no glia cells it is possible to use the whole cell population without subcultivation after reaching confluence. Also a subcultivation of the whole cell-population is practicable. Cells in a confluent monolayer show the typical spindle-shape endothelial cell morphology and they express common as well as blood-brain barrier specific endothelial markers. Expression of von Willebrand-factor (*factor VIII*-related antigen (Phillips et al., 1979a) as well as tight junction proteins claudin-5, occludin, and ZO-1 were demonstrated in indirect immunofluorescence staining. The latter proteins have also been identified in western blot analysis. On RNA-level all tested blood brain-barrier markers like γ -glutamyltranspeptidase (Orlowski et al., 1974), alkaline phosphatase (Karnushina et al., 1980b) and endothelial cell markers like angiotensin converting-enzyme (Gimbrone et al., 1979) and transferrin (Jefferies et al., 1984) have been detected. Furthermore the proteins ZO-1, claudin-5 and occludin were found to be highly expressed by QRT-PCR. A special property of the microvascular endothelial cells in the brain is the presence of numerous transporters which protect the brain against toxic compounds. The presence of P-glycoprotein and BMDP is a further hint that the cultured brain endothelial cells express blood-brain barrier related transport proteins. P-glycoprotein and BMDP were found to be expressed on RNA-level and BMDP could be additionally observed on protein level by immunofluorescence staining.

The transendothelial electrical resistance is much lower in cultured MBCEC *in vitro*. The TEER of PBCEC *in vitro* under serum-free conditions increases in the presence of hydrocortisone up to $2000 \Omega \cdot \text{cm}^2$ which correlates with the *in vivo*-situation (brain capillaries of frog $\sim 2000 \Omega \cdot \text{cm}^2$, (Crone and Olesen 1982); brain capillaries of rat $\sim 1500 \Omega \cdot \text{cm}^2$ (Butt and Jones, 1992). MBCEC develop in serum-containing medium resistance values of up to $50 \Omega \cdot \text{cm}^2$ were detected whereas cultures of MBCEC in hydrocortisone-containing serum-free medium reached rarely values of up to $600 \Omega \cdot \text{cm}^2$ but usually averaged to $200 \Omega \cdot \text{cm}^2$. This correlates with the high permeability for sucrose of $2.5 \cdot 10^{-5} \text{ cm/s}$. These data indicate that the primary culture of MBCEC express all typical markers of cerebral microvessel endothelial cells except the barrier function that lags behind the *in vivo* situation or the properties of PBCEC in culture. However, the measured values of transendothelial resistance are in the range of other cell culture systems (Hurst and Clark, 1998; Ramsohoye and Fritz, 1998; Reardon and Audus, 1993a). The low resistances and high permeability may be the result of incomplete tight junction formation in culture caused by a dedifferentiation as response to the *in vitro* situation. The differentiation of MBCEC *in vitro* is apparently not identical with the *in vivo* situation (Joo 1992; Reardon and Audus 1993b).

5.2 Influence of hydrocortisone on electrical properties of MBCEC

The transendothelial resistance is a strong indicator for the integrity of blood brain-barrier culture systems *in vitro*. While *in vivo* the TEER reaches values of about $2000 \Omega \cdot \text{cm}^2$ (section 5.1) a lot of groups work with primary culture systems or cell lines with much lower resistances. The porcine brain capillary endothelial cell system in our group expresses high resistances *in vitro* when the cells are cultured under serum-free conditions in hydrocortisone-supplemented medium (Hoheisel et al., 1998a). The lipophilic glucocorticoid-hormone hydrocortisone diffuses across the plasma membrane into the cytoplasm of the cells. In the porcine system it was shown that the TEER increased when the cells were exposed to hydrocortisone. The applied concentration of this hormone was physiological (550 nM, (Karlson 1994)) and the increase was independent from apical or basolateral application of the glucocorticoid. The question arose, if this effect is pig-specific or whether hydrocortisone has an influence on other primary cultures of brain derived microvascular endothelial cells as well. The new established murine model of the blood-brain barrier was analysed with respect

to a response upon hydrocortisone exposure. To investigate the effect of hydrocortisone, the cells were cultured 2 days *in vitro* in hydrocortisone-containing medium and, for comparison, in medium supplemented with foetal calf serum. Hydrocortisone induces the blood-brain barrier phenotype and allows the investigation of the cultured cells in serum-free and therefore chemically defined medium. This influence of hydrocortisone on the murine *in vitro* model will be discussed in the course of the following passage.

Using the mouse model, the glucocorticoid increases the resistance up to five-fold compared to serum containing and serum-free medium. In some cultures, cells reached electrical resistances in hydrocortisone-supplemented medium between 150 and 600 $\Omega \cdot \text{cm}^2$. Mostly the values lay around 180 $\Omega \cdot \text{cm}^2$. The effect was time-dependent and detectable after a lag period of 2 hours. During the following 20 hours the TEER increased linearly and the maximum value was reached after 40 hours while cells cultured in presence of serum and serum-free medium respectively reached maximum values of 40 $\Omega \cdot \text{cm}^2$.

From ECIS and QCM measurements it became clear that the parameter α and R_b depend on the culture conditions especially on the presence of hydrocortisone. The parameter α indicates the resistance underneath the cells between the cell monolayer and the substrate while R_b quantifies the resistance due to the cells-cell contacts. The change of these two parameters can be followed separately by ECIS and QCM. As mentioned earlier, a change of R_b indicates alterations in paracellular resistance while higher values for α point to a closer cell-substrate contact. For both, α and R_b higher values could be detected in hydrocortisone-containing medium. The value for the parameter α increases about 75% while R_b even reaches values of 250% of the value of MBCEC treated with serum. This clearly shows that the paracellular electrical permeability of MBCEC is reduced mainly by R_b which gives evidence for an improved cell-cell contact. The increase of the parameter α after treatment of cells with hydrocortisone may be the result of several factors. First, a change of cell-substrate contact can result in altered values for α . Cells, which are attached close to the substrate inhibit the flow of inorganic ions. An increase in production or secretion of extracellular matrix proteins can also reduce the flow of inorganic ions in the electrical field beneath the cells. Secondly, at high electrical resistances received in PBCEC-culture the total resistance is dominated by R_b . The impact of α becomes almost negligible. In cell cultures with lower electrical resistances like the MBCEC used here, an increase of α becomes more important and contributes more to the overall TEER. Normally, the TEER is measured without discrimination of cell-cell and cell-substrate contributions. This may lead to a false conclusion with respect to the mechanism since some mediators influence the TEER by acting on the cell-matrix interaction

indicated by a change of α . For this it is necessary to investigate both, α and R_b which is technically impossible on permeable filters which are mainly used.

The influence of hydrocortisone on the TEER may be the result of many subcellular changes. It is known for long that glucocorticoids increase the barrier properties of vascular cells (Ingraham et al., 1952; Jarden et al., 1989; Long et al., 1966a; Long et al., 1966b; Yamada et al., 1983). It was also shown that hydrocortisone increases barrier properties in term of TEER and permeability for ^{14}C -mannitol in epithelial cells (Zettl et al., 1992). A similar influence was found in a breast cancer tumour cell line (con8) (Buse et al., 1995a). Using PBCEC, Engelbertz et al. (2000) could show by concentration dependent measurements and experiments including antagonists for glucocorticoid receptors that the influence of hydrocortisone directly correlated with the occupation of glucocorticoid receptors. This leads to the conclusion that hydrocortisone somehow influences the process of transcription of genes either by enhancing or repressing the transcription. The main role of hydrocortisone is the enhancer effect in transcription. Targets of glucocorticoids are several genes encoding for enzymes which are involved in glucose and energy metabolism of the cell as there are gluconeogenesis and lipolysis (Jungermann and Möhler, 1980). A repression mediated by glucocorticoids was observed by (Vrtovsnik et al., 1994) who found a protein kinases C (PKC) mediated hydrocortisone and dexamethasone-induced repression of the expression of Na-P_i-co-transporter in renal kidney epithelial cells. In an immortalised endothelial cell-line a PKC-mediated dexamethasone induced increase of P-glycoprotein activity was found while no influence on the expression of the corresponding gene was found (Regina et al., 1999). The effect of hydrocortisone may be based on two different mechanisms. Most target-genes possess cis-stimulating enhancer elements (glucocorticoid response elements, GRE). These elements are able to interact with a hormone-receptor complex by, for instance, interaction of zinc-finger motives. Most of these elements also include binding regions for transcription factors. Together with the glucocorticoid-receptor-complex these factors regulate the transcription of the target genes. Another example is the direct interaction between the glucocorticoid-receptor complexes with transcription factors. This interaction enhances or represses the expression of genes without GRE (Brostjan et al., 1997). Via this signal-transduction pathway, glucocorticoids may influence the expression of matrix metalloproteinases (MMP). These enzymes play an important role in the remodelling of the extracellular matrix proteins (Nishino et al., 2002; Pirila et al., 2003; Sternlicht and Werb, 2001). The expression of MMP can be down-regulated by supplementing medium with glucocorticoids. Jonat et al. (1990) found a hydrocortisone induced down-regulation of

transcription of collagenases gene. The repression was observed to be dependent on the interaction of the hormone receptor complex with the transcription factors AP-1 (*fos/jun*). Altogether the glucocorticoid-regulated genes are rather low in particular cell-types (Miesfeld 1989). The variable inducibility of target-genes within different cell-types may be a cell-specific difference in the concentration of transcription factors within the cell that are needed as cofactors. Recent studies noted that matrix-metallo-proteinases (MMP) expression in PBCEC *in vitro* is influenced by hydrocortisone (Lohmann 2003). The secretion of MMP-9 to the extracellular matrix is significantly decreased after incubation in hydrocortisone-supplemented medium. In correlation with this result the parameter α could be increased since higher MMP expression would lead to a degradation of ECM-proteins followed by a lower value of α . Furthermore, Lohmann also observed that higher activity of MMP leads to a degradation of occludin. This could explain the lower value for the parameter R_b .

The incubation of MBCEC in serum containing medium has no significantly effect on the TEER in experiments on permeable filter membranes. The electrical resistance is stable for 72 hours after addition (figure 4.6). In contrast the withdrawal of serum induces a decrease of the TEER of about $10 \Omega \cdot \text{cm}^2$. This result is contradictory to the data received in the porcine system. The TEER in PBCEC is increased after withdrawal of serum. The difference in the response of MBCEC and PBCEC may be a species differences between porcine and murine microvascular endothelial cells. One of the main functions of serum is to supply the cells with growth factors and mitogens. Furthermore, serum acts as a buffer system and neutralises acidic metabolites. Nitz et al. (2003) observed that several compounds of serum influence the electrical resistances of PBCEC. A 66 kDa-fraction could be identified by MALDI which was shown to influence the TEER significantly after application to PBCEC. Heat-inactivated serum induces a decrease in TEER similar to not heat-inactivated serum although reduced in amplitude. Different compounds contained in serum were shown to influence the permeability and the TEER respectively. Lysophosphatidic acid (LPA) was shown by (Alexander et al., 1998) to decrease the permeability for cyanocobalamine in bovine pulmonary aortic endothelial cells (BPAEC). In conflict to that (English et al., 1999) observed an increase of TEER in BPAEC caused by LPA. (Schulze et al., 1997) noticed that LPA in physiological conditions decreases the TEER and increases the permeability in PBCEC. Vascular endothelial growth factor (VEGF) is also known to influence permeability and electrical resistance of vascular endothelial cells (Esser et al., 1998; Keck et al., 1989; Senger et al., 1983). VEGF was also shown to decrease TEER in the PBCEC *in vitro* model. Discussing the effect of serum on cultured brain microcapillary endothelial cells it should be taken into

account that different sera provide different results. Foetal calf serum and ox serum cause a strong influence on PBCEC while TEER from pig serum-treated cells is not as much affected. Horse and human serum have almost no effect on PBCEC⁶. These data indicate that species differences always have to be taken into account.

5.3 Influence of hydrocortisone and serum on morphology and mechanical properties of MBCEC

Mouse brain capillary endothelial cells were investigated for their morphological and mechanical properties when cultured under different conditions. All cells were treated the first two days with puromycin-containing medium. Puromycin is known to be an inducer of apoptosis and thus an additive to select different cell-lines with introduced resistant against puromycin (de la Luna and Ortin, 1992; Suzuki et al., 2001). For further experiments the cells were either treated with serum-containing medium, serum-free medium or serum-free medium supplemented with hydrocortisone (550 nM). The cells cultured in petri dishes showed the typical spindle-shaped morphology. They reached confluence after 3-4 days in culture in serum-containing medium. The cells cultured in serum-containing medium had less contrast than serum-treated cells in phase contrast imaging and expressed a spindle-shaped morphology. After withdrawal of serum the cells changed their morphology to cobble-stone shape with pads of spindle-shaped cells. These findings correlate with the results from immunostaining analysis of MBCEC. The cells cultured with hydrocortisone show a homogenous morphology while cells in hydrocortisone form cobble-stone areas and in between extended parts of spindle-shaped cells. The staining of tight junction proteins like occludin and claudin-5 indicate that the cell-cell-contact points of spindle-shaped cells are more distinct while the cell-cell contact in areas with cobble-stone morphology especially at contact points of three cells express a frayed pattern. This result was supported by the finding that indirect immunofluorescence staining against the membrane-localised brain multidrug resistance protein shows a similar pattern. This fact leads to the conclusion that not only the tight junction strands are involved in the morphological change but with re-orientation of the cells the membrane morphology changes.

⁶ Hüwel, Sabine; Institut für Biochemie, WWU Münster; personal communication

The different shape of the cells can also be observed in atomic force microscopy. The cell-cell contacts in cells cultured with hydrocortisone-containing medium are seen as distinct lines between the cells (figure 4-15). The region of contact points between two endothelial cells indicates cambered structures and the contact-region is elevated in comparison to serum-treated cells. These structures are also known from *in vivo* as marginal folds, small areas in which the edge of one of the cells protrudes and associates with the adjacent cells. These structures could also be observed in transmission electron microscopy of MBCEC as described later. AFM-imaging also shows a flat morphology of the cell-body with the exception of the nucleus whereas serum-treated cell are not as flat. Furthermore, in deflection and height profile imaging, cells cultured in presence of hydrocortisone show the expression of cable-like structures in the longitudinal direction which can be assigned to f-actin stress fibres. In correlation with this, force curves of AFM indicate that the cells cultured in presence of hydrocortisone possess 60% higher Young's modulus than cells cultured without hydrocortisone. Recent studies on elasticity of cells under physiological conditions indicate that actin stress fibres and intermediary filaments influence the elastic properties of cells while microtubulus structures have no influence on the force mapping of cells (Haga et al., 2000; Hassan et al., 1998). These structures can be detected in both, the nucleus-area and the cytoplasmic area of the cells indicating well developed stress fibres with hydrocortisone. Theoretically, stress fibres increase the elasticity modulus of endothelial cells by a factor 2-10 (Satcher and Dewey, 1996). In correlation with this, actin filaments could be observed in longitudinal direction of the cells by direct staining with rhodamine-labelled phalloidin. Phalloidin staining in cells cultured in serum-containing medium show a membrane located belt of actin filaments known as perijunctional actomyosin ring (PAMR) (Fanning et al., 1998; Madara et al., 1992). The withdrawal of serum and cultivation in serum-free medium leads to a redistribution or formation of actin filaments to the longitudinal direction of the cells. In the presence of hydrocortisone, this effect is intensified; however, the PAMR is still visible at the borders of the cells.

Several factors are responsible for the formation and redistribution of actin. LPA is known to induce formation of actin stress fibres (English et al., 1999; Schulze et al., 1997) and is, as described recently, one component of serum. The influence of serum and especially of LPA on the transendothelial resistance was already described (Miki et al., 2000). The influence on the redistribution and formation of stress fibres may result in a change of permeability and electrical resistance, respectively, especially since it has been found that dexamethasone and hydrocortisone induce an increased contractility in human lung fibroblasts caused by a *de-*

novo synthesis of filamentous actin in three-dimensional gel-matrix culture. The fibroblasts were cultured under serum-free conditions with dexamethasone (10^{-5} M). In contrast (Coulomb et al., 1984) reported a decrease of fibroblast contractility cultured in a gel-lattice in presence of serum and hydrocortisone in a concentration range of $2 \cdot 10^{-4}$ to $1.5 \cdot 10^{-3}$ M. The glucocorticoid dexamethasone was also applied to phenotypically stable cultures of untransformed mouse mammary epithelial cells (31EG4) (Zettl et al., 1992). This group could find no indication that glucocorticoids influence the de-novo synthesis or redistribution of actin stress fibres. Rubenstein et al., (2003) recently showed that RhoA small GTPase is regulated by glucocorticoids. They demonstrated that the glucocorticoid down-regulation of RhoA is a required step in the steroid signalling pathway which controls the organization of the apical junctional complex and the actin cytoskeleton in mammary epithelial cells. The tight junction, the adherens junction, and the cytoskeleton form an integrated functional unit based on multiprotein complexes. For example, the cadherin proteins of the adherens junction are structurally connected to F-actin polymers through β -catenin and α -catenin (Tsukita et al., 1992). Also, the actin cytoskeleton interacts with the tight junction-related protein ZO-1 (Fanning et al., 1999) or potentially indirectly through ZO-1-binding proteins such as spectrin (Mattagajasingh et al., 2000) and cortactin (Katsube et al., 1998). Furthermore, the actin cytoskeleton interacts with additional proteins localized to the tight junction, such as ZO-2, ZO-3, occludin (Wittchen et al., 1999) and cingulin (D'Atri and Citi, 2001). Therefore, one mechanism by which cellular RhoA activity could potentially disrupt the junctional complex is by selectively altering the cytoskeleton (Rubenstein et al., 2003). Rubenstein proposed that the steroid-induced down-regulation of RhoA leads to an apical F-actin organization that permits β -catenin accumulation at the lateral plasma membranes by generating a cytoskeletal scaffold to which β -catenin, and possibly ZO-1, can bind at points of cell-cell contacts. Alternatively, a dominant negative RhoA may cause the adherens and tight junction proteins to organize at the lateral plasma membrane and thus provide anchorage for actin filaments. Interestingly, in the quartz-mode of QCM (section 3.1.7) no difference was detectable in the mechanical properties of cells from both culture conditions. Changes in the resonance frequency of the quartz are results from the attachment and changes of structures close to the basolateral membrane of the cells. Thus, by QCM-experiments, changes to the basolateral membrane can be observed while by AFM changes at the apical membrane are detectable. Taking the results of ECIS into account, the changes of the electrical parameter α result from a closer cell-substrate interaction, but no significant changes of the mechanical properties of

the cells are detectable. These differences mainly base on the redistribution of the cytoskeleton to the apical membrane of the cells.

Transmission electron microscopy indicated also a morphological change in MBCEC. In cross-sections of MBCEC-monolayers the hydrocortisone-treated cells appear more flat than serum-treated cells. Tight junctions are expressed under both culture conditions but appear more intensely expressed with hydrocortisone. The cell-cell contact region expresses marginal folds in hydrocortisone-containing medium whereas serum leads to a loss of these structures from adjacent cells. The images indicate a higher contrast of structures beneath the cells. This is a possible hint on a higher content of extracellular matrix proteins. In parallel the cells cultured with hydrocortisone are closely attached to the substrate especially at the cell-cell contact regions while serum treated cells are detached in these areas. The cell-cell contact regions show also the main differences between these two culture conditions. Cells under serum-containing conditions either form blunt end contact points with gaps between adjacent cells or an extensive overlapping region with adjacent cells. Hydrocortisone treated cells show, as already described contact points with marginal folds and tight connections with neighbouring cells. The double layer is also detectable but not as extended as under serum conditions. This finding correlates with the capacitance C_M found in ECIS experiments. The capacitance of a cell-monolayer with a smooth cell surface amounts to $1 \mu\text{F}/\text{cm}^2$. The determined capacitance for cells cultured with hydrocortisone reaches values of approximately $0.82 \mu\text{F}/\text{cm}^2$. This value can be explained by the formation of double layer regions at the cell-cell contacts. The more expanded these regions are, the lower are the values for the membrane capacitance C_M . The values detected in MBCEC in both culture conditions confirm these findings. The serum treated cells show partial double layer formation at contact regions but not as extended as serum-treated cells. Taking into account that cells cultured onto permeable filters show in immunofluorescence staining of tight junction proteins a heterogenic morphology (either spindle- shaped with distinct cell borders or cobble stone-shaped with frayed staining pattern at cell-cell contacts) the influence of the reduce of capacitance may be caused by cobble-stone regions with overgrowth. A possible explanation of the frayed pattern in immunofluorescence staining caused by the overlapping of cells is given in figure 5-1. The TEM picture shows the contact region of three adjacent cells. The lower cell expresses tight junctions to both overlaying cells (see also figure 4-18). As recently described the tight junctions are directly linked to the actin filaments of the cytoskeleton. A redistribution of stress fibres may lead to a redistribution of tight junctions. The withdrawal of serum leads to a redistribution of F-actin in cultured MBCEC. The homogenous frayed

staining pattern in serum-treated cells vanishes and a more heterogeneous morphology of the cells appears. The addition of hydrocortisone leads as already described to cytoplasmic localised actin filaments in longitudinal direction within the cells in correlation with spindle-shaped morphology of the cells. Some areas still appear as cobble-stone shaped. Hydrocortisone may influence the cytoskeletal elements of MBCEC in a way that redistribution leads to the morphological change of some but not all cells. The cells forming pads in spindle-like manner can induce a change in cells between these pads.

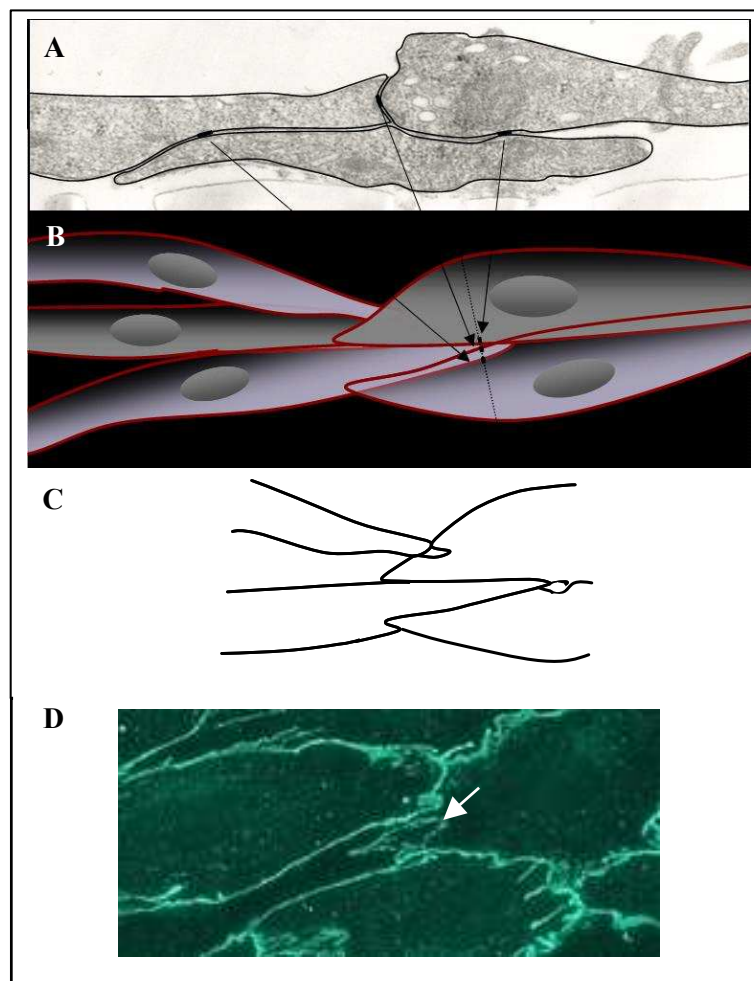


Figure 5-1: Model for tight junction localisation and resulting staining pattern in immunofluorescence detection of tight junction proteins. *A:* TEM image of cells cultured in serum. Tight junctions are indicated by black bars. *B:* model of overgrowth of adjacent cells and possible cross section of the TEM image indicated by the dotted line (view from the top). Arrows indicate the localisation of the corresponding tight junctions in the TEM-image and the model. *C:* Possible result of immunofluorescence staining against tight junction proteins in overlapping-region of adjacent cells. *D:* Immunofluorescence staining of ZO-1. The arrow indicates a region with possible overgrowth of the contact point between three adjacent cells.

5.4 Influence of hydrocortisone on RNA- and protein expression

The expression of tight junction-relevant proteins was quantified to determine if the increase of TEER after hydrocortisone-application is caused by altered expression. Occludin, ZO-1 and claudins are known to be involved in tight junction formation in endothelial and epithelial cells. For this reason, occludin, claudin-1 and -5 as well as ZO-1 were investigated for their expression in MBCEC. To quantify the influence of hydrocortisone on expression on RNA-level quantitative real-time PCR (QRT-PCR) was applied as described in section 3.2.7.2. The received data indicate that hydrocortisone has no influence on the mRNA expression of the investigated tight junction proteins. Claudin-1 was nearly not detectable by QRT-PCR. Also in western blot analysis and immunofluorescence staining no signal was detectable for claudin-1 indicating that this protein is not involved in tight junction formation in MBCEC *in vitro*. This finding goes confirm with the observations of Perrière et al.⁷ who could detect claudin-1 neither in freshly isolated capillaries nor in cultured rat microvessel endothelial cells. In the porcine BBB-*in vitro* model, claudin-1 was not detectable by western blot analysis. However, it could be detected in PBCEC by immunofluorescence staining after long incubation with the primary antibody and on RNA level by northern blot analysis after long-term exposure of the probes.. The mRNA content of the tight junction proteins occludin and claudin-5 is unaffected in all tested mRNA species. These proteins are expressed on the same level after one and two days in culture and after treatment with hydrocortisone or serum. ZO-1 mRNA content is not influenced by addition of the hydrocortisone as well. These findings correlate with the observations in PBCEC. Thus, the altered transendothelial resistance and the differences in immunofluorescence staining are no effects of the expression level of the investigated tight junction proteins. Detection of mRNA of specific proteins allows estimating the presence of the gene product but it is necessary to detect the protein by western blot analysis to observe the transcription rate. To examine the expression of occludin, claudin-5 and ZO-1 on protein level, western blot analysis of these proteins were performed. Occludin, claudin-5 and ZO-1 are expressed similar in both, hydrocortisone and serum-treated MBCEC. In contrast, (Antonetti et al., 2002) reported, that occludin expression on both, RNA- and protein-level is increased after glucocorticoid treatment of endothelial cells of the blood-retina barrier. Stelwagen et al., (1999) observed an increase in occludin expression after

⁷ Pierrère, N., Chaverot, N., Couraud, P.O., Deli, M.A., Cazaubon, S. Roux, F. Characterization of an *in vitro* rat blood-brain barrier model; poster on the “Sixth Symposium on Signal Transduction in the Blood-Brain Barrier” 2003, Szeged, Hungary

treatment of mouse HC11 epithelial cells in combination with prolactin. Also an increase of occludin and ZO-1 expression was detected in cultured rat brain endothelial cells after dexamethasone-treatment (Romero et al., 2003). Since no altered expression of the investigated tight junction proteins is detectable in MBCEC, the blood-brain barrier properties in this system are regulated somehow different. As already described, the withdrawal of serum and the addition of hydrocortisone induce a redistribution of f-actin. The formation of stress fibres together with the redistribution of actin-linked tight junctions may cause higher electrical resistance and enhanced barrier functioning in MBCEC.

Another main function of brain capillary endothelial cells is the protection of the brain from toxic substances by special transport systems. Transporters like multi-drug resistance proteins are known to be involved in this process. For this reason, expression level of the transporters BMDP and P-glycoprotein were examined. QRT-PCR showed that hydrocortisone has no influence on the expression of P-glycoprotein and BMDP on RNA-level. Both are highly expressed independent from the culture conditions. Eisenblatter and Galla (2002) observed an induction of expression after treatment of PBCEC with hydrocortisone. Furthermore, BMDP is higher expressed on RNA level in cultured brain microvascular endothelial cells than P-glycoprotein. The expression pattern of BMDP in whole brain tissue in comparison with P-glycoprotein was also investigated by (Eisenblätter 2002). Porcine brain tissue indicates a higher content of BMDP-RNA than a lysate of mouse brain tissue. In MBCEC P-glycoprotein and BMDP were shown to be highly expressed on the same level *in vitro*. Regina et al., (1999) could show that the synthetic glucocorticoid dexamethasone increases the expression of P-glycoprotein on protein level. Also a higher activity was observed in the investigated immortalised rat brain endothelial cell line GPNT.

The application of hydrocortisone had no influence on markers of blood-brain barrier endothelial cells as proven on mRNA-level by northern blot and QRT-PCR.. Therefore, hydrocortisone seems not to change the differentiation of the cells. But expression of the markers has still to be examined on protein level by western blot analysis or immunofluorescence staining.

5.5 Application of RNA interference method on primary cultures of microvascular endothelial cells

After the establishment and characterisation of the primary culture of mouse-derived brain capillary endothelial cells, RNA interference-technique (RNAi) was tested for its application on the blood-brain barrier systems based on both, MBCEC and on PBCEC. The application of RNAi gives the opportunity to investigate the down-regulation of target-proteins *in vitro* and *in vivo*. While less genomic data is available for pig, the blood-brain barrier *in vitro* model of MBCEC completes the PBCEC-culture by the knowledge of complete genome data.

RNAi was shown to work in both culture systems. The chosen target protein was lamin A/C, a nuclear membrane located protein. Successful knock down of this protein by RNAi was previously shown by Elbashir et al., (2002) and Harborth et al., (2001). Both, PBCEC and MBCEC were cultured until reaching 70% confluence as described in section 3.1.1 and transfected with siRNA against lamin A/C. Immunofluorescence staining indicates that the nuclear membrane localised lamin A/C is down-regulated in transfected cells. The staining indicates that lamin disappears in 70% of the cultured MBCEC and PBCEC (figure 4-23). Western blot analysis goes confirm with this finding. A significant down regulation of the investigated proteins is detectable but there is still a signal of lamin A/C. Some cells express lamin A/C as non-transfected cells, while other cells show only weak expression. The down-regulation is dose-dependent and the best effect is detectable after application a concentration of 100 nM of silence inducing double stranded RNA. The fact, that some cells still express lamin A/C can be the result of incomplete transfection with siRNA. The target of the transfected oligo-siRNA is the cytoplasmic localised mRNA. Due to the fact, that primary cultures are difficult to transfect with vectors, which express their antisense sequences within the nucleus, the advantage of RNAi is that it works in the cytoplasm. Furthermore, the RNA consists of only 21 nucleotides which are easier to transfect than plasmids. Cells, once transfected with siRNA, keep the silencing effect when dividing. However, some cells are not affected by siRNA indicating incomplete transfection efficiency. To observe effects after down-regulation of proteins in a cell culture model and to get facile assays for loss of function in a well-defined cellular system it is necessary to reach a significant down-regulation of the target proteins in all cells. Interestingly, the down-regulation of lamin A/C was not detectable by northern blot analysis (data not shown). So far, the down-regulation of occludin, ve-cadherin and BMDP was unsuccessful as well (data not shown). As described by (Tuschl et al., 2001) the parameters for selecting targets of siRNA are well defined and the siRNAs need

to be highly specific (base composition, target position, beginning and ending of the sequence and G/C-content). But considering all these parameters there is no guarantee for effective silencing of the target protein. The silence-inducing effect was observed in several groups after application of several different siRNA with sequence homology to the target-mRNA. For the silencing of occludin and ve-cadherin effective target sequences were not found so far.

6 Conclusion

With the isolation and cultivation of murine brain capillary endothelial cells (MBCEC) a new primary culture system as an *in vitro* model for blood-brain barrier is available. The cultured cells express a highly differentiated phenotype with specific endothelial and microvascular markers. They show the typical morphology of brain capillary endothelial cells and express transporters as P-glycoprotein and BMDP which were shown to be involved in multidrug resistance phenomena in cerebral microvessels. Thus, observations of drug transport are practicable in this culture system. Furthermore, MBCEC express well developed tight junction complexes. Proteins as occludin, claudin-5 and ZO-1 could be shown to be involved in these tight cell-cell contacts by immunofluorescence staining, northern blot- and western blot analysis. Together with the well established porcine culture of microvascular endothelial cells derived from brain, two models are available to investigate the regulation of barrier function and the transport properties of endothelial cells.

The MBCEC were shown to be influenced by the glucocorticoid hormone hydrocortisone. In serum-free medium, supplemented with 550 nM hydrocortisone, the cells express a 5-fold higher electrical resistance than cells cultured in serum containing medium. Hydrocortisone has no influence on the expression of the investigated tight junction proteins but influences the mechanical properties of the cells. In immunofluorescence staining could be shown that actin forms bundle-like structures in the longitudinal direction of the cells after hydrocortisone treatment, while cells, cultured in serum-containing medium indicate perijunctional-localised staining of f-actin. This finding correlates with observations made by atomic force microscopy. The Young's modulus of cells after hydrocortisone treatment is significantly increased and actin filaments can be detected in AFM imaging of hydrocortisone-treated MBCEC. The higher elasticity modulus indicates a distribution of f-actin within the whole cell. However, this finding is different from phenomena reported in the literature. The perijunctional actin-myosin ring (PAMR) was observed in cells with high electrical resistance in the literature, while MBCEC express lower TEER in this case. However, the PAMR is still detectable but a formation of stress fibres in the longitudinal direction of the cells takes part. Taking into consideration that the cytoskeleton is directly linked to the tight junction region by interaction with ZO-1, the redistribution of the cytoskeleton may have a more important influence than expression of tight junction proteins. In transmission electron micrographs differences in the cell-cell contact regions were obvious.

MBCEC cultured in presence of serum show wide overlapping regions at the contact of adjacent cells while this effect was not detectable in this extent after hydrocortisone treatment. This may also be an effect of changes in the structure of the cytoskeleton.

The down-regulation of specific proteins involved in tight junction formation in the cell culture would give important information about the regulation of the barrier properties. If it is possible to inhibit specific signal transduction pathways in developing cultures of microvascular endothelial cells, investigations of protein targeting and distribution would give important hints, which proteins and enzymes are involved in the formation of the tight junctions or which effects are responsible for the distribution of the cytoskeleton. RNA-interference gives the opportunity to inhibit the expression of specific target proteins within the cell culture. First observations showed that this method is practicable in primary cultures of isolated brain microvascular endothelial cells. PBCEC and MBCEC transfected with siRNA against lamin A/C showed a significant down-regulation of this nuclear-localised protein. The effect could be observed by western blot analysis and immunofluorescence staining. The protein was significantly down-regulated but still expressed in some cells. For this reason, the transfection efficiency has to be elevated and RNAi has to be optimised in future.

7 Materials and devices

7.1 Materials

| | |
|---------------------------------|--|
| acetic acid | <i>Merck</i> (Darmstadt, Germany) |
| acetone | <i>Merck</i> (Darmstadt, Germany) |
| acrylamid/bisacrylamid (37.5/1) | <i>AppliChem</i> (Darmstadt, Germany) |
| acrylamid/bisacrylamid (50/0.8) | <i>USB</i> (Cleveland, Ohio/USA) |
| Advantage cDNA Polymerase Mix | <i>Clontech</i> (Palo Alto, California/USA) |
| AdvanTAge PCR Cloning Kit | <i>Clontech</i> (Palo Alto, California/USA) |
| agar | <i>Sigma-Aldrich</i> (Deisenhofen, Germany) |
| agarose NEE0 | <i>ROTH</i> (Karlsruhe, Germany) |
| Albumine, bovine | <i>Sigma-Aldrich</i> (Deisenhofen, Germany) |
| ammonium acetate | <i>Riedel-de Haën</i> (Seelze, Germany) |
| ammonium sulfate | <i>Merck</i> (Darmstadt, Germany) |
| ampicillin | <i>Sigma-Aldrich</i> (Deisenhofen, Germany) |
| APS | <i>Sigma-Aldrich</i> (Deisenhofen, Germany) |
| Basic fibroblast growth factor | <i>Boehringer Mannheim</i> (Germany) |
| bromophenol blue | <i>ICN Biochemicals</i> (Eschwege, Germany) |
| BSA | <i>Sigma-Aldrich</i> (Deisenhofen, Germany) |
| CaCl ₂ | <i>Merck</i> (Darmstadt, Germany) |
| chloroform | <i>Merck</i> (Darmstadt, Germany) |
| collagen G | <i>Seromed</i> (Berlin, Germany) |
| Collagen type IV | <i>Sigma-Aldrich</i> (Deisenhofen, Germany) |
| Collagenase CLS2 | <i>Worthington</i> (Lakewood, USA) |
| collagenase/dispace (for PBCEC) | <i>Roche</i> (Basel, Swiss) |
| collagenase/dispace (for MBCEC) | <i>Boehringer Mannheim</i> |
| Coomassie Brilliant Blue G250 | <i>Sigma-Aldrich</i> (Deisenhofen, Germany) |
| 32P-dCTP | <i>Amersham Biotech</i> (Uppsala, Sweden) |
| dextran (~ 1632 kDa/mol) | <i>Sigma-Aldrich</i> (Deisenhofen, Germany) |
| dextran sulfate sodium salt | <i>Sigma-Aldrich</i> (Deisenhofen, Germany) |
| DMEM | <i>Biochrom KG</i> (Berlin, Germany) |
| DMEM/Ham's F12 | <i>Sigma-Aldrich</i> (Deisenhofen, Germany) |
| DMF | <i>Sigma-Aldrich</i> (Deisenhofen, Germany) |
| DMPC | <i>Sigma-Aldrich</i> (Deisenhofen, Germany) |
| DNA ladders (100 bp and 1 kb) | <i>Life Technologies</i> (Eggenstein, Germany) |
| DNase I | <i>Sigma-Aldrich</i> (Deisenhofen, Germany) |
| dNTPs, 10mM | <i>Sigma-Aldrich</i> (Deisenhofen, Germany) |
| DTT | <i>Sigma-Aldrich</i> (Deisenhofen, Germany) |
| EDTA | <i>Merck</i> (Darmstadt, Germany) |
| Emerald Enhancer | <i>Perkin Elmer</i> (Weiterstadt, Germany) |
| ethanol | <i>Merck</i> (Darmstadt, Germany) |
| ethidiumbromide | <i>ROTH</i> (Karlsruhe, Germany) |
| FCS | <i>Life Technologies</i> (Eggenstein, Germany) |
| Fibronectin | <i>Sigma-Aldrich</i> (Deisenhofen, Germany) |
| Ficoll 400 | <i>Sigma-Aldrich</i> (Deisenhofen, Germany) |
| formaldehyde (37%) | <i>Merck</i> (Darmstadt, Germany) |
| formamide | <i>Janssen</i> (Neuss, Germany) |
| Galacton | <i>Perkin Elmer</i> (Weiterstadt, Germany) |
| gentamicin | <i>Biochrom KG</i> (Berlin, Germany) |
| glucose | <i>Sigma-Aldrich</i> (Deisenhofen, Germany) |
| L-glutamine | <i>Seromed</i> (Berlin, Germany) |
| glutaraldehyde | <i>Sigma-Aldrich</i> (Deisenhofen, Germany) |
| glycerol | <i>Merck</i> (Darmstadt, Germany) |

| | |
|---|---|
| glycine | <i>Sigma-Aldrich</i> (Deisenhofen, Germany) |
| HCl | <i>Sigma-Aldrich</i> (Deisenhofen, Germany) |
| HEPES | <i>Merck</i> (Darmstadt, Germany) |
| hering sperm DNA | <i>Sigma-Aldrich</i> (Deisenhofen, Germany) |
| High Pure RNA Isolation Kit | <i>Roche</i> (Basel, Swiss) |
| hydrocortisone | <i>Sigma-Aldrich</i> (Deisenhofen, Germany) |
| Hyperfilm MP | <i>Amersham Biotech</i> (Uppsala, Sweden) |
| IPTG | <i>Biomol</i> (Hamburg, Germany) |
| isopropyl alcohol | <i>Merck</i> (Darmstadt, Germany) |
| kanamycin | <i>Sigma-Aldrich</i> (Deisenhofen, Germany) |
| KCl | <i>Merck</i> (Darmstadt, Germany) |
| KH ₂ PO ₄ | <i>Merck</i> (Darmstadt, Germany) |
| lysozyme | <i>Sigma-Aldrich</i> (Deisenhofen, Germany) |
| M 199 Earle | <i>Seromed</i> (Berlin, Germany) |
| MegaPrime DNA Labelling System | <i>Sigma-Aldrich</i> (Deisenhofen, Germany) |
| methanol | <i>Merck</i> (Darmstadt, Germany) |
| MgCl ₂ | <i>Merck</i> (Darmstadt, Germany) |
| MicroSpin G-50 Columns | <i>Amersham Biotech</i> (Uppsala, Sweden) |
| molecular weight marker (HMW and LMW) | <i>Amersham Biotech</i> (Uppsala, Sweden) |
| MOPS | <i>Sigma-Aldrich</i> (Deisenhofen, Germany) |
| Na ₂ HPO ₄ | <i>Merck</i> (Darmstadt, Germany) |
| NaCl | <i>Merck</i> (Darmstadt, Germany) |
| NaHCO ₃ | <i>Sigma-Aldrich</i> (Deisenhofen, Germany) |
| NaOH | <i>Sigma-Aldrich</i> (Deisenhofen, Germany) |
| NCS | <i>Seromed</i> (Berlin, Germany) |
| NGS | <i>Sigma-Aldrich</i> (Deisenhofen, Germany) |
| nylon membrane (GeneScreen Plus) | <i>NEN Life Science Products</i> (Boston, MA/USA) |
| Oligo(dT)12-18 Primer | <i>Life Technologies</i> (Eggenstein, Germany) |
| Oligofectamin | <i>Invitrogen</i> Karlsruhe (Germany) |
| oligonucleotides MWG | <i>Biotech</i> (Ebersberg, Germany) |
| Oligotex™ mRNA Mini Kit | <i>Qiagen</i> (Hilden, Germany) |
| OptiMem | <i>Invitrogen</i> (Karlsruhe, Germany) |
| ox serum | <i>PAA</i> (Linz, Austria) |
| paraformaldehyde | <i>Merck</i> (Darmstadt, Germany) |
| Paramount | <i>Polysciences Inc.</i> (Warrington, PA/USA) |
| penicillin/streptomycin | <i>Seromed</i> (Berlin, Germany) |
| peptone | <i>Life Technologies</i> (Eggenstein, Germany) |
| percoll | <i>Sigma-Aldrich</i> (Deisenhofen, Germany) |
| PDS | <i>First Link</i> (Brierley Hill, UK) |
| phenol/chloroform/isoamyl alcohol (25/24/1) | <i>Sigma-Aldrich</i> (Deisenhofen, Germany) |
| polyvinylpyrrolidone | <i>Sigma-Aldrich</i> (Deisenhofen, Germany) |
| protease inhibitor cocktail | <i>Roche</i> (Basel, Swiss) |
| protease/dispace | <i>Sigma-Aldrich</i> (Deisenhofen, Germany) |
| proteinase K | <i>Sigma-Aldrich</i> (Deisenhofen, Germany) |
| pT-Adv | <i>Clontech</i> (Palo Alto, California/USA) |
| QIAprep Spin Mini and Maxi Kit | <i>Qiagen</i> (Hilden, Germany) |
| QIAquick Gel Extraction Kit | <i>Qiagen</i> (Hilden, Germany) |
| restriction endonucleases | <i>New England Biolabs</i> (Beverly, MA/USA) |
| RNeasy Maxi-Kit | <i>Qiagen</i> (Hilden, Germany) |
| SDS | <i>Sigma-Aldrich</i> (Deisenhofen, Germany) |

| | |
|--------------------------------------|--|
| shrimp alkaline phosphatase | <i>Roche</i> (Basel, Swiss) |
| SMART DNA ladders (100bp and 1 kb) | <i>Eurogentec</i> (Seraing, Belgium) |
| sodium acetate | <i>Sigma-Aldrich</i> (Deisenhofen, Germany) |
| sodium citrate | <i>Sigma-Aldrich</i> (Deisenhofen, Germany) |
| ¹⁴ C-sucrose | <i>Amersham Biotech</i> (Uppsala, Sweden) |
| Superscript II Reverse Transcriptase | <i>Life Technologies</i> (Eggenstein, Germany) |
| T4 DNA ligase | <i>New England Biolabs</i> (Beverly, MA/USA) |
| Taq DNA polymerase | <i>Life Technologies</i> (Eggenstein, Germany) |
| TEMED | <i>AppliChem</i> (Darmstadt, Germany) |
| Tris | <i>ICN Biochemicals</i> (Eschwege, Germany) |
| Triton X-100 | <i>Sigma-Aldrich</i> (Deisenhofen, Germany) |
| trypsin | <i>Seromed</i> (Berlin, Germany) |
| trypsin/EDTA | <i>Biochrom KG</i> (Berlin, Germany) |
| Tween-20 | <i>ICN Biochemicals</i> (Eschwege, Germany) |
| urea | <i>Merck</i> (Darmstadt, Germany) |
| X-GAL | <i>ROTH</i> (Karlsruhe, Germany) |
| xylene cyanole | <i>ICN Biochemicals</i> (Eschwege, Germany) |
| yeast extract | <i>Life Technologies</i> (Eggenstein, Germany) |

7.2 Devices

Incubator

| | |
|-------------------------|--|
| Vortex | <i>IKA Labortechnik</i> (Staufen, Germany) |
| Hybridisation incubator | <i>Merck</i> (Darmstadt, Germany) |
| Thermomixer comfort | <i>Eppendorf</i> (Hamburg, Germany) |

PCR

| | |
|----------------------------------|---|
| Mastercycler gradient | <i>Eppendorf</i> (Hamburg, Germany) |
| Mastercycler personal | <i>Eppendorf</i> (Hamburg, Germany) |
| Gen Read IR4200 (for sequencing) | <i>LI-COR</i> (Lincoln, Nebraska/USA) |
| GeneAmp [®] 5700 | <i>PE Biosystems[®]</i> (Weiterstadt, Germany) |

Centrifuge

| | |
|--|--------------------------------------|
| Avanti 300 | <i>Beckman</i> (München, Germany) |
| Centrifuge 5415 C | <i>Eppendorf</i> (Hamburg, Germany) |
| Centrifuge 5804 R | <i>Eppendorf</i> (Hamburg, Germany) |
| Centrifuge J2-21 with rotors JA-14 and JA-20 | <i>Beckman</i> (München, Germany) |
| Type universal 16 R | <i>Hettich</i> (Tuttlingen, Germany) |
| Ultra centrifuge Optima-L70 | <i>Beckman</i> (München, Germany) |
| Sepatech Megafuge 1.0 | <i>Heraeus</i> (Hanau, Germany) |
| Mikro Rapid/K 1306 | <i>Hettich</i> (Tuttlingen, Germany) |

pH-meter

| | |
|--------|-----------------------------------|
| pH 213 | <i>Merck</i> (Darmstadt, Germany) |
|--------|-----------------------------------|

Photometer

| | |
|------------------------------|---|
| Perkin-Elmer 320 | <i>Perkin-Elmer</i> (Überlingen, Germany) |
| Shimadzu UV-2100 | <i>Shimadzu</i> (Düsseldorf, Germany) |
| Shimadzu UV-1601 PC | <i>Shimadzu</i> (Düsseldorf, Germany) |
| Microplate reader MR700 | <i>Dynatech</i> (Denkendorf, Germany) |
| UV spectrometer GeneQuant II | <i>Pharmacia</i> (Freiburg, Germany) |

Electrophoresis

| | |
|---------------------------------------|---|
| Mupid 2 | <i>Eurogentec</i> (Seraing, Belgium) |
| Electrophoresis Power Supply EPS 1000 | <i>Amersham Biotech</i> (Uppsala, Sweden) |

Power Pac 200
MultiSmall

BioRAD (Hercules, Californien/USA)
Amersham Biotech (Uppsala, Sweden)

Sonification

Branson Sonifier 250

Heinemann (Schwäbisch Gmünd, Germany)

Cell culture

Laminar flow hood Flow BSB 6A and BSB 4A
Water bath GFL 1004
Incubator BB 6220 CU
Incubator IG 150
Autoclave –steam sterilizer 3870EL
Sterilisator UT 6120
Hemocytometer (Bürker)

Gelaide (Meckenheim, Germany)
GFL (Burgwedel, Germany)
Heraeus (Hanau, Germany)
Astel (Chateau Gontier, France)
Jürgens (Münster, Germany)
Heraeus (Hanau, Germany)
Fischer (Frankfurt, Germany)

Microscope

Inverse phase-contrast microscope
Fluorescence microscope Diaphot TMD
Fluorescence microscope DM IRB
Confocal laser-scanning microscope TCS

Leika (Wetzlar, Germany)
Nikon (Düsseldorf, Germany)
Leika (Wetzlar, Germany)
Leika (Wetzlar, Germany)

Radioactive work

Scintillation counter
Autoradiography cassettes *Oncor*
Agfa Curix60
XOMAT AR Scientific Imaging Films

Beckman (München, Germany)
Appligene (Geithersburg, MD/USA)
Agfa AG (Leverkusen, Germany)
Eastman Kodak Comp. (Rochester, NY/USA)

8 References

- Abbott, N. J. 1992. Comparative physiology of the blood-brain barrier. Pages 371-96. *Physiology and pharmacology of the blood-brain barrier*. Springer-Verlag, Berlin, Heidelberg.
- Abbott, N. J., C. C. Hughes, P. A. Revest, and J. Greenwood. 1992. Development and characterisation of a rat brain capillary endothelial culture: towards an in vitro blood-brain barrier. *J Cell Sci* 103 (Pt 1): 23-37.
- Abraham, M. H., H. S. Chadha, and R. C. Mitchell. 1994. Hydrogen bonding. 33. Factors that influence the distribution of solutes between blood and brain. *J Pharm Sci* 83: 1257-68.
- Alberts, B., D. Bray, A. Johnson, J. Lewis, K. Roberts, and P. Walter. 1998. *Essential cell biology: an introduction to the molecular biology of the cell*. Garland Publishing Inc., New York.
- Alberts, B., D. Bray, J. Lewis, M. Raff, K. Roberts, and J. D. Watson. 1994. *Molecular biology of the cell*. Garland Publishing, Inc., New York.
- Alexander, J. S., and J. W. Elrod. 2002. Extracellular matrix, junctional integrity and matrix metalloproteinase interactions in endothelial permeability regulation. *J Anat* 200: 561-74.
- Alexander, J. S., W. F. Patton, B. W. Christman, L. L. Cuiper, and F. R. Haselton. 1998. Platelet-derived lysophosphatidic acid decreases endothelial permeability in vitro. *Am J Physiol* 274: H115-22.
- Anderson, J. M., M. S. Balda, and A. S. Fanning. 1993. The structure and regulation of tight junctions. *Curr Opin Cell Biol* 5: 772-8.
- Antonetti, D. A., E. B. Wolpert, L. DeMaio, N. S. Harhaj, and R. C. Scaduto, Jr. 2002. Hydrocortisone decreases retinal endothelial cell water and solute flux coincident with increased content and decreased phosphorylation of occludin. *J Neurochem* 80: 667-77.
- Antonov, A. S., M. E. Lukashev, Y. A. Romanov, V. A. Tkachuk, V. S. Repin, and V. N. Smirnov. 1986. Morphological alterations in endothelial cells from human aorta and umbilical vein induced by forskolin and phorbol 12-myristate 13-acetate: a synergistic action of adenylate cyclase and protein kinase C activators. *Proc Natl Acad Sci U S A* 83: 9704-8.
- Audus, K. L., and R. T. Borchardt. 1986. Characteristics of the large neutral amino acid transport system of bovine brain microvessel endothelial cell monolayers. *J Neurochem* 47: 484-8.
- . 1987. Bovine brain microvessel endothelial cell monolayers as a model system for the blood-brain barrier. *Ann N Y Acad Sci* 507: 9-18.
- Audus, K. L., L. Ng, W. Wang, and R. T. Borchardt. 1996. Brain microvessel endothelial cell culture systems. *Pharm Biotechnol* 8: 239-58.
- Bacic, F., S. Uematsu, R. M. McCarron, and M. Spatz. 1992. Secretion of immunoreactive endothelin-1 by capillary and microvascular endothelium of human brain. *Neurochem Res* 17: 699-702.
- Balabanov, R., and P. Dore-Duffy. 1998. Role of the CNS microvascular pericyte in the blood-brain barrier. *J Neurosci Res* 53: 637-44.

- Baranczyk-Kuzma, A., K. L. Audus, F. L. Guillot, and R. T. Borchardt. 1992. Effects of selected vasoactive substances on adenylate cyclase activity in brain, isolated brain microvessels, and primary cultures of brain microvessel endothelial cells. *Neurochem Res* 17: 209-14.
- Barrand, M. A., K. J. Robertson, and S. F. von Weikersthal., 1995. Comparisons of P-glycoprotein expression in isolated rat brain microvessels and in primary cultures of endothelial cells derived from microvasculature of rat brain, epididymal fat pad and from aorta. *FEBS Lett* 374: 179-83.
- Beuckmann, C. T., and H.-J. Galla. 1998. Tissue culture of brain endothelial cells - induction of blood-brain barrier properties by brain factors. Pages 79-86 in W. M. Pardridge, ed. *Introduction to the blood-brain barrier*. Cambridge University Press, Cambridge.
- Bosher, J. M., P. Dufourcq, S. Sookhareea, and M. Labouesse. 1999. RNA interference can target pre-mRNA: consequences for gene expression in a *Caenorhabditis elegans* operon. *Genetics* 153: 1245-56.
- Bowman, P. D., A. L. Betz, D. Ar, J. S. Wolinsky, J. B. Penney, R. R. Shivers, and G. W. Goldstein. 1981. Primary culture of capillary endothelium from rat brain. *In Vitro* 17: 353-62.
- Bowman, P. D., S. R. Ennis, K. E. Rarey, A. L. Betz, and G. W. Goldstein. 1983. Brain microvessel endothelial cells in tissue culture: a model for study of blood-brain barrier permeability. *Ann Neurol* 14: 396-402.
- Bradbury, M. W. 1993. The blood-brain barrier. *Exp Physiol* 78: 453-72.
- Brightman, M. W. 1989. The anatomic basis of the blood-brain barrier. Pages 53-84 in E. A. Neuwelt, ed. *Implications of the blood-brain barrier and its manipulation*. Plenum medical book company, New York.
- Brightman, M. W., and T. S. Reese. 1969. Junctions between intimately apposed cell membranes in the vertebrate brain. *J Cell Biol* 40: 648-77.
- Brostjan, C., J. Anrather, V. Csizmadia, G. Natarajan, and H. Winkler. 1997. Glucocorticoids inhibit E-selectin expression by targeting NF-kappaB and not ATF/c-Jun. *J Immunol* 158: 3836-44.
- Brown, H., T. T. Hien, N. Day, N. T. Mai, L. V. Chuong, T. T. Chau, P. P. Loc, N. H. Phu, D. Bethell, J. Farrar, K. Gatter, N. White, and G. Turner. 1999. Evidence of blood-brain barrier dysfunction in human cerebral malaria. *Neuropathol Appl Neurobiol* 25: 331-40.
- Buse, P., P. L. Woo, D. B. Alexander, H. H. Cha, A. Reza, N. D. Sirota, and G. L. Firestone. 1995a. Transforming growth factor-alpha abrogates glucocorticoid-stimulated tight junction formation and growth suppression in rat mammary epithelial tumor cells. *J Biol Chem* 270: 6505-14.
- Buse, P., P. L. Woo, D. B. Alexander, A. Reza, and G. L. Firestone. 1995b. Glucocorticoid-induced functional polarity of growth factor responsiveness regulates tight junction dynamics in transformed mammary epithelial tumor cells. *J Biol Chem* 270: 28223-7.
- Butt, A. M., and H. C. Jones. 1992. Effect of histamine and antagonists on electrical resistance across the blood-brain barrier in rat brain-surface microvessels. *Brain Res* 569: 100-5.
- Cancilla, R., J. Bready, and J. Berliner. 1993. Astrocyte-endothelial cell interactions. Pages 383-97 in Murphy, ed. *Astrocytes: Pharmacology and Function*. Academic, San Diego.

- Catalan, R. E., A. M. Martinez, M. D. Aragones, and I. Fernandez. 1989. Substance P stimulates translocation of protein kinase C in brain microvessels. *Biochem Biophys Res Commun* 164: 595-600.
- Cecchelli, R., B. Dehouck, L. Descamps, L. Fenart, V. V. Buee-Scherrer, C. Duhem, S. Lundquist, M. Rentfel, G. Torpier, and M. P. Dehouck. 1999. In vitro model for evaluating drug transport across the blood-brain barrier. *Adv Drug Deliv Rev* 36: 165-178.
- Chamoux, M., M. P. Dehouck, J. C. Fruchart, G. Spik, J. Montreuil, and R. Cecchelli. 1991. Characterization of angiogenin receptors on bovine brain capillary endothelial cells. *Biochem Biophys Res Commun* 176: 833-9.
- Chasan, B., N. A. Geisse, K. Pedatella, D. G. Wooster, M. Teintze, M. D. Carattino, W. H. Goldmann, and H. F. Cantiello. 2002. Evidence for direct interaction between actin and the cystic fibrosis transmembrane conductance regulator. *Eur Biophys J* 30: 617-24.
- Citi, S. 1993. The molecular organization of tight junctions. *J Cell Biol* 121: 485-9.
- Citi, S., H. Sabanay, J. Kendrick-Jones, and B. Geiger. 1989. Cingulin: characterization and localization. *J Cell Sci* 93 (Pt 1): 107-22.
- Cordon-Cardo, C., J. P. O'Brien, D. Casals, L. Rittman-Grauer, J. L. Biedler, M. R. Melamed, and J. R. Bertino. 1989. Multidrug-resistance gene (P-glycoprotein) is expressed by endothelial cells at blood-brain barrier sites. *Proc Natl Acad Sci U S A* 86: 695-8.
- Coulomb, B., L. Dubertret, E. Bell, and R. Touraine. 1984. The contractility of fibroblasts in a collagen lattice is reduced by corticosteroids. *J Invest Dermatol* 82: 341-4.
- Crone, C. 1965. Facilitated transfer of glucose from blood into brain tissue. *J Physiol* 181: 103-13.
- Crone, C., and S. P. Olesen. 1982. Electrical resistance of brain microvascular endothelium. *Brain Res* 241: 49-55.
- D'Atri, F., and S. Citi. 2001. Cingulin interacts with F-actin in vitro. *FEBS Lett* 507: 21-4.
- Davison, P. M., and M. A. Karasek. 1981. Human dermal microvascular endothelial cells in vitro: effect of cyclic AMP on cellular morphology and proliferation rate. *J Cell Physiol* 106: 253-8.
- de la Luna, S., and J. Ortin. 1992. pac gene as efficient dominant marker and reporter gene in mammalian cells. *Methods Enzymol* 216: 376-85.
- Dehouck, B., M. P. Dehouck, J. C. Fruchart, and R. Cecchelli. 1994. Upregulation of the low density lipoprotein receptor at the blood-brain barrier: intercommunications between brain capillary endothelial cells and astrocytes. *J Cell Biol* 126: 465-73.
- Dehouck, M. P., S. Meresse, P. Delorme, J. C. Fruchart, and R. Cecchelli. 1990. An easier, reproducible, and mass-production method to study the blood-brain barrier in vitro. *J Neurochem* 54: 1798-801.
- Deli, M. A., C. S. Abraham, M. Niwa, and A. Falus. 2003. N,N-diethyl-2-[4-(phenylmethyl)phenoxy]-ethan-amine increases the permeability of primary mouse cerebral endothelial cell monolayers. *Inflamm Res* 52 Suppl 1: S39-40.
- Deli, M. A., and F. Joo. 1996. Cultured vascular endothelial cells of the brain. *Keio J Med* 45: 183-98; 198-9.

- Deli, M. A., F. Joo, I. Krizbai, I. Lengyel, M. G. Nunzi, and J. R. Wolff. 1993. Calcium/calmodulin-stimulated protein kinase II is present in primary cultures of cerebral endothelial cells. *J Neurochem* 60: 1960-3.
- Dermietzel, R., and D. Krause. 1991. Molecular anatomy of the blood-brain barrier as defined by immunocytochemistry. *Int Rev Cytol* 127: 57-109.
- Diglio, C. A., P. Grammas, F. Giacomelli, and J. Wiener. 1982. Primary culture of rat cerebral microvascular endothelial cells. Isolation, growth, and characterization. *Lab Invest* 46: 554-63.
- Domke, J., Rademacher, M. 1998. Measuring the Elastic Properties of Thin Polymer Films with the AFM. *Langmuir* 14: 3320-25.
- Drake, B., C. B. Prater, A. L. Weisenhorn, S. A. Gould, T. R. Albrecht, C. F. Quate, D. S. Cannell, H. G. Hansma, and P. K. Hansma. 1989. Imaging crystals, polymers, and processes in water with the atomic force microscope. *Science* 243: 1586-9.
- Durieu-Trautmann, O., C. Federici, C. Creminon, N. Foignant-Chaverot, F. Roux, M. Claire, A. D. Strosberg, and P. O. Couraud. 1993. Nitric oxide and endothelin secretion by brain microvessel endothelial cells: regulation by cyclic nucleotides. *J Cell Physiol* 155: 104-11.
- Durieu-Trautmann, O., N. Foignant-Chaverot, J. Perdomo, P. Gounon, A. D. Strosberg, and P. O. Couraud. 1991. Immortalization of brain capillary endothelial cells with maintenance of structural characteristics of the blood-brain barrier endothelium. *In Vitro Cell Dev Biol* 27A: 771-8.
- Eggert, M., M. Muller, and R. Renkawitz. 1995. *The Glucocorticoid Hormone Receptor*. Birkhäuser, Boston.
- Ehrlich, P. 1885. *Eine farbanalytische Studie: Das Sauerstoffbedürfnis des Organismus*, Hirschwald.
- Eisenblätter, T., and H.-J. Galla. 2002. A new multidrug resistance protein at the blood-brain barrier. *Biochem Biophys Res Commun* 293: 1273-8.
- Eisenblätter, T. 2002. Identification and characterisation of a new multidrug resistance protein at the blood-brain barrier. Dissertation: *Institut für Biochemie*. Westfälische Wilhelms-Universität, Münster.
- Eisenblätter, T., K. Psathaki, T. Nitz, H.-J. Galla, and J. Wegener. 2001. Cell Culture Media: Selection and Standardization. in C. M. Lehr, ed. *Cell Culture Models of Biological Barriers: In-vitro test systems for Drug Absorption and Delivery*. Haarwood Academic Publishers, UK.
- Elbashir, S. M., J. Harborth, W. Lendeckel, A. Yalcin, K. Weber, and T. Tuschl. 2001. Duplexes of 21-nucleotide RNAs mediate RNA interference in cultured mammalian cells. *Nature* 411: 494-8.
- Elbashir, S. M., J. Harborth, K. Weber, and T. Tuschl. 2002. Analysis of gene function in somatic mammalian cells using small interfering RNAs. *Methods* 26: 199-213.
- Encio, I. J., and S. D. Detera-Wadleigh. 1991. The genomic structure of the human glucocorticoid receptor. *J Biol Chem* 266: 7182-8.
- Engelbertz, C., D. Korte, T. Nitz, H. Franke, M. Haselbach, J. Wegener, and H.-J. Galla. 2000. The development of in vitro models for the blood-brain and blood-CSF barriers. in D. J. Begley, M. W. Bradbury, and J. Kreuter, eds. *The Blood-Brain Barrier and Drug Delivery to the CNS*. Marcel Dekker, Basel, New York.

- English, D., A. T. Kovala, Z. Welch, K. A. Harvey, R. A. Siddiqui, D. N. Brindley, and J. G. Garcia. 1999. Induction of endothelial cell chemotaxis by sphingosine 1-phosphate and stabilization of endothelial monolayer barrier function by lysophosphatidic acid, potential mediators of hematopoietic angiogenesis. *J Hematother Stem Cell Res* 8: 627-34.
- Esser, S., M. G. Lampugnani, M. Corada, E. Dejana, and W. Risau. 1998. Vascular endothelial growth factor induces VE-cadherin tyrosine phosphorylation in endothelial cells. *J Cell Sci* 111 (Pt 13): 1853-65.
- Fagard, M., S. Boutet, J. B. Morel, C. Bellini, and H. Vaucheret. 2000. AGO1, QDE-2, and RDE-1 are related proteins required for post-transcriptional gene silencing in plants, quelling in fungi, and RNA interference in animals. *Proc Natl Acad Sci U S A* 97: 11650-4.
- Fanning, A. S., B. J. Jameson, L. A. Jesaitis, and J. M. Anderson. 1998. The tight junction protein ZO-1 establishes a link between the transmembrane protein occludin and the actin cytoskeleton. *J Biol Chem* 273: 29745-53.
- Fanning, A. S., L. L. Mitic, and J. M. Anderson. 1999. Transmembrane proteins in the tight junction barrier. *J Am Soc Nephrol* 10: 1337-45.
- Ferfer, R. 2000. Differentielle Genexpression an der Blut-Hirn Schranke. Examensarbeit: *Institut für Biochemie*. Westfälische Wilhelms-Universität, Münster.
- Fernandez, L., M. Romero, H. Soto, and J. Mosquera. 2001. Increased apoptosis in acute puromycin aminonucleoside nephrosis. *Exp Nephrol* 9: 99-108.
- Franke, H., H. Galla, and C. T. Beuckmann. 2000. Primary cultures of brain microvessel endothelial cells: a valid and flexible model to study drug transport through the blood-brain barrier in vitro. *Brain Res Brain Res Protoc* 5: 248-56.
- Franke, H., H.-J. Galla, and C. T. Beuckmann. 1999. An improved low-permeability in vitro-model of the blood-brain barrier: transport studies on retinoids, sucrose, haloperidol, caffeine and mannitol. *Brain Res* 818: 65-71.
- Freshney, R. I. 2000. *Culture of animal cells: a manual of basic techniques*. Wiley-Liss.
- Frick, E. 1965. Barriers of the central nervous system and physiology of proteins. *Int Ophthalmol Clin* 5: 683-712.
- Furuse, M., K. Fujita, T. Hiiiragi, K. Fujimoto, and S. Tsukita. 1998. Claudin-1 and -2: novel integral membrane proteins localizing at tight junctions with no sequence similarity to occludin. *J Cell Biol* 141: 1539-50.
- Furuse, M., T. Hirase, M. Itoh, A. Nagafuchi, S. Yonemura, and S. Tsukita. 1993. Occludin: a novel integral membrane protein localizing at tight junctions. *J Cell Biol* 123: 1777-88.
- Gaillard, P. J., I. C. van der Sandt, L. H. Voorwinden, D. Vu, J. L. Nielsen, A. G. de Boer, and D. D. Breimer. 2000. Astrocytes increase the functional expression of P-glycoprotein in an in vitro model of the blood-brain barrier. *Pharm Res* 17: 1198-205.
- Gaillard, P. J., L. H. Voorwinden, J. L. Nielsen, A. Ivanov, R. Atsumi, H. Engman, C. Ringbom, A. G. de Boer, and D. D. Breimer. 2001. Establishment and functional characterization of an in vitro

- model of the blood-brain barrier, comprising a co-culture of brain capillary endothelial cells and astrocytes. *Eur J Pharm Sci* 12: 215-22.
- Gardner, W. J. 1968. The barriers of the central nervous system. *Clin Neurosurg* 15: 80-100.
- Gecse, A., A. Ottlecz, Z. Mezei, G. Telegdy, F. Joo, E. Dux, and I. Karnushina. 1982. Prostacyclin and prostaglandin synthesis in isolated brain capillaries. *Prostaglandins* 23: 287-97.
- Gecse, A., A. Ottlecz, Z. Mezei, G. Telegdy, F. Joó, E. Dux, and I. L. Karnushina. 1981. Capillaries as the source of prostacyclin and prostaglandin synthesases in brain. Pages 107-15 in K. A.G.B., J. Hamar, and L. Szaboó, eds. *Advances in Physiological Sciences*. Akadémiai Kiadó, Budapest.
- Gehring, U. 1993. The structure of glucocorticoid receptors. *J Steroid Biochem Mol Biol* 45: 183-90.
- Gerritsen, M. E., T. P. Parks, and M. P. Printz. 1980. Prostaglandin endoperoxide metabolism by bovine cerebral microvessels. *Biochim Biophys Acta* 619: 196-206.
- Giaever, I., and Keese. C.R. 1993. A morphological biosensor for mammalian cells. *Nature*: 291-2.
- Gibson, U. E., C. A. Heid, and P. M. Williams. 1996. A novel method for real time quantitative RT-PCR. *Genome Res* 6: 995-1001.
- Gimbrone, M. A., Jr., G. R. Majeau, W. J. Atkinson, W. Sadler, and S. A. Cruise. 1979. Angiotensin-converting enzyme activity in isolated brain microvessels. *Life Sci* 25: 1075-83.
- Goehlert, U. G., N. M. Ng Ying Kin, and L. S. Wolfe. 1981. Biosynthesis of prostacyclin in rat cerebral microvessels and the choroid plexus. *J Neurochem* 36: 1192-201.
- Goldmann, E. E. 1913. Vitalfärbung am zentralen Nervensystem. Pages 1-60. *Agh. Preus. Akad. Wiss. Phys. Math. Kl. I, 1*.
- Goldstein, G. W., and A. L. Betz. 1986. The blood-brain barrier. *Sci Am* 255: 74-83.
- Grebenkamper, K., and H.-J. Galla. 1994. Translational diffusion measurements of a fluorescent phospholipid between MDCK-I cells support the lipid model of the tight junctions. *Chem Phys Lipids* 71: 133-43.
- Greenwood, J., G. Pryce, L. Devine, D. K. Male, W. L. dos Santos, V. L. Calder, and P. Adamson. 1996. SV40 large T immortalised cell lines of the rat blood-brain and blood-retinal barriers retain their phenotypic and immunological characteristics. *J Neuroimmunol* 71: 51-63.
- Greig, N. H. 1992. Drug entry into the brain and its pharmacologic manipulation. Pages 417-37 in M. W. B. Bradbury, ed. *Physiology and pharmacology of the blood-brain barrier*. Springer, Berlin, Heidelberg.
- Gruenau, S. P., K. J. Oscar, M. T. Folker, and S. I. Rapoport. 1982. Absence of microwave effect on blood-brain barrier permeability to [¹⁴C]sucrose in the conscious rat. *Exp Neurol* 75: 299-307.
- Habgood, M. D., D. J. Begley, and N. J. Abbott. 2000. Determinants of passive drug entry into the central nervous system. *Cell Mol Neurobiol* 20: 231-53.
- Habgood, M. D., Z. D. Liu, L. S. Dehkordi, H. H. Khodr, J. Abbott, and R. C. Hider. 1999. Investigation into the correlation between the structure of hydroxypyridinones and blood-brain barrier permeability. *Biochem Pharmacol* 57: 1305-10.

- Haga, H., S. Sasaki, K. Kawabata, E. Ito, T. Ushiki, and T. Sambongi. 2000. Elasticity mapping of living fibroblasts by AFM and immunofluorescence observation of the cytoskeleton. *Ultramicroscopy* 82: 253-8.
- Hanson-Painton, O., K. Morgenstern, D. R. Cooper, B. Moore, T. Botchlet, and P. Grammas. 1993. Protein kinase C in rat cerebral microvessels. *Mol Chem Neuropathol* 20: 245-61.
- Harborth, J., S. M. Elbashir, K. Bechert, T. Tuschl, and K. Weber. 2001. Identification of essential genes in cultured mammalian cells using small interfering RNAs. *J Cell Sci* 114: 4557-65.
- Hartwig, J. H., and D. J. Kwiatkowski. 1991. Actin-binding proteins. *Curr Opin Cell Biol* 3: 87-97.
- Haskins, J., L. Gu, E. S. Wittchen, J. Hibbard, and B. R. Stevenson. 1998. ZO-3, a novel member of the MAGUK protein family found at the tight junction, interacts with ZO-1 and occludin. *J Cell Biol* 141: 199-208.
- Hassan, A., W. F. Heinz, M. D. Antonik, N. P. D'Costa, S. Nageswaran, C. A. Schoenenberger, and J. H. Hoh. 1998. Relative microelastic mapping of living cells by atomic force microscopy. *Biophys J* 74: 1564-78.
- Hein, M., C. Madefessel, B. Haag, K. Teichmann, A. Post, and H.-J. Galla. 1992. Implications of a non-lamellar lipid phase for the tight junction stability. Part II: Reversible modulation of transepithelial resistance in high and low resistance MDCK-cells by basic amino acids, Ca²⁺, protamine and protons. *Chem Phys Lipids* 63: 223-33.
- Hertz, H. 1881. Über die Berührung fester elastischer Körper. *J. reine und angew. Math.* 92: 156-57.
- Hertz, L. 1989. Regulation of potassium homeostasis by glial cells. Pages 225-34 in G. Levi, ed. *Differentiation and function of glial cells*. Wiley-Liss, New York.
- Higuchi, R., G. Dollinger, P. S. Walsh, and R. Griffith. 1992. Simultaneous amplification and detection of specific DNA sequences. *Biotechnology (N Y)* 10: 413-7.
- Higuchi, R., C. Fockler, G. Dollinger, and R. Watson. 1993. Kinetic PCR analysis: real-time monitoring of DNA amplification reactions. *Biotechnology (N Y)* 11: 1026-30.
- Hoheisel, D., T. Nitz, H. Franke, J. Wegener, A. Hakvoort, T. Tilling, and H.-J. Galla. 1998. Hydrocortisone reinforces the blood-brain barrier properties in a serum free cell culture system. *Biochem Biophys Res Commun* 244: 312-6.
- Holash, J. A., D. M. Noden, and P. A. Stewart. 1993. Re-evaluating the role of astrocytes in blood-brain barrier induction. *Dev Dyn* 197: 14-25.
- Homayoun, P., W. D. Lust, and S. I. Harik. 1989. Effect of several vasoactive agents on guanylate cyclase activity in isolated rat brain microvessels. *Neurosci Lett* 107: 273-8.
- Huai-Yun, H., D. T. Secrest, K. S. Mark, D. Carney, C. Brandquist, W. F. Elmquist, and D. W. Miller. 1998. Expression of multidrug resistance-associated protein (MRP) in brain microvessel endothelial cells. *Biochem Biophys Res Commun* 243: 816-20.
- Hurst, R. D., and J. B. Clark. 1998. Alterations in transendothelial electrical resistance by vasoactive agonists and cyclic AMP in a blood-brain barrier model system. *Neurochem Res* 23: 149-54.
- Hurst, R. D., and I. B. Fritz. 1996. Properties of an immortalised vascular endothelial/glioma cell co-culture model of the blood-brain barrier. *J Cell Physiol* 167: 81-8.

- Igarashi, Y., H. Utsumi, H. Chiba, Y. Yamada-Sasamori, H. Tobioka, Y. Kamimura, K. Furuuchi, Y. Kokai, T. Nakagawa, M. Mori, and N. Sawada. 1999. Glial cell line-derived neurotrophic factor induces barrier function of endothelial cells forming the blood-brain barrier. *Biochem Biophys Res Commun* 261: 108-12
- Imaizumi, S., T. Kondo, M. A. Deli, G. Gobbel, F. Joo, C. J. Epstein, T. Yoshimoto, and P. H. Chan. 1996. The influence of oxygen free radicals on the permeability of the monolayer of cultured brain endothelial cells. *Neurochem Int* 29: 205-11.
- Ingraham, F. D., D. D. Matson, and R. L. McLaurin. 1952. Cortisone and ACTH as an adjunct to the surgery of craniopharyngiomas. *New Eng. J. Med*: 568-71.
- Janzer, R. C., and M. C. Raff. 1987. Astrocytes induce blood-brain barrier properties in endothelial cells. *Nature* 325: 253-7.
- Jarden, J. O., V. Dhawan, J. R. Moeller, S. C. Strother, and D. A. Rottenberg. 1989. The time course of steroid action on blood-to-brain and blood-to-tumor transport of ^{82}Rb : a positron emission tomographic study. *Ann Neurol* 25: 239-45.
- Jefferies, W. A., M. R. Brandon, S. V. Hunt, A. F. Williams, K. C. Gatter, and D. Y. Mason. 1984. Transferrin receptor on endothelium of brain capillaries. *Nature* 312: 162-3.
- Jesaitis, L. A., and D. A. Goodenough. 1994. Molecular characterization and tissue distribution of ZO-2, a tight junction protein homologous to ZO-1 and the Drosophila discs-large tumor suppressor protein. *J Cell Biol* 124: 949-61.
- Johansson, B. B. 1990. The physiology of the blood-brain barrier. *Adv Exp Med Biol* 274: 25-39.
- Jonat, C., H. J. Rahmsdorf, K. K. Park, A. C. Cato, S. Gebel, H. Ponta, and P. Herrlich. 1990. Antitumor promotion and antiinflammation: down-modulation of AP-1 (Fos/Jun) activity by glucocorticoid hormone. *Cell* 62: 1189-204.
- Joo, F. 1971. Increased production of coated vesicles in the brain capillaries during enhanced permeability of the blood-brain barrier. *Br J Exp Pathol* 52: 646-9.
- . 1992. The cerebral microvessels in culture, an update. *J Neurochem* 58: 1-17.
- Joo, F., Z. Rakonczay, and M. Wollemann. 1975. cAMP-mediated regulation of the permeability in the brain capillaries. *Experientia* 31: 582-4.
- Joo, F., P. Temesvari, and E. Dux. 1983. Regulation of the macromolecular transport in the brain microvessels: the role of cyclic GMP. *Brain Res* 278: 165-74.
- Joo, F., and I. Toth. 1975. Brain adenylate cyclase: its common occurrence in the capillaries and astrocytes. *Naturwissenschaften* 62: 397-8.
- Jungermann, K., and H. Möhler. 1980. Stoffwechselsteuerung durch Glucagon, Catecholamine und andere Hormone. Pages 249-64 in K. Jungermann and H. Möhler, eds. *Biochemie*. Springer-Verlag, Berlin, Heidelberg, New York.
- Karchar, B., and T. S. Reese. 1982. Evidence for the lipidic nature of tight junction strands. *Nature* 296: 464-466.
- Karlsom, P. 1994. *Kurzes Lehrbuch der Biochemie für Mediziner und Naturwissenschaftler*. Georg Thieme Verlag, Stuttgart, New York.

- Karnushina, I., I. Toth, E. Dux, and F. Joo. 1980a. Presence of the guanylate cyclase in brain capillaries: histochemical and biochemical evidence. *Brain Res* 189: 588-92.
- Karnushina, I. L., J. M. Palacios, G. Barbin, E. Dux, F. Joo, and J. C. Schwartz. 1980b. Studies on a capillary-rich fraction isolated from brain: histaminic components and characterization of the histamine receptors linked to adenylate cyclase. *J Neurochem* 34: 1201-8.
- Katsube, T., M. Takahisa, R. Ueda, N. Hashimoto, M. Kobayashi, and S. Togashi. 1998. Cortactin associates with the cell-cell junction protein ZO-1 in both *Drosophila* and mouse. *J Biol Chem* 273: 29672-7.
- Keck, P. J., S. D. Hauser, G. Krivi, K. Sanzo, T. Warren, J. Feder, and D. T. Connolly. 1989. Vascular permeability factor, an endothelial cell mitogen related to PDGF. *Science* 246: 1309-12.
- Keep, R. F., and H. C. Jones. 1990. A morphometric study on the development of the lateral ventricle choroid plexus, choroid plexus capillaries and ventricular ependyma in the rat. *Brain Res Dev Brain Res* 56: 47-53.
- Kniesel, U., and H. Wolburg. 2000. Tight junctions of the blood-brain barrier. *Cell Mol Neurobiol* 20: 57-76.
- Krause, D., U. Mischeck, H.-J. Galla, and R. Dermietzel. 1991. Correlation of zonula occludens ZO-1 antigen expression and transendothelial resistance in porcine and rat cultured cerebral endothelial cells. *Neurosci Lett* 128: 301-4.
- Krause, D. N., I. E. Goetz, C. Estrada, and E. Roberts. 1982. Culture of vascular endothelial cells from adult bovine brain. *Fed Proc* 41: 1760.
- Krstić, R. V. 1988. *Die Gewebe des Menschen und der Säugetiere*. Springer-Verlag, Berlin Heidelberg New York.
- Krizbai, I., G. Szabo, M. Deli, K. Maderspach, C. Lehel, Z. Olah, J. R. Wolff, and F. Joo. 1995. Expression of protein kinase C family members in the cerebral endothelial cells. *J Neurochem* 65: 459-62.
- Laemmli, U. K. 1970. Cleavage of structural proteins during the assembly of the head of bacteriophage T4. *Nature* 227: 680-5.
- Lechardeur, D., B. Schwartz, D. Paulin, and D. Scherman. 1995. Induction of blood-brain barrier differentiation in a rat brain-derived endothelial cell line. *Exp Cell Res* 220: 161-70.
- Levin, V. A. 1980. Relationship of octanol/water partition coefficient and molecular weight to rat brain capillary permeability. *J Med Chem* 23: 682-4.
- Lewandowsky, M. 1900. Zur Lehre von der Cerebrospinal Flüssigkeit. *Z. Klin. Med.*: 480-94.
- Linnell, E. R., C. P. Lerner, K. A. Johnson, C. A. Leach, T. R. Ulrich, W. C. Rafferty, and E. M. Simpson. 2001. Transgenic mice for the preparation of puromycin-resistant primary embryonic fibroblast feeder layers for embryonic stem cell selection. *Mamm Genome* 12: 169-71.
- Lo, C. M., C. R. Keese, and I. Giaever. 1995. Impedance analysis of MDCK cells measured by electric cell-substrate impedance sensing. *Biophys J* 69: 2800-7.
- Lohmann, C., S. Huwel, and H.-J. Galla. 2002. Predicting blood-brain barrier permeability of drugs: evaluation of different in vitro assays. *J Drug Target* 10: 263-76.

- Lohmann, T. 2003. Die Blut-Hirn-Schranke in vitro: Regulation der Permeabilität durch Matrixmetalloproteasen. Dissertation: *Institut für Biochemie*. Westfälische Wilhelms-Universität, Münster.
- Long, D. M., J. F. Hartmann, and L. A. French. 1966a. The response of experimental cerebral edema to glucosteroid administration. *J Neurosurg* 24: 843-54.
- Long, D. M., J. F. Hartmann, and L. A. French. 1966b. The response of human cerebral edema to glucosteroid administration. An electron microscopic study. *Neurology* 16: 521-8.
- Madara, J. L. 1988. Tight junction dynamics: is paracellular transport regulated? *Cell* 53: 497-8.
- Madara, J. L., C. Parkos, S. Colgan, A. Nusrat, K. Atisook, and P. Kaoutzani. 1992. The movement of solutes and cells across tight junctions. *Ann N Y Acad Sci* 664: 47-60.
- Marceau, F., B. Tremblay, R. Couture, and D. Regoli. 1989. Prostacyclin release induced by neurokinins in cultured human endothelial cells. *Can J Physiol Pharmacol* 67: 159-62.
- Markovac, J., and G. W. Goldstein. 1988. Transforming growth factor beta activates protein kinase C in microvessels isolated from immature rat brain. *Biochem Biophys Res Commun* 150: 575-82.
- Mattagajasingh, S. N., S. C. Huang, J. S. Hartenstein, and E. J. Benz, Jr. 2000. Characterization of the interaction between protein 4.1R and ZO-2. A possible link between the tight junction and the actin cytoskeleton. *J Biol Chem* 275: 30573-85.
- Maurer, P., M. A. Moskowitz, L. Levine, and E. Melamed. 1980. The synthesis of prostaglandins by bovine cerebral microvessels. *Prostaglandins Med* 4: 153-61.
- McNamara, R. K., and R. H. Lenox. 1998. Distribution of the protein kinase C substrates MARCKS and MRP in the postnatal developing rat brain. *J Comp Neurol* 397: 337-56.
- Meresse, S., M. P. Dehouck, P. Delorme, M. Bensaid, J. P. Tauber, C. Delbart, J. C. Fruchart, and R. Cecchelli. 1989. Bovine brain endothelial cells express tight junctions and monoamine oxidase activity in long-term culture. *J Neurochem* 53: 1363-71.
- Miesfeld, R. L. 1989. The structure and function of steroid receptor proteins. *Crit Rev Biochem Mol Biol* 24: 101-17.
- Miki, H., T. Mio, S. Nagai, Y. Hoshino, T. Tsutsumi, T. Mikuniya, and T. Izumi. 2000. Glucocorticoid-induced contractility and F-actin content of human lung fibroblasts in three-dimensional culture. *Am J Physiol Lung Cell Mol Physiol* 278: L13-8.
- Minakawa, T., J. Bready, J. Berliner, M. Fisher, and P. A. Cancilla. 1991. In vitro interaction of astrocytes and pericytes with capillary-like structures of brain microvessel endothelium. *Lab Invest* 65: 32-40.
- Mischek, U., J. Meyer, and H.-J. Galla. 1989. Characterisation of g-Glutamyl transpeptidase activity of cultured endothelial cells from porcine brain capillaries. *Cell Tissue Research* 256: 221-226.
- Mitra, P., C. R. Keese, and I. Giaever. 1991. Electric measurements can be used to monitor the attachment and spreading of cells in tissue culture. *Biotechniques* 11: 504-10.
- Moore, S. A., L. J. Prokuski, P. H. Figard, A. A. Spector, and M. N. Hart. 1988a. Murine cerebral microvascular endothelium incorporate and metabolize 12-hydroxyeicosatetraenoic acid. *J Cell Physiol* 137: 75-85.

- Moore, S. A., A. A. Spector, and M. N. Hart. 1988b. Eicosanoid metabolism in cerebromicrovascular endothelium. *Am J Physiol* 254: C37-44.
- Morin, A. M., and A. Stanboli. 1993. Nitric oxide synthase in cultured endothelial cells of cerebrovascular origin: cytochemistry. *J Neurosci Res* 36: 272-9.
- Muruganandam, A., L. M. Herx, R. Monette, J. P. Durkin, and D. B. Stanimirovic. 1997. Development of immortalized human cerebromicrovascular endothelial cell line as an in vitro model of the human blood-brain barrier. *Faseb J* 11: 1187-97.
- Nakane, M., M. Ichikawa, and T. Deguchi. 1983. Light and electron microscopic demonstration of guanylate cyclase in rat brain. *Brain Res* 273: 9-15.
- Neuhaus, J., W. Risau, and H. Wolburg. 1991. Induction of blood-brain barrier characteristics in bovine brain endothelial cells by rat astroglial cells in transfilter coculture. *Ann N Y Acad Sci* 633: 578-80.
- Nishino, K., K. Yamanouchi, K. Naito, and H. Tojo. 2002. Matrix metalloproteinases regulate mesonephric cell migration in developing XY gonads which correlates with the inhibition of tissue inhibitor of metalloproteinase-3 by Sry. *Dev Growth Differ* 44: 35-43.
- Nitz, T. 2001. Modulation der interendothelialen Permeabilität an der BHS. *Institut für Biochemie*. Westfälische Wilhelms-Universität, Münster.
- Nitz, T., T. Eisenblätter, K. Psathaki, and H.-J. Galla. 2003. Serum-derived factors weaken the barrier properties of cultured porcine brain capillary endothelial cells in vitro. *Brain Res* 981: 30-40.
- Nitz, T., T. Eisenblätter, M. Haselbach, and H.-J. Galla. 2001. Recent Advances in the development of Cell Culture Models for the Blood-Brain and the Blood-CSF-Barrier. Pages 45-62 in D. Kobilier, S. Lustig, and S. Shapira, eds. *Blood-Brain Barrier Drug Delivery and Brain Pathology*. Kluwer Academic/Plenum, New York.
- Oakley, R. H., C. M. Jewell, M. R. Yudt, D. M. Bofetiado, and J. A. Cidlowski. 1999. The dominant negative activity of the human glucocorticoid receptor beta isoform. Specificity and mechanisms of action. *J Biol Chem* 274: 27857-66.
- Oldendorf, W. H., M. E. Cornford, and W. J. Brown. 1977. The large apparent work capability of the blood-brain barrier: a study of the mitochondrial content of capillary endothelial cells in brain and other tissues of the rat. *Ann Neurol* 1: 409-17.
- Oldendorf, W. H., and J. Szabo. 1976. Amino acid assignment to one of three blood-brain barrier amino acid carriers. *Am J Physiol* 230: 94-8.
- Orlowski, M., G. Sessa, and J. P. Green. 1974. Gamma-glutamyl transpeptidase in brain capillaries: possible site of a blood-brain barrier for amino acids. *Science* 184: 66-8.
- Palmer, G. C., R. B. Chronister, and S. J. Palmer. 1980a. Adenylate cyclase responses to neurohumoral agonists in microvascular elements of the rabbit brain. *J Neurobiol* 11: 503-8.
- Palmer, G. C., S. J. Palmer, and R. B. Chronister. 1980b. Cyclic nucleotide systems in the microcirculation of mammalian brain. *Adv Exp Med Biol* 131: 147-62.

- Panula, P., F. Joo, and L. Rechart. 1978. Evidence for the presence of viable endothelial cells in cultures derived from dissociated rat brain. *Experientia* 34: 95-7.
- Pardridge, W. M. 1993. Brain drug delivery and blood-brain barrier transport. *Durg Delivery*: 83-101.
- Pardridge, W. M., D. Triguero, J. Yang, and P. A. Cancilla. 1990. Comparison of in vitro and in vivo models of drug transcytosis through the blood-brain barrier. *J Pharmacol Exp Ther* 253: 884-91.
- Pegram, C. N., L. F. Eng, C. J. Wikstrand, R. D. McComb, Y. L. Lee, and D. D. Bigner. 1985. Monoclonal antibodies reactive with epitopes restricted to glial fibrillary acidic proteins of several species. *Neurochem Pathol* 3: 119-38.
- Phillips, P., P. Kumar, S. Kumar, and M. Waghe. 1979. Isolation and characterization of endothelial cells from rat and cow brain white matter. *J Anat* 129: 261-72.
- Pirila, E., A. Sharabi, T. Salo, V. Quaranta, H. Tu, R. Heljasvaara, N. Koshikawa, T. Sorsa, and P. Maisi. 2003. Matrix metalloproteinases process the laminin-5 gamma 2-chain and regulate epithelial cell migration. *Biochem Biophys Res Commun* 303: 1012-7.
- Rademacher, M. 2002. Measuring the Elastic Properties of Living Cells by the Atomic Force Microscope. *Method In Cell Biology* 68: 67-87.
- Ramsohoye, P. V., and I. B. Fritz. 1998. Preliminary characterization of glial-secreted factors responsible for the induction of high electrical resistances across endothelial monolayers in a blood-brain barrier model. *Neurochem Res* 23: 1545-51.
- Raub, T. J. 1996. Signal transduction and glial cell modulation of cultured brain microvessel endothelial cell tight junctions. *Am J Physiol* 271: C495-503.
- Reardon, P. M., and K. L. Audus. 1993a. Applications of primary cultures of brain microvessel endothelial cells monolayers in the study of vasoactive peptide interaction with the blood-brain barrier. *Pharma Science* 3: 63-8.
- Regina, A., I. A. Romero, J. Greenwood, P. Adamson, J. M. Bourre, P. O. Couraud, and F. Roux. 1999. Dexamethasone regulation of P-glycoprotein activity in an immortalized rat brain endothelial cell line, GPNT. *J Neurochem* 73: 1954-63.
- Rexin, M., W. Busch, and U. Gehring. 1988. Chemical cross-linking of heteromeric glucocorticoid receptors. *Biochemistry* 27: 5593-601.
- Rist, R. J., I. A. Romero, M. W. Chan, P. O. Couraud, F. Roux, and N. J. Abbott. 1997. F-actin cytoskeleton and sucrose permeability of immortalised rat brain microvascular endothelial cell monolayers: effects of cyclic AMP and astrocytic factors. *Brain Res* 768: 10-8.
- Robinson, R. A., C. J. TenEyck, and M. N. Hart. 1986. Establishment and preliminary growth characteristics of a transformed mouse cerebral microvessel endothelial cell line. *Lab Invest* 54: 579-88.
- Romero, I. A., K. Radewicz, E. Jubin, C. C. Michel, J. Greenwood, P. O. Couraud, and P. Adamson. 2003. Changes in cytoskeletal and tight junctional proteins correlate with decreased permeability induced by dexamethasone in cultured rat brain endothelial cells. *Neurosci Lett* 344: 112-6.

- Rosenthal, M. D., and J. E. Jones. 1988. Release of arachidonic acid from vascular endothelial cells: fatty acyl specificity is observed with receptor-mediated agonists and with the calcium ionophore A23187 but not with melittin. *J Cell Physiol* 136: 333-40.
- Rotsch, C., and M. Radmacher. 2000. Drug-induced changes of cytoskeletal structure and mechanics in fibroblasts: an atomic force microscopy study. *Biophys J* 78: 520-35.
- Roux, E., Borrel, A. 1889. Tétanos cérébral et immunité contre le tétanos. *Ann. Inst. Pasteur*: 225-39.
- Roux, F., O. Durieu-Trautmann, N. Chaverot, M. Claire, P. Mailly, J. M. Bourre, A. D. Strosberg, and P. O. Couraud. 1994. Regulation of gamma-glutamyl transpeptidase and alkaline phosphatase activities in immortalized rat brain microvessel endothelial cells. *J Cell Physiol* 159: 101-13.
- Rubenstein, N. M., Y. Guan, P. L. Woo, and G. L. Firestone. 2003. Glucocorticoid down-regulation of RhoA is required for the steroid-induced organization of the junctional complex and tight junction formation in rat mammary epithelial tumor cells. *J Biol Chem* 278: 10353-60.
- Rubin, L. L., D. E. Hall, S. Porter, K. Barbu, C. Cannon, H. C. Horner, M. Janatpour, C. W. Liaw, K. Manning, J. Morales, and et al., 1991. A cell culture model of the blood-brain barrier. *J Cell Biol* 115: 1725-35.
- Rubin, L. L., and J. M. Staddon. 1999. The cell biology of the blood-brain barrier. *Annu Rev Neurosci* 22: 11-28.
- Sackmann, E. 1994. Intra- and extracellular macromolecular networks: physics and biological function. *Macromol. Chem. Phys.* 195: 7-28.
- Sambrook, J., Fritsch, E.F., Maniatis, T.,. 1989. Molecular Cloning: A Laboratory Manual in C. S. H. Laboratory, ed. Press, New York.
- Sanwal, V., M. Pandya, M. Bhaskaran, N. Franki, K. Reddy, G. Ding, A. Kapasi, E. Valderrama, and P. C. Singhal., 2001. Puromycin aminonucleoside induces glomerular epithelial cell apoptosis. *Exp Mol Pathol* 70: 54-64.
- Satcher, R. L., Jr., and C. F. Dewey, Jr. 1996. Theoretical estimates of mechanical properties of the endothelial cell cytoskeleton. *Biophys J* 71: 109-18.
- Saunders, N. R., M. D. Habgood, and K. M. Dziegielewska. 1999. Barrier mechanisms in the brain, I. Adult brain. *Clin Exp Pharmacol Physiol* 26: 11-9.
- Schar-Zammaretti, P., U. Ziegler, I. Forster, P. Groscurth, and U. E. Spichiger-Keller. 2002. Potassium-selective atomic force microscopy on ion-releasing substrates and living cells. *Anal Chem* 74: 4269-74.
- Schinkel, A. H., J. J. Smit, O. van Tellingen, J. H. Beijnen, E. Wagenaar, L. van Deemter, C. A. Mol, M. A. van der Valk, E. C. Robanus-Maandag, H. P. te Riele, and et al., 1994. Disruption of the mouse *mdr1a* P-glycoprotein gene leads to a deficiency in the blood-brain barrier and to increased sensitivity to drugs. *Cell* 77: 491-502.
- Schneeberger, E. E., and R. D. Lynch. 1992. Structure, function, and regulation of cellular tight junctions. *Am J Physiol* 262: L647-61.
- Schulze, C., C. Smales, L. L. Rubin, and J. M. Staddon. 1997. Lysophosphatidic acid increases tight junction permeability in cultured brain endothelial cells. *J Neurochem* 68: 991-1000.

- Senger, D. R., S. J. Galli, A. M. Dvorak, C. A. Perruzzi, V. S. Harvey, and H. F. Dvorak. 1983. Tumor cells secrete a vascular permeability factor that promotes accumulation of ascites fluid. *Science* 219: 983-5.
- Shepro, D., and N. M. Morel. 1993. Pericyte physiology. *Faseb J* 7: 1031-8.
- Shi, F., and K. L. Audus. 1994. Biochemical characteristics of primary and passaged cultures of primate brain microvessel endothelial cells. *Neurochem Res* 19: 427-33.
- Sims, D. E. 1986. The pericyte--a review. *Tissue Cell* 18: 153-74.
- Singer, K. L., B. R. Stevenson, P. L. Woo, and G. L. Firestone. 1994. Relationship of serine/threonine phosphorylation/dephosphorylation signaling to glucocorticoid regulation of tight junction permeability and ZO-1 distribution in nontransformed mammary epithelial cells. *J Biol Chem* 269: 16108-15.
- Skalli, O., M. F. Pelte, M. C. Pecllet, G. Gabbiani, P. Gugliotta, G. Bussolati, M. Ravazzola, and L. Orci. 1989. Alpha-smooth muscle actin, a differentiation marker of smooth muscle cells, is present in microfilamentous bundles of pericytes. *J Histochem Cytochem* 37: 315-21.
- Sneddon, I. N. 1965. The relation between load and penetration in the axisymmetric Boussinesq problem for a punch of arbitrary profile. *Int. J. Eng. Sci.* 3: 47-57.
- Sobue, K., N. Yamamoto, K. Yoneda, M. E. Hodgson, K. Yamashiro, N. Tsuruoka, T. Tsuda, H. Katsuya, Y. Miura, K. Asai, and T. Kato. 1999. Induction of blood-brain barrier properties in immortalized bovine brain endothelial cells by astrocytic factors. *Neurosci Res* 35: 155-64.
- Spector, R., and C. E. Johanson. 1989. The mammalian choroid plexus. *Sci Am* 261: 68-74.
- Speth, R. C., and S. I. Harik. 1985. Angiotensin II receptor binding sites in brain microvessels. *Proc Natl Acad Sci U S A* 82: 6340-3.
- Stanimirovic, D., P. Morley, R. Ball, E. Hamel, G. Mealing, and J. P. Durkin. 1996. Angiotensin II-induced fluid phase endocytosis in human cerebrovascular endothelial cells is regulated by the inositol-phosphate signaling pathway. *J Cell Physiol* 169: 455-67.
- Stelwagen, K., H. A. McFadden, and J. Demmer. 1999. Prolactin, alone or in combination with glucocorticoids, enhances tight junction formation and expression of the tight junction protein occludin in mammary cells. *Mol Cell Endocrinol* 156: 55-61.
- Sternlicht, M. D., and Z. Werb. 2001. How matrix metalloproteinases regulate cell behavior. *Annu Rev Cell Dev Biol* 17: 463-516.
- Stevenson, B. R., J. D. Siliciano, M. S. Mooseker, and D. A. Goodenough. 1986. Identification of ZO-1: a high molecular weight polypeptide associated with the tight junction (zonula occludens) in a variety of epithelia. *J Cell Biol* 103: 755-66.
- Stewart, P. A., K. Hayakawa, and C. L. Farrell. 1994. Quantitation of blood-brain barrier ultrastructure. *Microsc Res Tech* 27: 516-27.
- Stewart, P. A., and M. J. Wiley. 1981. Developing nervous tissue induces formation of blood-brain barrier characteristics in invading endothelial cells: a study using quail--chick transplantation chimeras. *Dev Biol* 84: 183-92.
- Stins, M. F., N. V. Prasadarao, J. Zhou, M. Ardit, and K. S. Kim. 1997. Bovine brain microvascular endothelial cells transfected with SV40-large T antigen: development of an immortalized cell line to study pathophysiology of CNS disease. *In Vitro Cell Dev Biol Anim* 33: 243-7.

- Stryer, L. u. 1996. *Biochemie*. Spektrum, Heidelberg; Berlin; Oxford.
- Suzuki, T., H. Takemura, E. Noiri, K. Nosaka, A. Toda, S. Taniguchi, K. Uchida, T. Fujita, S. Kimura, and A. Nakao. 2001. Puromycin aminonucleoside induces apoptosis and increases HNE in cultured glomerular epithelial cells(1). *Free Radic Biol Med* 31: 615-23.
- Svendgaard, N. A., A. Bjorklund, J. E. Hardebo, and U. Stenevi. 1975. Axonal degeneration associated with a defective blood-brain barrier in cerebral implants. *Nature* 255: 334-6.
- Svoboda, P., P. Stein, and R. M. Schultz. 2001. RNAi in mouse oocytes and preimplantation embryos: effectiveness of hairpin dsRNA. *Biochem Biophys Res Commun* 287: 1099-104.
- Tan, K. H., M. S. Dobbie, R. A. Felix, M. A. Barrand, and R. D. Hurst. 2001. A comparison of the induction of immortalized endothelial cell impermeability by astrocytes. *Neuroreport* 12: 1329-34.
- Tatsuta, T., M. Naito, T. Oh-hara, I. Sugawara, and T. Tsuruo. 1992. Functional involvement of P-glycoprotein in blood-brain barrier. *J Biol Chem* 267: 20383-91.
- Teifel, M., and P. Friedl. 1996. Establishment of the permanent microvascular endothelial cell line PBMEC/C1-2 from porcine brains. *Exp Cell Res* 228: 50-7.
- Tewes, B., H. Franke, S. Hellwig, D. Hoheisel, S. Decker, D. Griesche, T. Tilling, J. Wegener, and H.-J. Galla. 1996. Preparation of endothelial cells in primary cultures obtained from the brain of 6-month-old pigs in D. B. B. S. W., ed. *Drug Transport across the Blood-Brain Barrier*. Harwood academic publishers, Amsterdam.
- Tontsch, U., and H. C. Bauer. 1989. Isolation, characterization, and long-term cultivation of porcine and murine cerebral capillary endothelial cells. *Microvasc Res* 37: 148-61.
- Trautmann, O. D., S. Bourdoulous, F. Roux, J. M. Bourre, A. D. Strosberg, and P.-O. Couraud. 1993. Immortalized rat brain microvessel endothelial cells: II. Pharmacological characterization. Pages 205-9 in L. R. Drewes and A. L. Betz, eds. *Frontiers in Cerebral Vascular Biology: Transport and Its Regulation*. Plenum Press, New York.
- Tsukita, S., A. Nagafuchi, and S. Yonemura. 1992. Molecular linkage between cadherins and actin filaments in cell-cell adherens junctions. *Curr Opin Cell Biol* 4: 834-9.
- Tuschl, T., S. Elbashir, J. Harborth, and K. Weber. 2001. The siRNA user guide. *HTML-online* -: -.
- van Meer, G., B. Gumbiner, and K. Simons. 1986. The tight junction does not allow lipid molecules to diffuse from one epithelial cell to the next. *Nature* 322: 639-41.
- van Meer, G., and K. Simons. 1986. The function of tight junctions in maintaining differences in lipid composition between the apical and the basolateral cell surface domains of MDCK cells. *Embo J* 5: 1455-64.
- Vorbrodt, A. W. 1988. Ultrastructural cytochemistry of blood-brain barrier endothelia. *Prog Histochem Cytochem* 18: 1-99.
- Vrtovsnik, F., M. Jourdain, G. Cherqui, J. Lefebvre, and G. Friedlander. 1994. Glucocorticoid inhibition of Na-Pi cotransport in renal epithelial cells is mediated by protein kinase C. *J Biol Chem* 269: 8872-7.

- Wagner, D. D., and V. J. Marder. 1984. Biosynthesis of von Willebrand factor protein by human endothelial cells: processing steps and their intracellular localization. *J. Cell. Biology* 99: 2123-30.
- Walter, E., T. Kissel, M. Reers, G. Dickneite, D. Hoffmann, and W. Stuber. 1995. Transepithelial transport properties of peptidomimetic thrombin inhibitors in monolayers of a human intestinal cell line (Caco-2) and their correlation to in vivo data. *Pharm Res* 12: 360-5.
- Wegener, J., and H.-J. Galla. 1996. The role of non-lamellar lipid structures in the formation of tight junctions. *Chemistry And Physics Of Lipids* 81: 229-255.
- Wegener, J., A. Hakvoort, and H.-J. Galla. 2000a. Barrier function of porcine choroid plexus epithelial cells is modulated by cAMP-dependent pathways in vitro. *Brain Res* 853: 115-24.
- Wegener, J., A. Janshoff, and H.-J. Galla. 1999. Cell adhesion monitoring using a quartz crystal microbalance: comparative analysis of different mammalian cell lines. *Eur Biophys J* 28: 26-37.
- Wegener, J., A. Janshoff, and C. Steinem. 2001. The quartz crystal microbalance as a novel means to study cell-substrate interactions in situ. *Cell Biochem Biophys* 34: 121-51.
- Wegener, J., C. R. Keese, and I. Giaever. 2000b. Electric cell-substrate impedance sensing (ECIS) as a noninvasive means to monitor the kinetics of cell spreading to artificial surfaces. *Exp Cell Res* 259: 158-66.
- Wegener, J., J. Seebach, A. Janshoff, and H.-J. Galla. 2000c. Analysis of the composite response of shear wave resonators to the attachment of mammalian cells. *Biophys J* 78: 2821-33.
- Weidenfeller, C. 2000. Analyse differentiell exprimierter Gene am Endothel der Blut-Hirn-Schranke in vitro. Diplomarbeit: *Institut für Biochemie*. Westfälische Wilhelms-Universität, Münster.
- Wittchen, E. S., J. Haskins, and B. R. Stevenson. 1999. Protein interactions at the tight junction. Actin has multiple binding partners, and ZO-1 forms independent complexes with ZO-2 and ZO-3. *J Biol Chem* 274: 35179-85.
- Wolburg, H., J. Neuhaus, U. Kniesel, B. Krauss, E. M. Schmid, M. Ocalan, C. Farrell, and W. Risau. 1994. Modulation of tight junction structure in blood-brain barrier endothelial cells. Effects of tissue culture, second messengers and cocultured astrocytes. *J Cell Sci* 107 (Pt 5): 1347-57.
- Yamada, K., Y. Ushio, T. Hayakawa, N. Arita, N. Yamada, and H. Mogami. 1983. Effects of methylprednisolone on peritumoral brain edema. A quantitative autoradiographic study. *J Neurosurg* 59: 612-9.
- Yamane, Y., H. Shiga, H. Haga, K. Kawabata, K. Abe, and E. Ito. 2000. Quantitative analyses of topography and elasticity of living and fixed astrocytes. *J Electron Microsc (Tokyo)* 49: 463-71.
- Zettl, K. S., M. D. Sjaastad, P. M. Riskin, G. Parry, T. E. Machen, and G. L. Firestone. 1992. Glucocorticoid-induced formation of tight junctions in mouse mammary epithelial cells in vitro. *Proc Natl Acad Sci U S A* 89: 9069-73.
- Zhang, J., Y. L. Wang, L. Gu, and J. Pan. 2003. Atomic force microscopy of actin. *Sheng Wu Hua Xue Yu Sheng Wu Wu Li Xue Bao (Shanghai)* 35: 489-94.

- Zhang, Y., H. Han, W. F. Elmquist, and D. W. Miller. 2000. Expression of various multidrug resistance-associated protein (MRP) homologues in brain microvessel endothelial cells. *Brain Res* 876: 148-53.
- Zhong, Y., T. Saitoh, T. Minase, N. Sawada, K. Enomoto, and M. Mori. 1993. Monoclonal antibody 7H6 reacts with a novel tight junction-associated protein distinct from ZO-1, cingulin and ZO-2. *J Cell Biol* 120: 477-83.

Appendix A: Abbreviations

| | |
|----------------|--|
| ABC | ATP-binding cassette |
| APS | ammonium peroxodisulfate |
| ATP | adenosine triphosphate |
| BBB | blood-brain barrier |
| BCEC | brain capillary endothelial cells |
| BCSFB | blood-cerebrospinal fluid barrier |
| BMDP | brain multidrug resistance protein |
| bp base | pair(s) |
| BSA | bovine serum albumin |
| cDNA | complementary deoxyribonucleic acid |
| CNS | central nervous system |
| CSF | cerebrospinal fluid |
| Da | Dalton |
| dATP | deoxyadenosine triphosphate |
| dCTP | deoxycytosine triphosphate |
| dd | double distilled |
| ddNTP | dideoxynucleoside triphosphate |
| dGTP | deoxyguanosine triphosphate |
| DIV | day(s) in vitro |
| DMEM | Dulbecco's Modified Eagle Medium |
| DMF | dimethylformamide |
| DMPC | dimethylpyrocarbonate |
| DMSO | dimethylsulfoxide |
| DNA | deoxyribonucleic acid |
| dNTP | deoxynucleoside triphosphate |
| ds | double-stranded |
| DTT | dithiothreitol |
| dTTP | desoxytyrosinetriphosphate |
| <i>E. coli</i> | <i>Escherichia coli</i> |
| ECIS | electric cell substrate sensing |
| EDTA | ethylenediamine tetraacetic acid |
| f.c. | final concentration |
| FCS | fetal calf serum |
| for | forward |
| g | acceleration due to gravity (9.81 m/s ²) |
| GAPDH | glyceraldehyde-3-phosphate dehydrogenase |
| GGT | γ -glutamyltranspeptidase |
| h | hour(s) |
| HC | hydrocortisone |
| Hepes | 2-[4-(2-hydroxyethyl)-1-piperazinyl]-ethanesulfonic acid |
| HUVEC | human umbilical vein endothelial cells |
| kb | kilo base |
| kDa | kilo Dalton |
| L | liter |
| LB | Luria and Bertami |
| LMW | low molecular weight marker |
| M | molar (mol/l) |

| | |
|----------------|---|
| MBCEC | murine brain capillary endothelial cells |
| min | minute(s) |
| MOPS | [N-morpholino]-propylsulfonic acid |
| mRNA | messenger ribonucleic acid |
| MRP | multidrug resistance associated protein |
| MW | molecular weight |
| NCBI | National Centre for Biotechnology Information |
| NCS | newborn calf serum |
| OD | optical density |
| p.a. | pro analysis |
| PAEC | porcine aortic endothelial cells |
| PAGE | polyacrylamide gel electrophoresis |
| PAMR | perijunctional actomyosin ring |
| PBCEC | porcine brain capillary endothelial cells |
| PBS | phosphate buffered saline |
| PCR | polymerase chain reaction |
| PDS | Plasma derived bovine serum |
| Pgp | P-glycoprotein |
| QCM | Quartz crystal microbalance |
| QRT-PCR | quantitative real-time polymerase chain reaction |
| ρ | density |
| RNA | ribonucleic acid |
| RNAi | RNA-interference method |
| Rev | revers |
| rpm | rounds per minute |
| rRNA | ribosomal ribonucleic acid |
| RT | reverse transcription |
| SDS | sodium dodecyl sulfate |
| sec | seconds |
| siRNA | silence-inducing ribonucleic acid |
| SSC | standard saline citrate |
| SSH | subtractive suppression hybridisation |
| TEMED | N,N,N',N'-tetramethylethyldiamine |
| TEER | transendothelial/epithelial electrical resistance |
| Tris | tris-(hydroxymethyl)-aminomethane |
| T _A | Annealing temperature |
| U | unit |
| UV | ultra violet |
| V | voltage |
| VE | vascular endothelial |
| VIS | visible |
| v/v | volume per volume |
| vol | volume |
| W | watt |
| w/v | weight per volume |
| WWU | Westfälische Wilhelms-Universität |
| ZO | zonula occludens |

Appendix B: WWW links

www.ub.uni-bielefeld.de/netahtml/jaso1.html

www.uni-muenster.de/ULB/Welcome.html

www.embl-heidelberg.de/srs5/

www.ncbi.nlm.nih.gov/

www.pubmed.de/index.plip3

www.expasy.ch/

Jason: ordering of literature

Uni-Muenster: download of papers

Medline: literature search

Genbank, EMBL: sequence data bases

NCBI: sequence alignment, basic blast search, PubMed

Literature data bases

Expert Protein Analysis System Molecular Biology Server

Appendix C: Genotypes of *Escherichia coli* K12 strains

TOP10F This strain can be used for general cloning and blue/white screening without IPTG.

F- *mcrA* $\Delta(mrr-hsdRMS-mcrBC)$ $\Phi80lacZ\Delta M15$ $\Delta lacX74recA1$ *deoR* *araD139*
 $\Delta(ara-leu)7697$ *galU* *galK* *rpsL* (StrR) *endA1* *nupG*

TOP10F' This strain expresses the Lac repressor (*lacIq* gene). For blue/white screening IPTG has to be added to obtain expressing from the lac promoter. This strain contains the F episome and can be used for single-strand rescue of plasmid DNA containing an f1 origin.

F' $\{lacIq$ Tn10(TetR) $\}$ *mcrA* $\Delta(mrr-hsdRMS-mcrBC)$ $\Phi80lacZ\Delta M15$
 $\Delta lacX74recA1$ *deoR* *araD139* $\Delta(ara-leu)7697$ *galU* *galK* *rpsL* (StrR) *endA1*
nupG

Appendix D: Sequences

Primer sequences: PCR

Primers for PCR were purchased from MWG Biotech.

| | | |
|---------------------|------------|---|
| porcine GAPDH | for rev | ACCACAGTCCATGCCATCAC TGAGCTTGACAAAGTGGTCG |
| porcine lamin A/C | for rev | GAGCACTGCTCTCAGTGAGAAGCGC CTCTCAGCAGACTGCCTGGCATTGT |
| porcine ve-cadherin | for rev | CGTGGTGGACAAGAACAAGTGGGAG GAGTGATGAACACAGTGGCTGTGCC |
| porcine occludin | for rev | CTACACAAGTGGCGGCGAGTCCTGC CTCCAACCATCTTCTTGATGTGTGAC |

Primer sequences: QRT-PCR

Primers for QRT-PCR were purchased from Proligo

| | | |
|----------------------------------|------------|---|
| Alkaline phosphatase | for rev | CCAAAAACCTCAAAGGCTTCTTC CTGCTTGGCCTTACCCTCATG |
| Angiotensin-converting enzyme | for rev | GACAAACCCAACCTCGATGTCA CCTCTGATACCCGGAACATGTG |
| β -Actin | for rev | CCTGACGGACTACCTCATGAA TCACGCACGATTACCCTCTCA |
| BMDP | rev for | GTGGTAACCTGCTGATGCAAA CCTTACTGGCTTCCGGGAAA |
| Claudin-1 | for rev | TCCCCGGAAAACAACCTCTT TGTCACACATAGTCTTTCCCA |
| Claudin-5 | for rev | GGTGGAACGCTCAGATTTTCAT AGTGCCCCCAGGATCTCAGT |
| Ferritintransferase | for rev | AGCCCAGAGAGACGCTTTGG GCAAGTTTCAACAGAAGACCTGTTC |
| γ -Glutamyltranspeptidase | for rev | CGGTTTGCCTATGCCAAGAG CATGTTGCGGATCACCTGAGA |

| | | |
|----------------|-----|-----------------------|
| GAPDH | for | CAAGGCCGAGAATGGGAAG |
| GAPDH | rev | GGCCTCACCCCATTTGATGT |
| Occludin | for | TGACAGACGGAAACCTTAGAG |
| | rev | AGACATCGTGCAGGCAGATG |
| P-glycoprotein | for | TTACCCGTGGCTGGAAGCTA |
| | rev | CAAATACCAGCTGACAGTCCA |
| ZO-1 | for | TGGACAACCAGATGTGGATTT |
| | rev | TCCCGTCTTCATGAGCTGAAT |

siRNA sequences

| | | |
|--------------------------|-----------------|-------------------------------|
| Lamin A/C ¹ | sense siRNA | CUG GAC UUC CAG AAG AAC AdTdT |
| | antisense siRNA | UGU UCU UCU GGA AGU CCA GdTdT |
| Occludin ² | sense siRNA | GAC UAC ACA ACU GGC GGC GdTdT |
| | antisense siRNA | CGC CGC CAG UUG UGU AGU CdTdT |
| VE-Cadherin ² | sense siRNA | GGU GCU CGU GAU GCU GCU CdTdT |
| | antisense siRNA | GAG CAG CAU CAC GAG CAC CdTdT |
| BMDP ² | | |
| target 3: | sense siRNA | AUC UUC GUU GUU AGA UGU CdTdT |
| | antisense siRNA | GAC AUC UAA CAA CGA AGA UdTdT |
| target 5: | sense siRNA | ACA AGG ACG GAC CAT CAT CdTdT |
| | antisense siRNA | CAU GAU CCU CCG UCC UUG UdTdT |

¹ purchased from Xeragon

² purchased from Eurogentec

Appendix E: Clone charts

Vectors designed for probing and sequencing

porcine GAPDH in pT-Adv (provided by *Tanja Eisenblätter*)

RT-PCR (total RNA from PBCEC, GAPDH-F and GAPDH-R, T_A 55°C); TA-cloning.

porcine ve-cadherin in pT-Adv

RT-PCR (total RNA from PBCEC, ve-cadherin for and ve-cadherin rev, T_A 58°C); TA-cloning

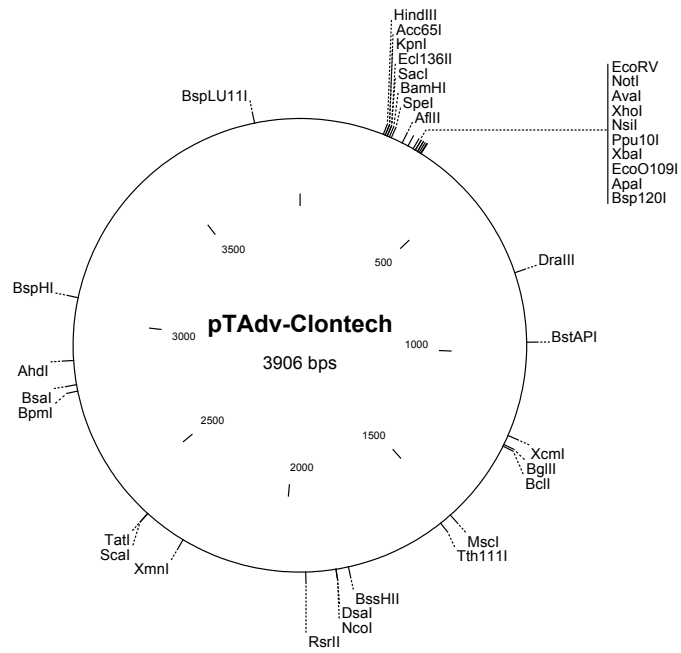
porcine lamin A/C in PCR2.3

RT-PCR (total RNA from PBCEC, lamin A/C for and lamin A/C rev, T_A 58°C); TA-cloning

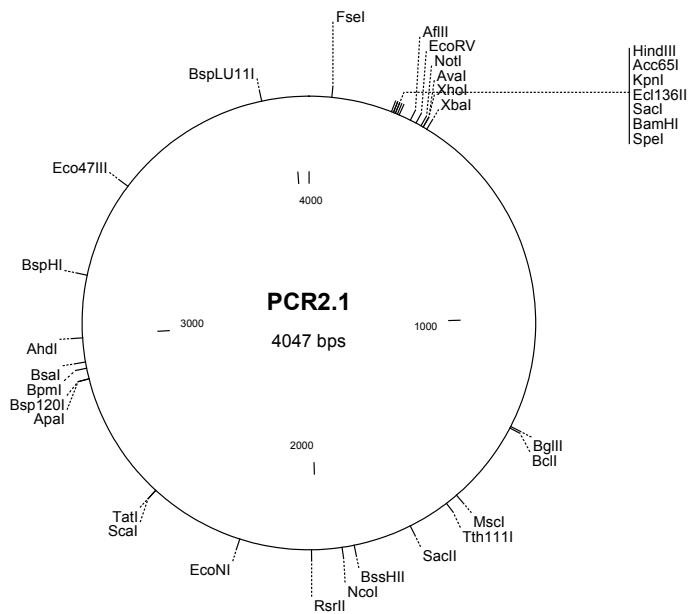
porcine occludin in pT-Adv (provided by *Tanja Eisenblätter*)

RT-PCR (total RNA from PBCEC, occludin for and occludin rev, T_A 54°C); TA-cloning.

pT-Adv-Vector (Clontech)



PCR 2.1-Vector (Invitrogen)



Appendix F: List of table and figure captions

Table captions

| | |
|---|----|
| Table 2_1: Common Features of Endothelial Cells (Deli and Joo, 1996) | 12 |
| Table 2_2: Effects of compounds on different blood-brain barrier models <i>in vitro</i> | 15 |
| Table 3_1: Overview of amounts and concentrations of used solutions during transfection with siRNA | 27 |
| Table 3_2: Primary antibodies used in immunofluorescence staining | 28 |
| Table 3_3: Secondary antibodies used in immunofluorescence staining | 28 |
| Table 3_4: Concentrations of agarose gels..... | 39 |
| Table 3_5: Acrylamide concentration for separation of proteins | 53 |
| Table 3_6: Compounds of SDS-gels..... | 53 |
| Table 3_7: Antibodies for western blotting..... | 55 |

Figure captions

| | |
|--|----|
| Figure 2-1: Schematic view of the mammalian brain. Overview about the ventricles of the choroid plexus. (Spector and Johanson, 1989)..... | 5 |
| Figure 2-2: Micrograph of a Cross-section of a brain capillary (Krstic, 1988). | 7 |
| Figure 2-3: Molecular structure of the tight junctions.. | 8 |
| Figure 2-4: Regulation of glucocorticoid secretion. | 17 |
| Figure 2-5: Schematic representation of the human GR gene and the alternatively spliced cDNAs encoding the α and β isoforms of this receptor. | 18 |
| Figure 2-6: Signal transduction pathway of glucocorticoids.. | 19 |
| Figure 3-1: <i>In vitro</i> model of BBB and experimental setup for TEER measurement..... | 32 |
| Figure 3-2: Setup for electric cell substrate sensing (ECIS). | 32 |
| Figure 3-3: ECIS electrode in 8-well format (8W10E, <i>Applied BioPhysics, Troy, NY</i>)..... | 33 |
| Figure 3-4: A: Experimental setup for QCM. | 35 |
| Figure 3-5: Semilog diagram of the fluorescence signal intensity versus cycle..... | 45 |
| Figure 4-1 Endothelial cell morphology after 4 DIV determined by phase contrast microscopy..... | 57 |
| Figure 4-2: Immunofluorescence stain of MBCEC <i>in vitro</i> | 58 |
| Figure 4-3: Tight junction expression in MBCEC.. | 59 |
| Figure 4-4: Immunofluorescence labelling of tight junction proteins in MBCEC.. | |
| Figure 4-5: Localisation of brain multidrug resistance protein and factor VIII in MBCEC..... | 61 |

| | |
|---|----|
| Figure 4-6: Expression of mRNA of blood-brain barrier related proteins and house-keeping genes..... | 63 |
| Figure 4-7: Influence of hydrocortisone on transendothelial resistance on MBCEC under different culture conditions..... | 65 |
| Figure 4-8: Time-dependent effect of hydrocortisone in MBCEC..... | 66 |
| Figure 4-9: A the motional inductance ΔL and the motional resistance ΔR of MBCEC..... | 67 |
| Figure 4-10: Results of ECIS..... | 68 |
| Figure 4-11: Permeability of MBCEC..... | 69 |
| Figure 4-12: Morphology of cells treated either with serum- or with hydrocortisone-containing medium..... | 71 |
| Figure 4-13: Effect of hydrocortisone on tight junctions..... | 73 |
| Figure 4-14: Direct phalloidin-staining of actin in MBCEC..... | 74 |
| Figure 4-15: Topography images of MBCEC <i>in vitro</i> | 76 |
| Figure 4-16: Height of tight junctions in different media..... | 77 |
| Figure 4-17: Force mapping of MBCEC under different conditions..... | 78 |
| Figure 4-18: Micrograph of a TEM-image of MBCEC..... | 79 |
| Figure 4-19: TEM images of MBCEC..... | 80 |
| Figure 4-20: Results of QRT-PCR in MBCEC..... | 81 |
| Figure 4-21: Expression pattern on RNA-level of blood-brain barrier markers in MBCEC..... | 82 |
| Figure 4-22: Western blot analysis of tight junction proteins..... | 83 |
| Figure 4-23: Immunodetection of lamin A/C in cultured murine and porcine brain capillary endothelial cells..... | 85 |
| Figure 4-24: Change in expression of lamin A/C on protein level after transfection of cells with siRNA against lamin A/C..... | 86 |
| Figure 5-1: Model for tight junction localisation and resulting staining pattern in immunofluorescence detection of tight junction proteins..... | 96 |

Lebenslauf

Name: Christian Weidenfeller

Geburtsdatum: 10.10.1973

Geburtsort: Oberhausen

Familienstand: ledig

Namen der Eltern: Ulrich Weidenfeller
Elisabeth Weidenfeller, geb. Hübner

Schulbildung:

1980-1984: Besuch der St. Vincentius Grundschule in Rees-Mehr

1984-1993: Besuch des Gymnasiums Aspel der Stadt Rees

17.06.1993 Abschluss mit Erhalt der Allgemeinen Hochschulreife, Rees

Zivildienst

08/93-09/94 St. Willibrord-Spital Emmerich-Rees

Studium:

10/1994: Grundstudium der Biologie, Chemie Lehramt (Sek. II/I) und Philosophie
Lehramt (Sek. II/I) an der Westfälischen Wilhelms-Universität Münster.

17.04.1996 Zwischenprüfung im Fach Chemie (Lehramt Sek. II)

05/1996 Hauptstudium Chemie Lehramt (Sek. II/I) an der Westfälischen
Wilhelms-Universität, Münster

25.09.1996 Vordiplom im Fach Biologie

10/1996 Hauptstudium der Biologie an der Westfälischen Wilhelms-Universität,
Münster

30.05.2000 Abschluss des Studiums mit dem Diplom im Fach Biologie

Promotionsstudiengang:

06.2000 Beginn der Dissertation unter der Betreuung von Prof. Dr. H.-J. Galla,
Institut für Biochemie

Tätigkeiten:

06/2000-08/2003: Wissenschaftlicher Mitarbeiter am Institut für Biochemie der
Westfälischen Wilhelms-Universität, Münster